COMENIUS UNIVERSITY IN BRATISLAVA,
FACULTY OF NATURAL SCIENCES
&
UNIVERSITÄT BREMEN,
FACHBEREICH GEOWISSENSCHAFTEN

THE EFFECT OF POPULATION DYNAMICS, GROWTH AND CALCIFICATION OF PLANKTONIC FORAMINIFERA ON THE PELAGIC CARBONATE FLUX

Dissertation

Study programme:	Paleontology, dPAL
Field of study:	Earth Sciences (Vedy o Zemi)
Department/Research faculty:	Department of Geology and Paleontology & MARUM - Center for Marine Environmental Sciences
Supervisors:	doc. Mgr. Natália Hudáčková, PhD. & Prof. Michal Kučera
Date of Defense:	30 August 2021

BRATISLAVA & BREMEN 2021 **Mgr. Peter Kiss**

Versicherung an Eides Statt / *Affirmation in lieu of an oath*

gem. § 5 Abs. 5 der Promotionsordnung vom 18.06.2018 /
according to § 5 (5) of the Doctoral Degree Rules and Regulations of 18 June, 2018

Ich / I, Peter Kiss
(Vorname / First *Name*, Name / *Name*, Anschrift / *Address*, ggf. Matr.-Nr. / *student ID no., if applicable)*

versichere an Eides Statt durch meine Unterschrift, dass ich die vorliegende Dissertation selbständig und ohne fremde Hilfe angefertigt und alle Stellen, die ich wörtlich dem Sinne nach aus Veröffentlichungen entnommen habe, als solche kenntlich gemacht habe, mich auch keiner anderen als der angegebenen Literatur oder sonstiger Hilfsmittel bedient habe und die zu Prüfungszwecken beigelegte elektronische Version (PDF) der Dissertation mit der abgegebenen gedruckten Version identisch ist. / *With my signature I affirm in lieu of an oath that I prepared the submitted dissertation independently and without illicit assistance from third parties, that I appropriately referenced any text or content from other sources, that I used only literature and resources listed in the dissertation, and that the electronic (PDF) and printed versions of the dissertation are identical.*

Ich versichere an Eides Statt, dass ich die vorgenannten Angaben nach bestem Wissen und Gewissen gemacht habe und dass die Angaben der Wahrheit entsprechen und ich nichts verschwiegen habe*. / I affirm in lieu of an oath that the information provided herein to the best of my knowledge is true and complete.*

Die Strafbarkeit einer falschen eidesstattlichen Versicherung ist mir bekannt, namentlich die Strafandrohung gemäß § 156 StGB bis zu drei Jahren Freiheitsstrafe oder Geldstrafe bei vorsätzlicher Begehung der Tat bzw. gemäß § 161 Abs. 1 StGB bis zu einem Jahr Freiheitsstrafe oder Geldstrafe bei fahrlässiger Begehung. / *I am aware that a false affidavit is a criminal offence which is punishable by law in accordance with § 156 of the German Criminal Code (StGB) with up to three years imprisonment or a fine in case of intention, or in accordance with § 161 (1) of the German Criminal Code with up to one year imprisonment or a fine in case of negligence.*

Bremen, 28. Juni 2021

Ort / *Place*, Datum / *Date* | Unterschrift / *Signature*

Univerzita Komenského v Bratislave
Prírodovedecká fakulta

61781885

ZADANIE ZÁVEREČNEJ PRÁCE

Meno a priezvisko študenta: Mgr. Peter Kiss
Študijný program: paleontológia (Jednoodborové štúdium, doktorandské III. st., denná forma)
Študijný odbor: vedy o Zemi
Typ záverečnej práce: dizertačná
Jazyk záverečnej práce: anglický
Sekundárny jazyk: slovenský

Názov: The effect of population dynamics, growth and calcification of planktonic foraminifera on the pelagic carbonate flux
Vplyv populačnej dynamiky, rastu a kalcifikácie schránky planktonických dierkavcov na morský spád karbonátu

Anotácia: 1) Definícia mechanizmov určujúcich variabilitu v kalcitovom spáde planktonických dierkavcov
2) Zmeny v spáde, veľkosti a kalcifikácie schránok planktonických dierkavcov počas obdobia poslednej deglaciácie
3) Štúdium kalcifikácie schránok planktonických dierkavcov v sedimentoch stredného miocénu Centrálnej Paratetýdy

Školiteľ: doc. Mgr. Natália Hlavatá Hudáčková, PhD.
Katedra: PriF.KGP - Katedra geológie a paleontológie
PriF vedúci katedry: prof. RNDr. Michal Kováč, DrSc.

Dátum zadania: 18.01.2017

Dátum schválenia: 19.01.2017

prof. RNDr. Daniela Reháková, CSc.
garant študijného programu

.....
študent

.....
školiteľ

Comenius University in Bratislava
Faculty of Natural Sciences

THESIS ASSIGNMENT

Name and Surname:	Mgr. Peter Kiss
Study programme:	Palaeontology (Single degree study, Ph.D. III. deg., full time form)
Field of Study:	Earth Sciences
Type of Thesis:	Dissertation thesis
Language of Thesis:	English
Secondary language:	Slovak

Title: The effect of population dynamics, growth and calcification of planktonic foraminifera on the pelagic carbonate flux

Annotation: 1) Mechanisms modulating the variability in the planktonic foraminifera calcite flux
2) Changes in shell flux, shell size and calcification intensity of planktonic foraminifera during the last deglaciation
3) Calcification intensity of planktonic foraminifera from mid-Miocene sediments of the Central Paratethys

Tutor:	doc. Mgr. Natália Hlavatá Hudáčková, PhD.
Department:	PriF.KGP - Katedra geológie a paleontológie
Head of Department:	prof. RNDr. Michal Kováč, DrSc.
Assigned:	18.01.2017
Approved:	19.01.2017

prof. RNDr. Daniela Reháková, CSc.
Guarantor of Study Programme

.....
Student

.....
Tutor

Čestné vyhlásenie

Čestne vyhlasujem, že dizertačnú prácu som vypracoval samostatne, s použitím uvedenej literatúry.

Bratislava, 15.06.2021 .....

podpis

Content

Acknowledgements

I would like to express my deepest gratitude to my supervisors, doc. Mgr. Natália Hudáčková, PhD. and Prof. Michal Kučera, for their patient guidance, unlimited support and trusting me with my freedom and creativity within this PhD project. I am genuinely grateful to Dr. Lukas Jonkers for his great support and for the valuable discussions that enabled me to grow in my academic life. Many thanks for Dr. Julie Meilland for her help that she provided in and outside of the laboratories during my research stays in Bremen. I would like to thank all my colleagues in Bremen and Bratislava for their assistance, for creating a friendly working environment and for their selfless support during my PhD journey.

I am thankful for the Graduate School GLOMAR for the courses, workshops, and support for attending scientific meetings that allowed me to extend my scientific knowledge. Thanks for the foundations Collegium Talentum Programme of Hungary, German Academic Exchange Service (DAAD), National Scholarship Programme of the Slovak Republic and Erasmus+ Programme of the European Commission for providing financial support enabling me to stay for 2 years in Bremen and conduct my research at the institution MARUM.

There are many people outside academia who believed in me and strongly supported my work over my PhD. They sometimes had difficult times with a frustrated Peter (sorry for my unconscious behaviour), but they always got me back. For this I will be forever grateful for my loved family and fiancé Emma. Furthermore, as a PhD student I got motivation and support from my friends. A special thanks for Peter for the coffee breaks and tea sessions, for the A33 corridor of the Galileo Residenz (Amanda, Rebeka and Fernando) for the long nights, for Felipe and Igor for our discussions and cooking together - I will miss you all!

This work has been financially supported by the Slovak Research and Development Agency under the contracts APVV 15-0575 and APVV 16-0121, by the German Research Foundation (DFG) through the Research Center Ocean Margins (RCOM), by the Excellence Cluster “The Ocean in the Earth System” and the Cluster of Excellence “The Ocean Floor–Earth’s Uncharted Interface”.

Abstract in Slovak

Produkcia kalcitových schránok planktonických dierkavcov je základnou zložkou morského kolobehu uhlíka. Spád kalcitových schránok planktonických dierkavcov zaberá globálne takmer polovicu celkového množstva morského kalcitového spádu, avšak počas biomineralizácie kalcitu sa do morského prostredia uvoľňuje oxid uhličitý. Vzhľadom na význam planktonických dierkavcov v morskom uhlíkovom rozpočte a v efektivite biologického čerpadla z hľadiska sekvestrácie oxidu uhličitého z atmosféry je nevyhnutné porozumieť mechanizmom ovplyvňujúcim krátkodobú (ročnú a medziročnú) a dlhodobú (centeniálnu a mileniálnu) variabilitu kalcitového spádu planktonických dierkavcov. Spád kalcitových schránok planktonických dierkavcov je výsledkom kalcitového spádu jedincov, v ktorom variabilitu môžu vyvolať zmeny v i) spáde schránok, ii) veľkosti schránok, a iii) kalcifikačná intenzita. V populáciách, v ktorých sa odlišuje veľkosť a kalcifikačná intenzita medzi druhmi, môžu byť zmeny spôsobené i v dôsledku druhového zloženia populácie. Predchádzajúce výskumy neskúmali všetky tieto mechanizmy spoločne v kontexte kalcitového spádu planktonických dierkavcov. Z toho vyplýva, že nevieme koľko z potenciálnych kontrolných mechanizmov je dostatočných na modelovanie variability v kalcitovom spáde planktonických dierkavcov, a na rozpočet kalcitu produkovaného planktonickými dierkavcami. Za účelom definovania mechanizmov určujúcich krátkodobé (= ročné) zmeny v kalcitovom spáde planktonických dierkavcov sme interpretovali spád schránok, veľkosť schránok a kalcifikačnú intenzitu schránok planktonických dierkavcov počas dvoch rokov sedimentácie (v roku 1990-1991 a 2007-2008) získaných použitím pasce na sediment z lokality Cape Blanc v Atlantickom oceáne. Tieto pozorovania boli následne porovnané s dlhodobými trendami mechanizmov spôsobujúcich variabilitu v kalcitovom spáde planktonických dierkavcov (spád schránok, veľkosť schránok a kalcifikačná intenzita). Za účelom interpretácie ich reakcie na náhle environmentálne zmeny sme skúmali spoločenstvá planktonických dierkavcov z vrtného jadra (GeoB3104-1), pochádzajúcich z obdobia posledného ústupu ľadovcov z Atlantického oceánu a zo stredného miocénu z lokality Devínska Nová Ves (Slovensko). Naše pozorovania odhalili, že zmeny v kalcitovom spáde planktonických dierkavcov v rámci jedného roka sú spôsobené spádom schránok, ktorý vysvetľuje až 82 % variability v celkovom kalcitovom spáde planktonických dierkavcov. Na rozdiel od ročných zmien, medziročné zmeny sú spôsobené viacerými mechanizmami, kedy pozorujeme, že interakcia medzi spádom schránok a veľkosťou

schránok sú najdôležitejšími faktormi, ktoré ovplyvňujú variabilitu v kalcitovom spáde planktonických dierkavcov. Sedimentárne vzorky poukázali na to, že dlhodobé zmeny v kalcitom spáde planktonických dierkavcov spôsobuje spád schránok, kým veľkosť a kalcifikačná intenzita nie sú dôležitými mechanizmami. Tieto výsledky podporujú aj naše pozorovania zo vzoriek zo stredného momiocénu, ktoré odhaľujú, že veľkosť a kalcifikačná intenzita vybraných druhov zostala identickou, aj napriek ich dlhodobej evolúcie v odlišných podmienkach. Bez ohľadu na časovú škálu, spád schránok je najdôležitejším mechanizmom spôsobujúcim variabilitu v kalcitovom spáde planktonických dierkavcov, kým kalcifikačná intenzita je najmenej dôležitým. Spád schránok sa počas obdobia s veľkými klimatickými zmenami mení významným spôsobom, zatiaľ čo kalcifikačná intenzita a veľkosť schránok zostáva takmer rovnaká aj napriek glaciálnym a interglaciálnym cyklom, a aj medzi modernými a strednomiocénnymi vzorkami sú takmer identické. Z hľadiska predpovedania globálneho rozpočtu kalcitu produkovanými planktonickými dierkavcami je v prvom rade potrebné zistiť biotické a abiotické faktory ovplyvňujúce spád schránok planktonických dierkavcov.

Kľúčové slová: planktonické dierkavce, kolobeh uhlíka, pasca na sediment, Pleistocén, Miocén

Abstract in English

The planktonic foraminifera calcite production represents a fundamental component of the pelagic carbon cycle by contributing up to half of the biogenic carbonate export flux to the deep ocean, whilst simultaneously the calcite biomineralisation releases CO_2 from the surface waters. Due to its relevance for the pelagic carbonate budget and the biological pump, in terms of oceanic capacity of CO_2 sequestration from the atmosphere, it is crucial to understand the mechanisms constraining the short-term (intra-and interannual) and long-term (centennial to millennial) variability in the planktonic foraminifera calcite flux. The planktonic foraminifera calcite flux is the product of the species individual calcite fluxes where variability in calcite flux can be caused by changes in the species i) individual flux, ii) shell size, and iii) calcification intensity. In the exported assemblages, where size and calcification intensity vary among the species, changes can be caused by the species composition as well. Previous research has not investigated these three mechanisms comprehensively in the context of the planktonic foraminifera calcite flux. Thus, it is uncertain how many of the potential controlling mechanisms are sufficient to be considered to constrain the variability in the planktonic foraminifera calcite flux and to derive an accurate planktonic foraminifera calcite budget. To assess the importance of these mechanisms in regulating the short-term variability in planktonic foraminifera calcite flux, record of species-resolved shell flux, shell size, and calcification intensity variations during two years of sedimentation (from 1990-1991 and 2007-2008) from the Cape Blanc upwelling area in the Atlantic Ocean was generated. In order to compare how the short-term variability in the regulating mechanisms compares to long-term trends and to assess how these mechanisms responded to large amplitude environmental changes, we investigated exceptionally preserved planktonic foraminifera communities from a well-dated sediment core (GeoB3104-1) covering the period of the last deglaciation in the tropical Atlantic and sediment samples from the mid-Miocene Devínska Nová Ves (Slovakia) site. The sediment trap time series revealed that on the intra-annual timescales, the variability in calcite flux is largely due to changes in shell flux, which can alone explain 82 % of the variability in the planktonic foraminifera calcite flux. On the interannual timescale, multiple mechanisms act in concert to shape the variability in the planktonic foraminifera calcite flux, and next to shell flux shell size also emerges as an important predictor of calcite flux. The sedimentary time series revealed that on the centennial to millennial timescales, shell flux is the most important mechanism shaping the variability in the

planktonic foraminifera calcite flux. This conclusion is supported by observations from the Miocene site, which reveals that despite different background climate state and millions of years of evolution, the calcification intensity of the studied species remained similar. Thus, irrespective of the temporal scale, shell flux emerges as the most and calcification intensity the least important mechanism for predicting changes in the planktonic foraminifera calcite flux. Shell flux changed dramatically during large-scale environmental transition, whereas calcification intensity and shell size remained more similar during the glacial-interglacial cycle and between modern and mid-Miocene samples. Therefore, our analysis implies that in order to model/predict the global foraminifera calcite budget we first and foremost need to constrain the biotic and abiotic factors that control shell flux variability.

Keywords: planktonic foraminifera, carbon cycle, sediment trap time series, Pleistocene, Miocene

Summary

Planktonic foraminifera are undoubtedly one of the most successful marine protists, which thank to their fossiliferous shells created a continuous record in marine sediments since the Jurassic. Their shells are formed by calcite precipitation in the productive zone, which after the death of the organisms sink to the deep ocean. The rain of their empty shells become one of the most common sources of pelagic calcite during the Cenozoic, which at present comprises up to half of the global pelagic calcite flux. However, the export and production of planktonic foraminifera calcite releases carbon dioxide into the ambient seawater, partly offsetting the oceanic carbon dioxide uptake by the biological pump. Therefore, the presented doctoral thesis aims to constrain the regulating mechanisms of the planktonic foraminifera calcite flux on short-term and long-term timescales.

The planktonic foraminifera calcite flux is the sum of the individual species calcite fluxes. In theory, changes in the individual species calcite flux may result from changes in i) shell flux – reflecting changes in the population growth and ii) shell mass – reflecting changes in the individual growth. Shell mass is in turn the product of shell size and calcification intensity. Previous research has not analysed the comprehensive influence of these mechanisms in regulating the planktonic foraminifera calcite flux variability. Therefore, we present the first analysis of the relative contribution of variability in the individual species shell flux, size, and calcification intensity to the total planktonic foraminifera calcite on the seasonal up to millennial timescales.

In order to resolve to what degree, the shell flux, shell size, and calcification intensity shape the intra-annual (within the year) and inter-annual (between the years) variability in the planktonic foraminifera calcite flux, we analysed two time series (1990-1991 and 2007-2008) from the long-term sediment trap mooring array off Cape Blanc (Atlantic Ocean). Our results revealed that on the intra-annual timescale, the variability in the calcite flux was only matched by shell flux, which is the best predictor of seasonal variability in the planktonic foraminifera calcite flux. On the interannual timescales, the variability in the calcite flux was lower and shell flux and shell size varied with a comparable magnitude with the calcite flux. Therefore, predictions of variability in the planktonic foraminifera calcite flux beyond the seasonal timescale will require the knowledge about shell mass.

Afterwards, we assessed how the relative contribution of the mechanisms regulating (shell flux, shell size, and calcification intensity) the planktonic foraminifera calcite flux responded to major climate transitions. For this issue, the period of the last deglaciation provides an excellent opportunity, while the last ~22.000 years are characterised by changes in land and sea-surface temperature, atmospheric and oceanic carbon dioxide concentrations and ocean carbonate chemistry that far exceed the magnitude of modern intra-annual and inter-annual changes. Using a well-dated sediment core from the tropical Atlantic (GeoB3104-1) we generated a species resolved shell flux, shell size, and calcification intensity data from the period of the Last Glacial Maximum, Heinrich Stadial I., Younger Dryas and Holocene, and observed their variability in the context of the resulting planktonic foraminifer calcite flux. The sedimentary time series revealed that the most important predictor of the long-term variability in the planktonic foraminifera calcite flux is the shell flux. The long-term variability in shell size and calcification intensity was surprisingly low and interestingly they did not show significant changes in response to the major climatic events associated with the glacial-interglacial cycle.

In the next step we thus focused on the long-term variability in shell size, shell wall thickness, and calcification intensity of planktonic foraminifera. We measured the calcification aspects of *Globigerina bulloides* obtained from sediment samples from the mid-Miocene Devínska Nová Ves site (Slovakia), representing a climatic setting immediately postdating the prominent Miocene climatic optimum with high carbon dioxide content. We compared this data with the shell size and calcification intensity with two years of sedimentation from the Cape Blanc time series, where specimens calcified under lower dissolved inorganic carbon concentration. Our results showed that the variability in size and calcification are insignificant between the modern and mid-Miocene representatives of *Globigerina bulloides*, which indicates that the long-term evolution of this species from a generally warmer climate and elevated carbon dioxide concentration to the present did not lead to substantial modifications in the calcification process.

Our results thus yield a clear ranking of the mechanisms based on their significance for modulating the variability in the planktonic foraminifera calcite flux. Shell flux appears the most and calcification intensity the least important mechanisms, while the relevance of shell size depends on the timescale. Our analysis thus implies that in order to model the global foraminifera calcite budget, we first need to constrain the processes that control individual flux.

Zusammenfassung

Planktonische Foraminiferen sind zweifellos eine der erfolgreichsten marinen Protisten, die dank ihrer fossilhaltigen Schalen seit dem Jura eine kontinuierliche Dokumentation im marinen Sediment aufgebaut haben. Ihre Schalen entstehen durch das Ausfällen von Kalzit in der produktiven Zone, die nach dem Absterben der Organismen in die Tiefsee absinken. Dieses Absinken leerer Schalen wird während des Känozoikums zu einer der häufigsten Quellen für pelagischen Kalzit und macht in der Gegenwart bis zu fünfzig Prozent des globalen pelagischen Kalzitflusses aus. Der Export und die Produktion des Kalzits planktonischer Foraminiferen gibt jedoch Kohlenstoffdioxid in das umgebende Meerwasser ab, wodurch die ozeanische Kohlenstoffdioxidaufnahme durch die biologische Pumpe teilweise kompensiert wird. Daher zielt die vorliegende Dissertation darauf ab, die Regulationsmechanismen des planktonischen Foraminiferen-Kalzitflusses auf kurz- und langfristige Zeitskalen genauer zu definieren.

Der Kalizitfluss planktonischer Foraminiferen ist die Summe der Kalzitflüsse individueller Arten. Theoretisch können Änderungen des Kalzitflusses der einzelnen Arten aus Änderungen i) des Schalenflusses – der Änderungen des Populationswachstums widerspiegelt und ii) der Schalenmasse – die Änderungen des individuellen Wachstums widerspiegelt, resultieren. Die Schalenmasse ist wiederum das Produkt aus Schalengröße und Kalzifizierungsintensität. Bisherige Forschungen haben den umfassenden Einfluss dieser Mechanismen auf die Regulierung der planktonischen Foraminiferen-Kalzitflussvariabilität nicht analysiert. Daher präsentieren wir die erste Analyse des relativen Beitrags der Variabilität des Schalenflusses, der Größe und der Kalzifizierungsintensität einzelner Arten zum gesamten Kalzit planktonischer Foraminiferen auf Zeitskalen von saisonal bis hin zu Jahrtausenden.

Um auszumachen, inwieweit Schalenfluss, Schalengröße und Kalzifizierungsintensität die intra-annuelle (innerhalb des Jahres) und interannuelle (zwischen den Jahren) Variabilität des Kalzitflusses planktonischer Foraminiferen beeinflussen, haben wir zwei Zeitreihen (1990-1991 und 2007-2008) aus der Langzeit-Sedimentfalle vor Cap Blanc (Atlantischer Ozean) analysiert. Unsere Ergebnisse zeigten, dass auf der intra-annuellen Zeitskala die Variabilität des Kalizitflusses nur mit dem Schalenfluss übereinstimmte, welcher der beste Prädiktor für die saisonale Variabilität des planktonischen Foraminiferen-Kalzitflusses Flusses ist. Auf den interannuellen Zeitskalen war die Variabilität des Kalzitflusses geringer und Schalenfluss und

Schalengröße variierten in vergleichbarer Größenordnung. Daher erfordern Vorhersagen der Variabilität des planktonischen Foraminiferen-Kalzitflusses über die jahreszeitliche Zeitskala hinaus Kenntnisse über die Schalenmasse.

Anschließend bewerteten wir, wie der relative Beitrag der verschiedenen Kalzifizierungsaspekte (Schalenfluss, Schalengröße und Kalzifizierungsintensität) des planktonischen Foraminiferen-Kalzitflusses auf große Klimaveränderungen reagierte. Hierfür bietet der Zeitraum der letzten Entgletscherung eine hervorragende Gelegenheit, während die letzten ~22.000 Jahre durch Veränderungen der Land- und Meeresoberflächentemperatur, der atmosphärischen und ozeanischen Kohlenstoffdioxidkonzentrationen und der Ozeankarbonatchemie gekennzeichnet sind, die weit über das Ausmaß moderner intra- und interannueller Änderungen hinausgehen. Unter Verwendung eines gut datierten Sedimentkerns aus dem tropischen Atlantik (GeoB3104-1) haben wir unter Artenspezifikation Schalenfluss-, Schalengröße- und Kalzifizierungsintensitätsdaten aus der Zeit des letzten glazialen Maximums, Heinrich Ereignis I., Jüngere Dryaszeit und Holozän generiert und beobachteten ihre Variabilität im Kontext des Kalzitflusses planktonischer Foraminiferen. Die Sedimentzeitreihen zeigten auf, dass der Schalenfluss der wichtigste Prädiktor für die langfristige Variabilität des planktonischen Foraminiferen-Kalzitflusses. Die langfristige Variabilität der Schalengröße und der Kalzifizierungsintensität war überraschend gering. Interessanterweise zeigten sie keine signifikanten Veränderungen als Reaktion auf die großen klimatischen Ereignisse im Zusammenhang mit dem Glazial-Interglazial-Zyklus.

Im nächsten Schritt konzentrierten wir uns daher auf die langfristige Variabilität von Schalengröße, Schalenwanddicke und Kalzifizierungssintensität planktonischer Foraminiferen. Wir haben die Kalzifizierungskomponenten von *Globigerina bulloides* gemessen, die aus Sedimentproben aus dem mittelmiozänen Standort Devínska Nová Ves (Slowakei) gewonnen wurden und eine klimatische Situation unmittelbar nach dem miozänen Klimaoptimums mit hohem Kohlenstoffdioxidgehalt darstellen. Wir verglichen diese Daten mit Schalengröße und der Kalzifizierungsintensität aus Proben der zweijährigen Zeitreihe der Sedimentation vor Cap Blanc, in der Foraminiferen unter einer geringeren Konzentration an gelöstem anorganischem Kohlenstoff kalzifizierten. Unsere Ergebnisse zeigten, dass die Variabilität in Größe und Kalzifizierung zwischen modernen und mittleren Miozän-Vertretern von Globigerina bulloides

unbedeutend ist, was darauf hindeutet, dass eine langfristige Evolution dieser Art von einem allgemein wärmeren Klima und einer erhöhten Kohlendioxidkonzentration in die Gegenwart nicht zu erheblichen Veränderungen im Kalzifizierungsprozess führten.

Unsere Ergebnisse ergeben somit eine klare Rangordnung der Mechanismen, die die Variabilität der planktonischen Foraminiferen-Kalzitflüsse prägen: Der Schalenfluss erscheint als der wichtigste und die Kalzifizierungsintensität als der unwichtige Mechanismus, während die Relevanz der Schalengröße von der Zeitskala abhängt. Unsere Analyse zeigt daher, dass wir zur Modellierung des globalen Kalzitbudgets durch Foraminiferen zunächst die Prozesse definieren müssen, die individuelle Flüsse kontrollieren.

Own contribution to the manuscripts

The fundamental concept of the first study (**Chapter 1**) was formulated jointly by the candidate (PK), MK and LJ. Suitable material for the study was selected by PK with advice from BD and GF. Identification and counting of foraminifera were carried out by PK for time series 2007-2008 and RT for time series 1990-1991. The candidate carried out all shell size and weight measurements. Afterwards he harmonised all data, performed statistical analyses and drafted all figures. The analyses and interpretations, as well as the drafting of the first manuscript were carried out by PK with advice from MK and LJ. The final manuscript with its statistical backbone benefitted from contributions by all co-authors, as well from feedback by three referees, who provided constructive comments on the submitted version of the present manuscript.

For the second study (**Chapter 2**), the candidate jointly with MK and LJ designed the research goals. The selection of suitable sediment core for the study was carried out by PK with advice from LJ and SM. The candidate then sampled the chosen sediment core and under the supervision of MK and LJ carried out the laboratory processing of samples, including weighing and washing of all samples, extracting foraminifera, determining species fluxes and size and weight variation at species level. After this, the candidate performed the subsequent statistical analyses, benefitting from support of LJ for the interpretation of the age model and accumulation rates of the core. The candidate carried out all data visualizations and wrote the draft of the manuscript.

For the third study (**Chapter 3**), the candidate with MK and NH defined the research goals, with NH carried out the selection of the material and planned the preparation of polished thin sections in Bratislava with MG. NH ensured the sample accessibility and NH and MK provided assistance with taxonomical identification. The candidate extracted the foraminifera from the samples, measured the size and shell weight of the selected species and prepared the data set for statistical analyses. He extracted oceanographic data from online environmental repositories and data on shell calcification of the studied species available in public databases. The candidate then prepared the figures and data visualization, and wrote the first draft of the manuscript, which was discussed and commented by MK and LJ.

For the **Appendix Chapter 1**, NH and the candidate developed the objectives of the study. The candidate decided to add this appendix chapter to his dissertation by the suggestion of MK. AR helped in the taxonomic identification of the specimens, KH assisted in the choice of individuals suitable for CT scanning. The computer tomography was done by ZH in Prague. The candidate afterwards segmented the data obtained with the tomographic microscopy and conducted the measurements. He prepared the data visualization together with NH, the CT images were created by ZH. The candidate wrote the first draft of the manuscript, which benefited from contributions by all co-authors, as well as feedback by two referees, who provided constructive comments on the earlier versions of the present manuscript.

The **Appendix Chapter 2** was formulated by the candidate, NH and MK. The candidate added this chapter to his dissertation by the suggestion of MK. PK, AR and SL ensured the samples and picked the specimens suitable for the defined methodological approaches. The selected specimens were then studied by using computed tomography by ZH in Prague. Two more scanned individuals were given by SL to the candidate. The obtained tomographic data were segmented and the morphometric data from the segmented models were extracted by JT. Information about the coiling geometry was extracted by MGSR. SR helped in the preparation of the paleogeographic map. Afterwards, the candidate performed statistical analyses and prepared the data visualization with MK and NH. The candidate wrote the first version of the manuscript, which was sent around the co-authors, who provided constructive comments on the submitted version of the present manuscript.

1. Introduction

1.1 Oceans, the mass storages of carbon

The currently ongoing climate change is potentially the most challenging global threat that humanity has ever faced. Since the onset of the Industrial Revolution, the man-made energy-hungry industry triggered an abrupt increase of a wide variety of greenhouse-gases to the atmosphere, including carbon dioxide, with atmospheric concentration presently exceeding 400 ppmv (Fig. 1). The consequence of this increase influences the Earth's terrestrial and marine environments through continuous warming, such that the average surface temperature since the mid-20th century rose by approximately 1 °C (Hoegh-Guldberg et al., 2019, Fig. 1). Since the atmosphere and the global ocean are mutually interlaced by complex interactions facilitated via air-sea fluxes, a quarter of the carbon dioxide produced by human activities has been absorbed by the oceans (Sabine et al., 2004; Watson et al., 2020). In terms of oceanic capacity of carbon dioxide uptake, the subtropical and polar oceans of the Northern and Southern hemisphere represent the most important reservoirs due to their colder and more productive waters, whereas oceans along the equator appear as net sources for carbon dioxide (Takahashi, T. et al., 1997). The process of carbon dioxide sequestration by the oceans thus mitigating the degree of global warming comes at the cost of marine ecosystems, because as they absorb carbon, the oceans are becoming more acidic. The pH of the global ocean since the Industrial Revolution has already decreased by 0.1 unit (Orr et al., 2005). It appears as a small drop but indeed it means a powerful change for organisms that produce carbonate shells or skeletons such as planktonic foraminifera, coccoliths, pteropods, shellfish or corals (Comeau et al., 2009; Leclercq et al., 2000; Riebesell et al., 2000).

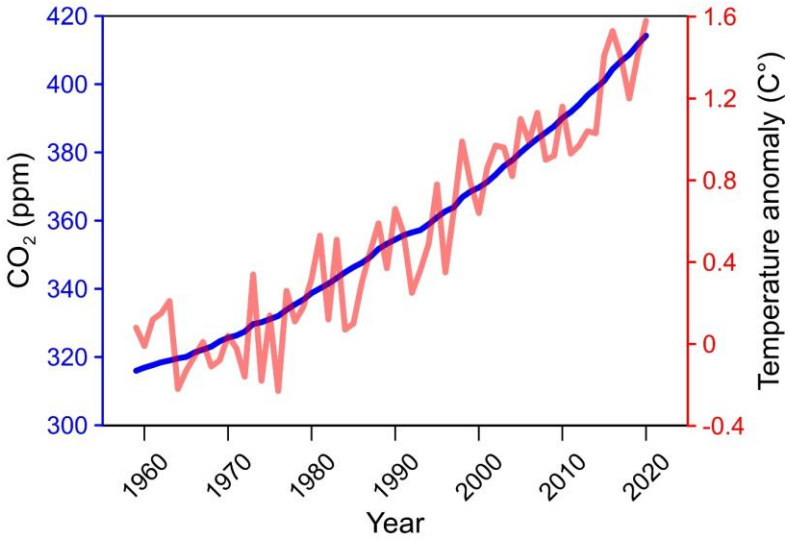

Figure 1. Global annual mean atmospheric carbon dioxide concentration (blue line) and global surface temperature anomalies (red line). CO_2 were taken from Tans & Keeling (2020) and temperature anomalies from the NOAA National Centers for Environmental information server website. The global temperature anomalies are calculated with respect to the 20th century average.

In the seawater, carbon dioxide can be found in dissolved forms as free carbon dioxide (CO_2 aq), bicarbonate (HCO_3^-) and carbonate ion (CO_3^{2-}, Zeebe and Wolf-Gladrow, 2001). Although marine phytoplankton (= unicellular algae) comprise less than 1 % of the total photosynthetic biomass on Earth, through photosynthesis they convert 50 Gt of dissolved carbon dioxide into organic carbon each year into organic matter associated with global primary productivity (Baumert & Petzoldt, 2008; Field et al., 1998). This organic carbon is then exported from the sea surface to the deep ocean by the biological pump. A part of the organic carbon flux degrades while settling through the water column, while the remaining part upon reaching the seafloor is buried in the sediment. The amount of exported organic carbon mediated by the biological pump display distinct tendencies under different climatic conditions and potentially its efficiency of carbon dioxide sequestration is strengthened during glacial periods (Sigman & Boyle, 2000), and thus the biological pump is a crucial component of the marine carbon cycle and global climate.

However, because of the process of biomineralisation, the production of biogenic carbonate by the plankton at the same time counterbalances the efficiency of the biological pump as well as the oceanic capacity of CO_2 uptake (Salter et al., 2014). Marine plankton use carbonate or

bicarbonate dissolved in the seawater to biomineralize calcite or aragonite, and this process releases carbon dioxide into the ambient sea water (Frankignoulle & Canon, 1994). Consequently, the efficiency of the biological pump in sequestering carbon dioxide from the atmosphere depends on the rain ratio between the export production of organic carbon and biogenic carbonate (Salter et al., 2014). At present, it is unclear how the oceanic capacity of carbon dioxide sequestration changes due to global warming, but it could be projected by quantitative characterisation of organic carbon and biogenic carbonate production.

The carbon uptake by photosynthesis has been extensively studied (e. g., Guidi et al., 2016; Young et al., 1991), whereas the export production of biogenic carbonate (calcite or aragonite) remained poorly understood (e. g., Balch et al., 2016). Planktonic foraminifera are fundamental components of the biogenic carbonate export and production. Their shells are made of calcite, and because calcite is less soluble in seawater compared to aragonite (Keir, 1980), biogenic calcite is the primary medium to export biogenic carbonate to the deep sea. The rest of the total carbonate flux is made up by coccoliths, ostracods or calcareous dinoflagellate cysts (Baumann et al., 2004; Milliman, 1993).

The atmospheric carbon dioxide concentration by the end of this century is expected to reach values about 550 ppmv (Smith & Myers, 2018). Considering this increase and the predicted decrease in planktonic foraminifera calcification (Lombard et al., 2010) in response to global warming, understanding the relative contribution of population and individual growth of planktonic foraminifera to the planktonic foraminifera calcite production and flux is essential for more accurate model predictions for the future.

1.2 Planktonic foraminifera: the exporters

Planktonic foraminifera are extremely successful symbiont-bearing heterotrophic protists, which produce calcite shells around their unicellular body. Their shells are made of low-Mg calcite that is well preserved in the sediment. In fact, the fossil record of planktonic foraminifera is one of the most continuous, which allows tracing of species transformation through time and in space (Bicknell et al., 2018; Malmgren et al., 1983), dating processes in the geological past (Wade et al., 2011) as well as conducting paleoenvironmental analysis including climatic studies (Fenton et al., 2016) and oceanography by providing reliable proxies (Kučera, 2007).

Planktonic foraminifera live in the pelagic zone. Upon death or sexual reproduction (gametogenesis), their shells are exported from the sea surface to the deep ocean and the resulting rain of their empty shells create the planktonic foraminifera calcite flux. The planktonic foraminifera calcite flux comprises up to half of the total calcite flux (Schiebel, 2002; Schiebel et al., 2007), although the contribution of planktonic foraminifera to the total calcite flux is variable in space and time. For example, a recent work in the Sargasso Sea (North Atlantic Ocean) show that their contribution ranged between 10 and 40 % (Salmon et al., 2015), and from 30 to 50 % in the Southern Ocean (Rigual Hernández et al., 2020; Salter et al., 2014). In the Indian Ocean, planktonic foraminifera comprised between 10 and 20 % of the total calcite flux (Rembauville et al., 2016). Yet, factors controlling this notable variability remained poorly constrained. The variability in the planktonic foraminifera calcite flux could be potentially caused by three mechanisms (Fig. 2):

1. **Shell flux**

   The shell flux is created by empty Foraminifera shells settling through the water column. It varies both spatially and temporally. For example, in the Sargasso Sea and in the Madeira Basin, the total planktonic foraminifera shell flux varies by almost two orders of magnitude (Deuser et al., 1981; Storz et al., 2009). Among a suite of factors influencing the total shell flux variability, sea-surface temperature (Žarić et al., 2005) and food availability (Bijma, W. et al., 1990) appear to be dominant. However, distinct species display different seasonal cycles due to their environmental preferences, in which clearly identifiable peak fluxes can be determined (Jonkers & Kučera, 2015). In addition, we distinguish 47 morphospecies of modern planktonic foraminifera that have different ecological optima with respect to environmental factors. Since the total planktonic foraminifera shell flux is the sum of individual species shell fluxes, thus it needs to be assessed from a species-specific perspective. Up today, several notable studies characterized the shell flux of planktonic foraminifera species (Jonkers & Kučera, 2015; Žarić et al., 2005), but they did not assess the contribution of variability in planktonic foraminifera shell flux to the planktonic foraminifera calcite flux.

2. Shell mass (calcification intensity)

The mass of planktonic foraminifera shells is the product of their size and calcification intensity (Fig. 2). Both parameters vary considerably between and within species (Malmgren & Kennett, 1976; Peeters et al., 1999; Rillo et al., 2020; Schmidt et al., 2004; Weinkauf et al., 2016). The mean shell size of planktonic foraminifera displays an increasing trend from the polar waters towards the tropical regions (Schmidt et al., 2004). This tendency leads to a general assumption that shell size is related to sea-surface temperature. However, most of the existing studies investigated the interspecific shell size (e. g., Malmgren & Kennett, 1976; Schmidt et al., 2004) difference instead of the intraspecific. Therefore, little is known about the contribution of intraspecific size variability to the planktonic foraminifera calcite flux. The existing studies show that the shell size within the species varies intra-annually by a factor 1.9 and 3.8 (Storz et al., 2009; Weinkauf et al., 2016) and hence the planktonic foraminifera calcite flux could be modulated by the intra-and interannual shell size variability.

Similarly, to shell size, the shell wall thickness is also not constant between and within the species (Henehan et al., 2017; Moller et al., 2013; Weinkauf et al., 2016). The species shell wall thickness provides information about their calcification intensity, which could be calculated based on the relationship of shell weight and shell size. In this way, we can calculate the amount of calcite precipitated in relation to size (Beer et al., 2010). Environmental parameters controlling the shell wall thickness (= calcification intensity) are challenging to quantify but are tough to be related to carbonate ion concentration in the ambient seawater (Barker & Elderfield, 2002; Marshall et al., 2013) or temperature and optimal growth condition (Beer et al., 2010; Qin et al., 2020; Weinkauf et al., 2016).

3. Species composition

In assemblages, where shell mass differs among the species, the species composition of the exported community is an important aspect potentially determining the resulting calcite flux (Fig. 2). There are species which are heavily calcified, and their contribution can intensify the planktonic foraminifera calcite flux (Salmon et al., 2015). These species are mainly deeper dwellers that often bear a crust, which constitute the majority of their

shell mass. The species composition of modern planktonic foraminifera assemblages appears to be driven by temperature, since the assemblage composition is well-predictable by sea-surface temperature, which creates the basis for transfer functions (Ortiz & Mix, 1997; Salgueiro et al., 2008). In the fossil record, planktonic foraminifera are one of the most important paleothermometers used in paleoceanographic studies containing past sea-surface temperature (Incarbona et al., 2019; Kučera et al., 2005).

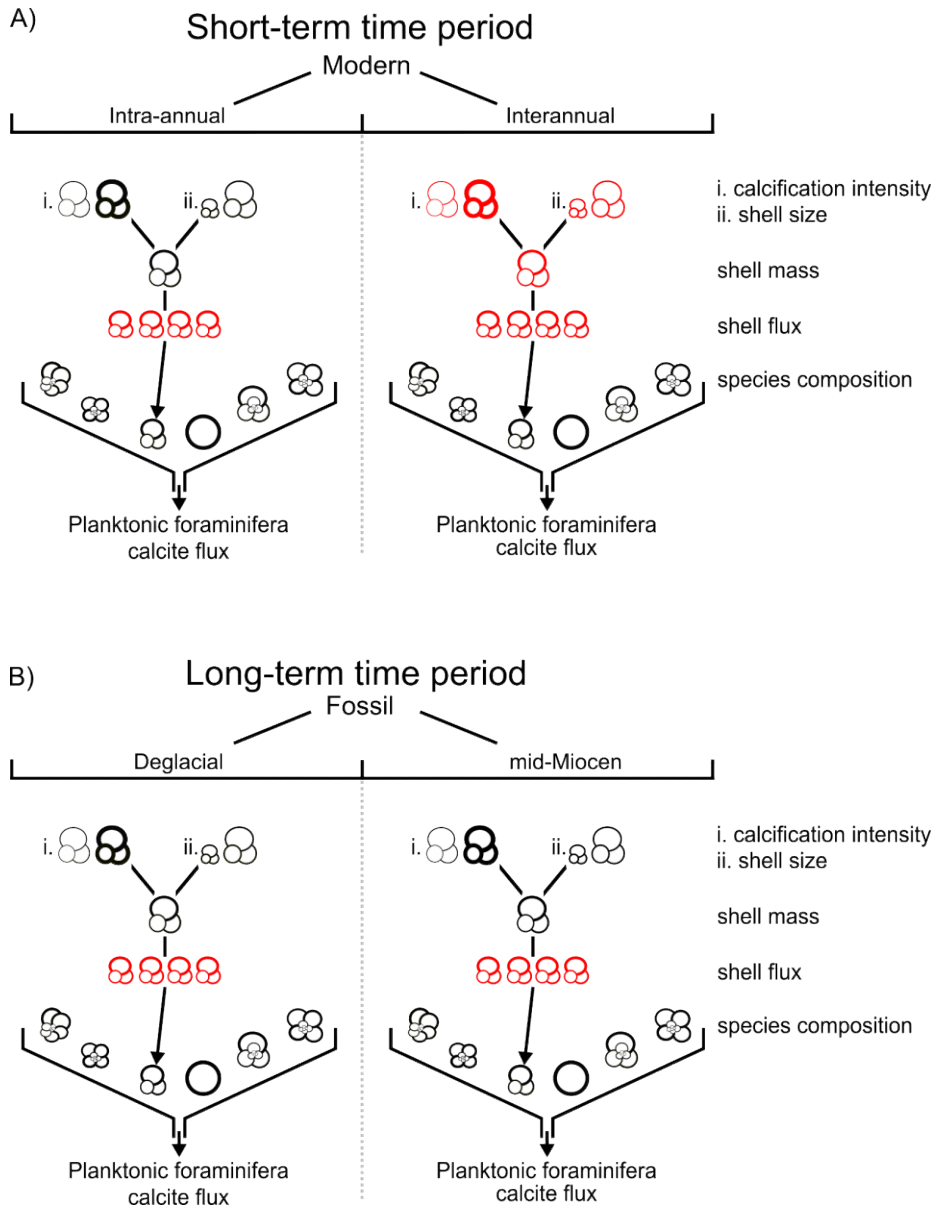

Figure 2. Schematic view of the mechanisms determining the planktonic foraminifera calcite flux of (A): modern assemblages on short-term and (B): fossil assemblages on long-term timescales. The most important mechanism(s) shaping the variability in the planktonic foraminifera calcite during the different time-periods (modern, deglacial and mid-Miocene) is highlighted with red colour. In general, the planktonic foraminifera calcite flux is the sum of the individual species calcite fluxes, which is the product of shell flux and shell mass, which in turn is a function of shell size and calcification intensity. On the intra-annual timescales, shell flux is the most important predictor of variability in the planktonic foraminifera calcite flux, whereas multiple mechanisms act in concert to shape the variability on the interannual timescales, where shell mass is as important as shell flux. On the long-term timescales, shell flux is the most relevant mechanism.

2. Thesis objectives and outline

The planktonic foraminifera calcite flux could be modulated by shell flux, reflecting changes in the population growth and shell mass (shell size and calcification intensity), indicating changes in the individual growth (Fig. 2). Up today, it has not been investigated how these aspects comprehensively shape the variability in the planktonic foraminifera calcite flux. There is a high chance, that these mechanisms act in concert to shape the variability of the planktonic foraminifera, but we do not know their relative contribution. Based on first impression, shell flux appears as the most important mechanisms modulating the planktonic foraminifera calcite flux, since higher shell flux means that more calcite is being exported and low shell flux indicates the export of less calcite. However, this simple relationship between shell flux and calcite flux can be quickly disturbed, since individuals with larger and/or more heavily calcified shells export more calcite (Salmon et al., 2015). Therefore, disentangling the relative contribution of shell flux, shell size, and calcification intensity in the individual species and predicting the way in which these mechanisms modulate the planktonic foraminifera calcite flux on different timescales form the major goal of this dissertation. At first, the partitioning of these mechanisms in modulating the spatial and temporal variability in the planktonic foraminifera calcite flux on the intra-annual (seasonal) timescale was aimed to understand. The two-time series yielded slightly different sea-surface temperature and atmospheric carbon dioxide concentration and by comparing the intra-annual observations the timescale was extended to interannual (between the years) and the way how the intra-annual variability in the modulating mechanisms translated into interannual was observed. Since different mechanisms shape the variability in the planktonic foraminifera calcite flux on the intra-and interannual timescales, in the next step, the relative contribution of the mechanisms in response to major climate transitions was documented. In addition, this approach provided an opportunity to find the mechanisms responsible for regulating the long-term variability (centennial to millennial) in the planktonic foraminifera calcite flux. By focusing on the period of the last deglaciation, when changes in land and sea-surface temperature, atmospheric and oceanic carbon dioxide concentrations and ocean carbonate chemistry far exceed the modern intra-and interannual magnitude, the variable contribution of shell flux, shell size and calcification intensity to the total planktonic foraminifera calcite flux under large-scale environmental changes was investigated.

While shell flux, shell size, and calcification intensity act together, their relative contribution likely varies both spatially and temporally. Certainly, some modifications in the planktonic foraminifera calcite flux emerge from dissolution of foraminifera shells while settling through the water column (Schiebel et al., 2007), but in this thesis the mechanisms controlling the export flux of foraminifera shells from the surface ocean was analysed. Thus, a species resolved shell flux, shell size and calcification intensity data of individual species was generated by using samples obtained by sediment trap time series, sedimentary time series and sediment samples. The sedimentary time series provided and excellent opportunity to gain a process-level understanding of the changes in the planktonic foraminifera calcite flux both on intra-and interannual timescales as well as regionally. The sedimentary time series was selected to extend our investigation beyond the interannual timescale, and to disentangle the effects of temperature and carbonate chemistry on the planktonic foraminifera calcite flux and its modulating mechanisms during the last deglaciation. Since shell mass (shell size and calcification intensity) surprisingly did not show large variability during the last deglaciation, the changes in the calcification aspects on geologically relevant timescales, from mid-Miocene sediments, of the selected species was observed. By comparing the mid-Miocene inferences with the outcomes of the sediment trap time series, the long-term changes in the calcification aspects under different climatic conditions was evaluated, which enabled to rank the regulating mechanism based on their efficiency and accuracy in predicting changes in the planktonic foraminifera calcite flux on different timescales.

This work is cumulative thesis consisting of three individual chapters. Manuscript of Chapter 1 is under consideration for publication in the journal *Global Biogeochemical Cycles*, Chapter 2 and 3 are in the preparation for submission.

The manuscript in Chapter 1 aims to understand the relative contribution of variability in shell flux, shell size, and calcification intensity in the individual species to the total planktonic foraminifera calcite flux on intra-and interannual timescales. For this issue, moored sediment trap time series 1990-1991 (Cape Blanc-3) and time series 2007-2008 (Cape Blanc-18) from the Northeastern Atlantic Ocean were investigated, which enabled to assess the partitioning of the mechanisms (shell flux, shell size, and calcification intensity) on intra-annual time scale as well as to observe how the intra-annual variability translates to inter-annual. Subsequently, the

locally observed variability in shell flux and shell size were put into a global context, thus indicating that the insights from Cape Blanc time series can be extrapolated to the special domain. Chapter 1 thus guides to set research priorities of which aspects of the planktonic foraminifera calcite flux should be parameterized in models predicting foraminifera calcite flux on the intra-and interannual timescales.

In Chapter 2, the magnitude and the relative contribution of shell flux, shell size, and calcification intensity of the planktonic foraminifera calcite flux in response to large amplitude environmental changes during the last deglaciation was assessed. Specifically, four periods were investigated: i) Last Glacial Maximum, ii) Heinrich Stadial I., iii) Younger Dryas and iv) Holocene, which covers the last ~22.000 years. This time span is characterized by major changes in land and sea-surface temperature, atmospheric and oceanic carbon dioxide concentration, and ocean carbonate chemistry that far exceed the magnitude of modern intra-and interannual changes. As such it provides an excellent opportunity to test the inferences obtained by analysing modern processes using sediment trap time series in Chapter 1. To investigate the outlined approach of Chapter 2, a gravity core GeoB3104-1 (Behling et al., 2000) from the western tropical Atlantic was selected and the importance of most the influential mechanisms (shell flux, shell size and calcification intensity) for modulating the long-term variability in the planktonic foraminifera calcite flux under different environmental forcing was quantified.

The last manuscript in Chapter 3 is dealing with the calcification aspects (shell size, shell wall thickness and calcification intensity) of *Globigerina bulloides* under different climatic conditions. As the outcomes of Chapter 1 and Chapter 2 indicate, shell mass is the least variable component of the planktonic foraminifera calcite flux. In order to observe if the long-term evolution under different environmental conditions could culminate into prominent differences in the calcification aspects that could change our final interpretations on geologically relevant timescales, the calcification aspects of mid-Miocene specimens with their modern representatives was compared. In this chapter, mid-Miocene sediment samples collected at Devínska Nová Ves locality was used from the Vienna basin (Slovakia), which specimens archived calcification under climatic setting immediately postdating the Miocene Climatic Optimum with high carbon dioxide content. This data was compared with the calcification aspects of specimens obtained from the Cape Blanc time series (Chapter 1), when specimens

calcified under lower dissolved inorganic carbon concentration. In this way, the long-term changes in shell size and calcification intensity of *Globigerina bulloides* in response to different climatic conditions was observed.

2.1 Appendix chapters

One of the reasons for differences in calcification intensity among species is the shell architecture. This is why I append two additional manuscripts to this thesis, showing results of work on the reconstruction of planktonic foraminifera shell architecture using X-ray tomography.

Appendix chapter 1 represents a reconstruction of ontogenetic trajectory of planktonic foraminifera species *Orbulina suturalis* from mid-Miocene sediments of the Central Paratethys Sea. Despite the investigated species being important biostratigraphic and paleoecological tools, its ontogeny is poorly understood. Here we use a specimen acquired from a bulk sample from Modrany-1 borehole (Slovakia) and by using X-ray computed tomography we revealed the species internal shell morphology. The study provides morphological description of each ontogenetic stage, which aim to help future taxonomic works in the identification of pre-adult forms of *Orbulina suturalis*. This study has been published in the journal *Acta Geologica Slovaca*.

Appendix chapter 2 aims to understand the mechanisms that induced the evolution of the spherical chamber in two mid-Miocene evolutionary lineages of planktonic foraminifera. The evolutionary lineage leading to the emergence of *Orbulina* is a textbook example of a complex character, whose morphological transition has been documented by a series of intermediate forms. In parallel with the *Orbulina* lineage, a convergent evolutionary transition is documented in the Central Paratethys Sea, leading to the appearance of the enigmatic lineage of *Velapertina*. Since the species external morphology is spectacularly similar, we use computed tomography in order to reveal their internal shell architecture and to reconstruct their ontogenetic trajectories to resolve the species relatedness. This manuscript has been submitted for publication in the journal *Paleobiology*.

3. Material

The influence of shell flux, shell size, and calcification intensity on the individual species and the total planktonic foraminifera calcite flux on short-term (seasonal or intra-annual) timescales can be the best studied by using seasonally resolved sediment trap time series. To investigate how the intra-annual variability in the mechanisms shaping the planktonic foraminifera calcite flux translates to interannual, thus continuous time series of at least two years captured by sediment traps is required. This is needed to understand the mechanisms determining the variability at first on the intra-annual timescales, which can be afterwards compared between the two-time series. On decadal timescales, long-term sediment trap time series are needed, and to disentangle the different contribution of shell flux, shell size, and calcification intensity on geologically relevant timescales (centennial to millennial), comprehensive analyses of sedimentary time series of planktonic foraminifera communities are required. In this thesis, I combine the outcomes derived from sediment trap time series and compare the observations with sedimentary time series in order to bring novel insights into the mechanisms shaping the short-term (from intra-annual to inter-annual) and the long-term (from centennial to millennial) contribution of shell flux, shell size, and calcification intensity to the planktonic foraminifera calcite flux.

To calculate the individual species calcification intensity, the shell-weighing method was applied. This approach requires exceptionally well-preserved foraminifera shells. Unlike the foraminifera shells from sediment traps, fossil material, extracted from the sediment could be affected by dissolution and/or filling or partial filling of the shells by sediment, in both cases producing biased results with calcification intensity being either lower or higher than in reality. This fact often limits the applicability of this method only for young (= pre-Quaternary) material. However, the planktonic foraminifera preservation was precisely the reason for selecting the studied areas for Chapter 2 and Chapter 3. I looked for locations, where the foraminifera shell preservation was unusually good from shallow setting and not affected by dissolution. Before the shell-weighing method was used, the preservation of foraminifera shells in each sample was carefully assessed. In case when some foraminifera shells displayed infill or signs of dissolution, they were considered as not suitable for the shell-weighing method and

they were separated from the unfilled and empty shells. In this way I could ensure that the weighed masses reflect the shell weight without any contribution of lithogenic infill.

3.1 Sediment trap time series

For the purpose of analysing the relative contribution of mechanisms modulating the variability in the planktonic foraminifera calcite flux on the intra-and interannual timescales, samples collected by sediment trap moorings from sediment trap mooring array off Cape Blanc (Atlantic Ocean, Fig. 3) were used. This time series is among the longest in the World. It serves as an excellent source of samples to characterise the particle flux variability in the upwelling system off Mauritania (Northwest Africa) since 1988 (Fischer et al., 1996; 2016; 2019). This subtropical region provides life habitat for a diverse assemblage of planktonic foraminifera, displaying high intra-and interannual flux variability on individual species and population levels, which is due to the seasonal upwellings (Romero et al., 2020; Žarić et al., 2006). In fact, the seasonal upwellings cause unusually large seasonal range in temperature and productivity and hence also in the foraminifera shell fluxes (Fischer et al., 2016), which was among the main reasons why this site was selected. From the Cape Blanc time series, 1990-1991 (CB-3, 730 m below the ocean surface) and 2007-2008 (CB-18, 1222 m below the ocean surface) were chosen based in part on the availability of pristine material. The foraminifera samples from the selected time series have been stored at the Bremen University/MARUM.

3.2 Quaternary sedimentary time series

For characterising the mechanisms controlling the variability in the planktonic foraminifera calcite flux beyond the intra-and interannual timescales and to assess the response of shell flux, shell size, and calcification intensity on large amplitude environmental changes across the last deglaciation, a well-dated sedimentary time series from the tropical Atlantic (Fig. 3) was used. The selected core is a 5 m long gravity core (GeoB3104-1) that covers the last 45.000 years (Arz et al., 1998b), which has thanks to its high sedimentation rates (~13 cm kyr^{-1}) thick deglacial layers. The GeoB3104-1 core is stored in the MARUM sediment core repository and has been extensively used for studying environmental changes during the last deglaciation (Arz et al., 1999; Voigt et al., 2017). The shells do not yield sedimentary infill inside their chambers and

thus can be used for the shell-weighing approach. The water depth at this site is relatively shallow (700 m), thus the foraminifera shells did not display signs of dissolution.

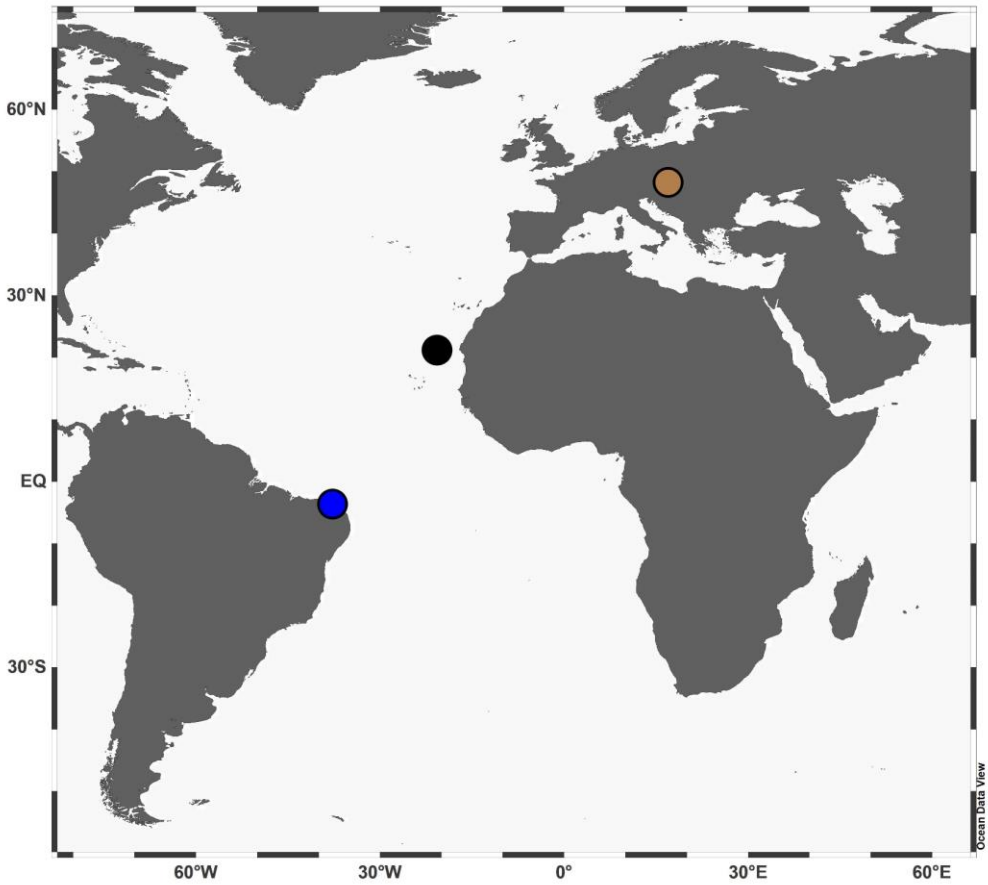

Figure 3. Position of sediment trap mooring off Cape Blanc (black filled symbol), Quaternary sedimentary time series GeoB3104-1 in the tropical Atlantic (blue filled symbol) and Miocene sediment samples from Devínska Nová Ves profile (brown filled symbol), plotted with Ocean Data View v. 5.2.0 (Schlitzer, 2019).

3.3 Miocene sediment samples

In order to observe the different calcification aspects (shell size, shell wall thickness and calcification intensity) of planktonic foraminifera under different climatic conditions, sediment samples from the mid-Miocene were used. The selected site is situated in the Vienna Basin (Slovakia, Fig. 3), where a 15 m long Devínska Nová Ves (DNV) outcrop could be found. The DNV profile covers the time period between 13.6 – 12.7 Ma years and is one of the most well-studied and most completely preserved outcrop from the mid-Miocene of the Vienna Basin (Doláková et al., 2020; Zlinská et al., 2013). This site exhibits extraordinarily well-preserved

planktonic foraminifera, which species composition is dominated (more than 90 %) by *Globigerina bulloides* (Kováčová & Hudáčková, 2009). Their shells are empty and therefore suitable the interpreting the calcification intensity by using their mean shell weight and size.

4. Methods

The applied methods of each chapter involved shell size and shell weight measurements of planktonic foraminifera specimens picked from different aliquots obtained by sediment trap time series (Chapter 1), sedimentary time series (Chapter 2) and sediment samples (Chapter 3). The applied methodological steps in each chapter followed the same sequence (Fig 4). At first, all planktonic foraminifera shells were picked and on species level identified, and specimens counts using a Zeiss Stemi 2000 binocular microscope from size fractions > 150 µm, except for the DNV samples, where the fraction > 125 µm was used, were generated. The taxonomical identification of modern planktonic foraminifera is based on the taxonomic concept of Schiebel & Hemleben (2017) as amended by Spezzaferri et al. (2015) and Morard et al. (2019). Following Spezzaferri et al. (2015), specimens of *Trilobatus sacculifer* with and without the terminal sac-shaped chamber were grouped into one category. The species identification from the mid-Miocene samples follows the taxonomic concepts of Kennett & Srinivasan (1983). After the species identification, specimens obtained from the sedimentary time series (Chapter 2) and from sediment samples (Chapter 3) were divided into unfilled and filled groups, where the unfilled category indicate their suitability for the shell-weighing method (Fig. 5).

3.4.1 Shell size measurements

The shell size measurements of the individuals were conducted by using a digital Keyence VHX-S650E microscope and its in-built Keyence 3D Shape Measurement Software v. 1.00 at the institution MARUM (Fig. 4). The filled and unfilled shells of each taxonomic category were placed with their aperture facing upwards on custom-made micropaleontological slides with blue background. These micropaleontological slides with flat background are required for this approach, since the slicing of the digital elevation model of the scanned slide surface using the classical micropaleontological slides failed in the segmentation of the foraminifera shells. The arranged foraminifera shells were photographed under 200-300x magnification, yielding a resolution of 1.0086-1.4663 µm per pixel. The foraminifera shell size in the snaped images was automatically determined and measured by the Keyence Software based on a digital elevation model of the scanned slide surface at 5 µm resolution, as well as by the combination of elevation information with colour images of the surface of the slide. The successfully segmented foraminifera shells are than characterized with a suite morphometric parameters such as the

surface area, maximum size, minimum size, and perimeter. This methodological approach enabled me to compile a tremendous data set involving in total 31 922 individual measurements.

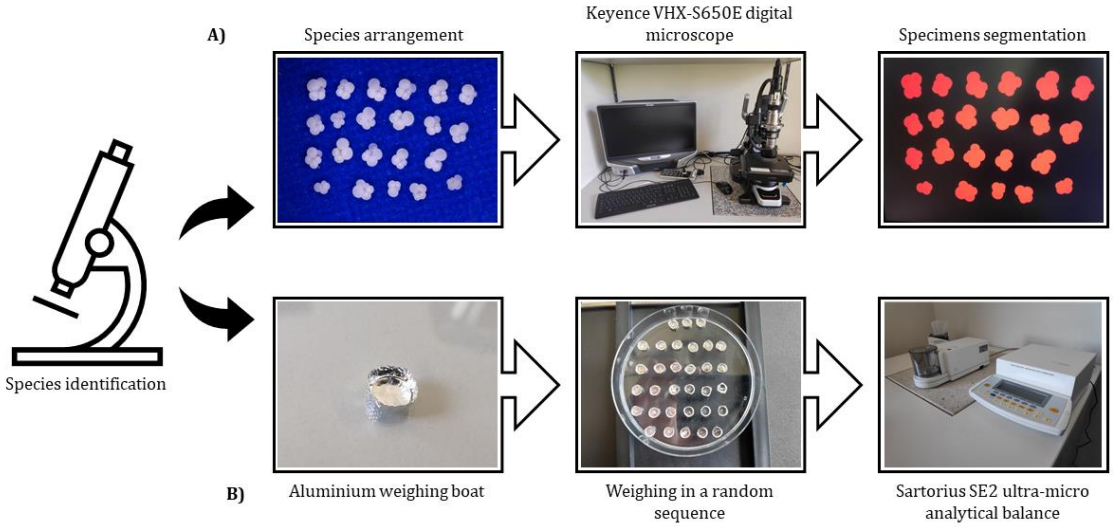

Figure 4. Schematic illustration of the (A): shell size and (B): shell weighing methodological approaches used in this thesis. Own visualisation.

3.4.2 Shell weighing

After the shell size measurements, the weighing of the specimens was conducted. Specimens from > 150 µm size fractions belonging to the same species were weighed together, while shells in the 63-150 size fraction were weighed together, without distinguishing them on species level. Foraminifera shell obtained by the Cape Blanc sediment trap moorings are empty and their shells are translucent and suitable for the shell-weighing approach. Foraminifera shells from the Quaternary sedimentary time series (GeoB3104-1) and Miocene sediment samples (Devínska Nová Ves site) were separated based on the shells preservation into unfilled and filled categories (Fig. 5). For the shell-weighing approach we used only the unfilled category. In this way we could ensure that weighed masses reflect the shell weight without any contribution of lithogenic infill.

The planktonic foraminifera were placed in three-times, pre-weighted, aluminium weighing boats (Fig. 4). The samples were than left for 24 hours in the MARUM weighing laboratory to

acclimate with the room moisture. The weighing boats with the foraminifera were weighed with a Sartorius SE2 ultra-micro analytical balance with a nominal resolution of 0.1 µg (Fig. 4). The weighing was done in a random sequence, each sample five-times (Weinkauf et al., 2016), in order to decrease the weighing bias caused by the analytical balance. The obtained weights were used to calculate the average weight of the specimens in each sample, which was further used to calculate their calcification intensity based on their shell weight and size ratio (see Beer et al., 2010). A step-by-step methodological description of shell size and weight determination is given in each chapter within the Material and Methods section.

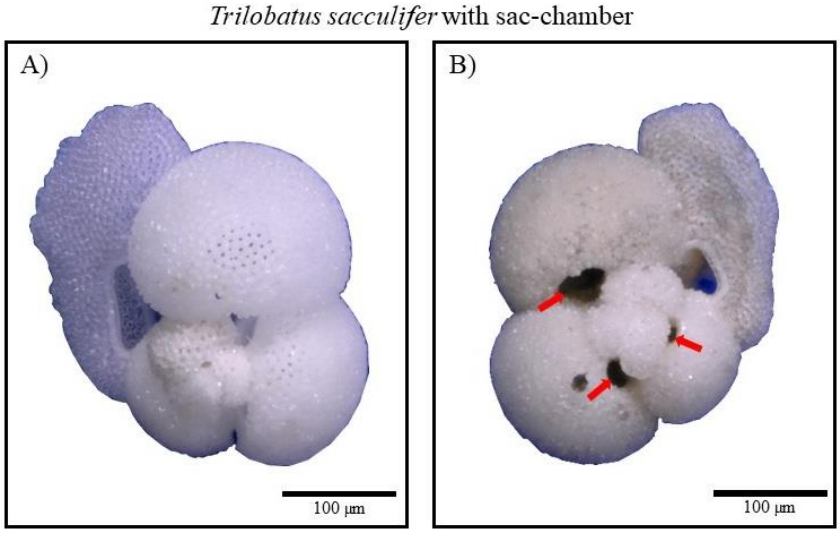

Figure 5. Example of specimens *Trilobatus sacculifer* with sac-chamber categorized prior to shell weighing as (A): unfilled and (B): filled shells. The shell of specimen (A) is empty and translucent. This specimen shows no signs of sedimentary infill that could be determined through the apertures and pores, as well as displays no signs of dissolution. Unlike specimen (B), which is not well-preserved and not translucent. Along the periphery of the apertures and inside in chamber (areas indicated by red coloured arrows), lithogenic infill could be determined. For the shell-weighing method only the unfilled category was used. The separation of unfilled (A) and filled (B) shells from each other ensured that the weighed masses reflect the actual shell weight of the specimens without any contribution of lithogenic infill. Both images were captured by using the digital Keyence VHX-S650E microscope.

Chapter 1

Determinants of Planktonic Foraminifera Calcite Flux: Implications for the Prediction of Intra-and Interannual Pelagic Carbonate Budgets

This work is under consideration for publication in the journal *Global Biogeochemical Cycles*.

P. Kiss[1,2*], L. Jonkers[2], N. Hudáčková[1], R. T. Reuter[3], B. Donner[2], G. Fischer[3] and M. Kučera[2]

[1]Department of Geology and Paleontology, Comenius University in Bratislava, Bratislava, Slovakia.

[2]MARUM - Center for Marine Environmental Sciences, University of Bremen, Bremen, Germany.

[3]Geosciences Department, University of Bremen, Bremen, Germany.

*Corresponding author: Peter Kiss (pkiss@marum.de)

Data availability: data generated in this study will be available on the public repository PANGAEA Data Publisher.

Abstract

Planktonic foraminifera precipitate calcite shells, which after the death of the organisms are exported to the seafloor. Globally, the resulting calcite flux constitutes up to half of the pelagic calcite flux. Given their importance for the marine calcite budget and for the carbonate counter pump, which counteracts the biological pump in terms of oceanic capacity for CO_2 uptake, it is crucial to understand the mechanisms regulating the planktonic foraminifera calcite flux. In principle, variability in individual species calcite flux could be caused by changes in i) shell flux, ii) shell size and iii) calcification intensity. Where size and calcification intensity differ among species, variations can be caused by changes in species composition. To assess the importance of these factors in regulating the planktonic foraminifera calcite flux, we investigated two sediment trap time series from the Cape Blanc upwelling area. On intra-annual timescales, 82 % of the variability in the calcite flux can be explained by shell flux alone. Since the intra-annual flux variability at the study site covers the global range of mean annual shell fluxes, our results indicate that a global prediction of steady-state planktonic foraminifera calcite flux can be predicted by shell flux variability in combination with species-specific average shell mass. However, our results show that on interannual timescales, shell mass variability can be as important as shell flux variability. Therefore, this implies that in order to predict temporal changes in the planktonic foraminifera calcite flux variability in shell size and calcification intensity also require considered.

1. Introduction

Pelagic carbonate production is an important element of the global carbon cycle. Through biomineralization of either calcite or aragonite, marine plankton binds large amounts of dissolved inorganic carbon in their shells, which are then exported from the productive zone (Milliman, 1993). A large part of the aragonite flux, which consists exclusively of pteropods (Buitenhuis et al., 2019; Fabry, 1989; Singh & Conan, 2008), is dissolved before being buried in the sediment (Berner & Honjo, 1981). However, calcite (especially low-magnesium calcite in planktonic foraminifera shells) is less prone to dissolution (Keir, 1980), making the burial of biogenic calcite the main mechanism to transfer carbon from the rapidly cycling ocean-atmosphere-biosphere to the slow geological reservoir (Archer, 1996; Catubig et al., 1998). In addition, biogenic carbonate production has an opposing fast effect on the carbon cycle, as well

as the marine biological carbon pump. By consuming alkalinity, it induces degassing of carbon dioxide and thus acts as a "counter pump" in the process of biological carbon sequestration in the ocean (Frankignoulle & Canon, 1994). Planktonic foraminifera shells are a key component of marine biogenic calcite production and flux. Upon death of these organisms, their shells begin to settle through the water column, and the resulting export flux is estimated to constitute up to half of the global calcite flux (Schiebel, 2002; Schiebel et al., 2007). The rest of the pelagic calcite flux is dominated by coccoliths (Baumann et al., 2004; Milliman, 1993). However, in order to quantify the pelagic calcite budget, planktonic foraminifera cannot be ignored. The planktonic foraminifera shell flux is a variable in both space and time (Jonkers & Kučera, 2015; Žarić et al., 2005), yet the factors controlling the shell flux variability are not completely constrained and understood. Furthermore, the subject concerning how shell flux variability relates to mass flux variability has not been explicitly studied before. In theory, variability in the planktonic foraminifera calcite flux could arise from changes in the shell flux and thus reflect population growth and/or changes in the shell mass, which consequently reflect individual growth. Shell mass is in turn determined by shell size and calcification intensity, i.e. the mass of calcite precipitated per unit size. At the species level, calcite flux is the product of shell flux, size, and calcification intensity, and the total planktonic foraminifera calcite flux therefore becomes the sum of the mass fluxes of the individual species (Figure 1). The effect of shell flux on calcite flux is intuitive: more shells equal more calcite. However, this simple relationship can be modulated by changes in the size and/or calcification intensity, since larger or thicker shells will export more calcite to the seafloor. Indeed, low numbers of heavily calcified shells can have a disproportionately large effect on the overall planktonic foraminifera calcite flux (Salmon et al., 2015). To date, the shell flux of planktonic foraminifera has been relatively well-studied and shown to vary by several orders of magnitude seasonally and regionally (Deuser, 1986; Deuser et al., 1981; Jonkers & Kučera, 2015; Žarić et al., 2005). Similarly, shell size and calcification intensity vary substantially among and within species (Henehan et al., 2017; Lombard et al., 2010; Malmgren & Kennett, 1976; Moller et al., 2013; Peeters et al., 1999; Schmidt et al., 2004; Weinkauf et al., 2013). Thus, in theory, calcite flux by planktonic foraminifera could be modulated by all of these processes.

At present, the importance of shell flux, size, and calcification intensity for the prediction of planktonic foraminifera calcite flux remains largely unquantified. Most studies have either

analysed time series of shell flux (Deuser, 1986; Jonkers & Kučera, 2015; Kincaid et al., 2000; Žarić et al., 2005) or considered factors affecting size individually (Elderfield et al., 2002; Hecht, 1976; Kahn, 1981; Moller et al., 2013; Schmidt et al., 2004) or calcification intensity (Beer et al., 2010; Henehan et al., 2017; Lombard et al., 2010; Marshall et al., 2013; Moy et al., 2009; Naik et al., 2013; Weinkauf et al., 2013); however, the combined effect of the three factors has never been comprehensively assessed. As a result, it is not clear at present how the planktonic foraminifera calcite flux can be parameterized in models, or whether all of the potential controlling factors (Figure 1) need to be considered in order to derive an accurate planktonic foraminifera calcite budget, including temporal changes therein. For example, if the majority of species produce shells with a similar mean size and weight, then a prediction of shell fluxes can be easily transformed into calcite fluxes. On the other hand, if size and/or calcification intensity vary significantly, then a prediction of calcite flux requires that all three factors are considered. At present, several models for some aspect(s) of the spatio-temporal distribution of planktonic foraminifera exist; however, none of them explicitly predict all three aspects that affect calcite flux (Fraile et al., 2008; Jonkers & Kučera, 2015; Kretschmer et al., 2018; Lombard et al., 2011; Žarić et al., 2006). Considering the results by Salmon et al. (2015), as well as the observed (Jonkers et al., 2019) and anticipated (Kretschmer, 2017; Roy et al., 2015) changes in planktonic foraminifera communities due to global change, it is unclear how the existing models need to be adapted to predict the impact of planktonic foraminifera community change on the resulting calcite flux, and hence evaluate its effect on the global carbon cycle.

In order to resolve this issue, we present the first analysis of the relative contribution of variability in shell flux, shell size, and calcification intensity in individual species to the total calcite flux by the planktonic foraminifera community on intra-annual (seasonal) and interannual timescales. We investigated the planktonic foraminifera calcite flux in two one-year sediment trap time series from the Northeastern Atlantic Ocean and placed the observed variability of shell flux, shell size, and calcification intensity of each species in the context of the resulting calcite flux. In this way, we provide new insight into the mechanisms shaping the planktonic foraminifera calcite flux, as well as identify factors necessary for the prediction of its spatial and temporal variability.

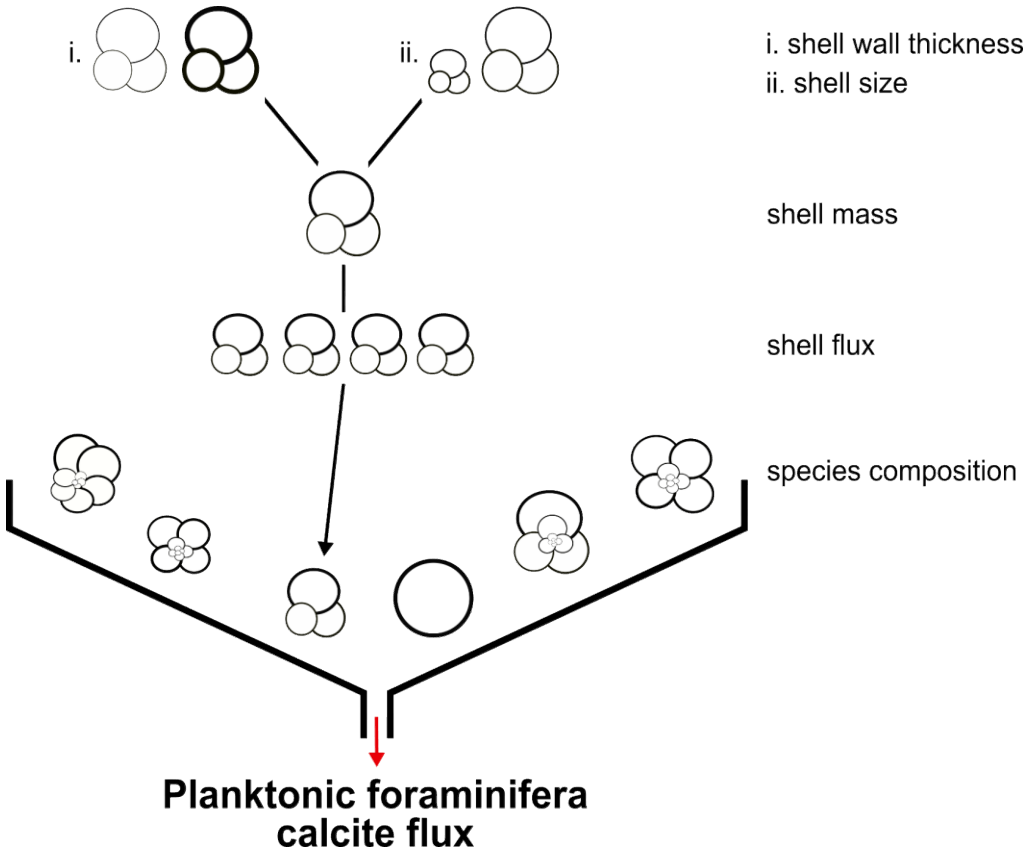

Figure 1. A schematic representation of factors determining the planktonic foraminifera calcite flux at a given point in time and space. The total planktonic foraminifera calcite flux is the result of calcite flux by individual species, which is the product of shell flux and shell mass, which in turn is a function of size and calcification intensity.

2. Materials and Methods

Throughout this manuscript "bulk carbonate flux" refers to the overall flux of carbonate measured with a CHN-Analyzer (Fischer et al., 2016). This bulk carbonate flux consists of both calcite and aragonite. The total calcite flux is the sum of planktonic foraminifera calcite flux (measured here) and coccolithophore calcite flux (not measured here), with a negligible contribution by ostracod or calcareous dinoflagellate cyst calcite fluxes. In this study, we thus calculated the calcite flux by subtracting the aragonite flux from the bulk carbonate flux. The effect of shell flux, size, and calcification intensity on the calcite flux of planktonic foraminifera can be best studied in a seasonally resolved and continuous time series of at least two years from a moored sediment trap. This is necessary for obtaining a first-order estimate of the seasonal variability of calcite flux, as well as to determine how the seasonal variability translates into

interannual variability. Here, we use samples from the long-term sediment trap mooring array off Cape Blanc, localized almost 400 km away from the NW African coast (Figure 2 and 3), which has been used to characterise particle flux variability in the upwelling system off Mauritania for over three decades (Fischer et al., 1996, 2016, 2019). We selected this site because it harbours a diverse assemblage of planktonic foraminifera, exhibiting high-amplitude intra-annual and interannual flux variability (Romero et al., 2020; Žarić et al., 2005). This is because the studied sediment trap is moored in an upwelling region (Figure 2 and 3), causing higher seasonality in many oceanographic parameters, as well as in the foraminifera export flux when compared to other locations at the same latitude. To indicate the productivity and its seasonality, we use the biogenic opal flux (Figure 2), which has been used to characterise productivity at this site (Fischer et al., 2016; Romero et al., 2008).

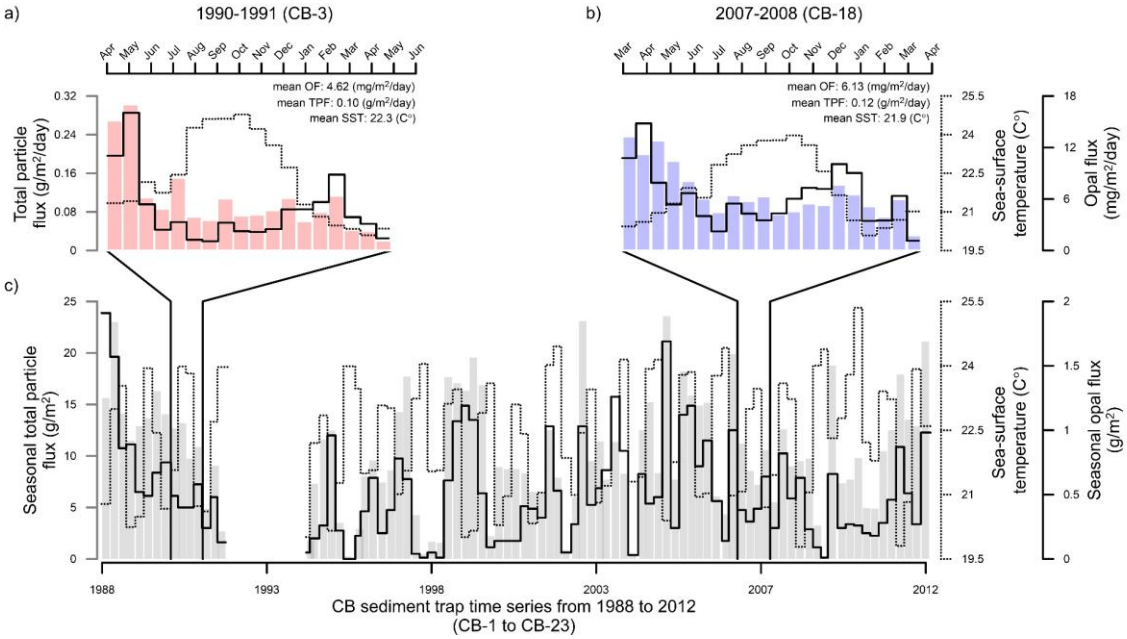

Figure 2. Total particle flux (TPF, coloured bars), opal flux (OF, black line), sea-surface temperature (SST, dotted line) and their seasonality in the upwelling area off Cape Blanc, plotted for (a): time series 1990-1991 (CB-3); time series 2007-2008 (CB-18); (c): from 1988 to the end of 2012 (CB-1 to CB-23). Bulk carbonate flux and opal flux data were taken from Fischer et al. (2016) and the average sea-surface temperature from Reynolds et al. (2007). Annual mean values are indicated where appropriate (a, b). These parameters help place the two analysed time series into a long-term environmental context.

From the 30-year time series, we selected 1990-1991 (CB-3, 730 m below the ocean surface) and 2007-2008 (CB-18, 1222 m below the ocean surface) based in part on the availability of

pristine material. Each of these deployments covered an entire year continuously, with an average sampling resolution of ~ 20 days (Table 1). The two sampled years are far apart and capture the typical amount of interannual foraminifera flux variability at this site (Romero et al., 2020). The traps are located > 3 km above the seafloor and contain no benthic foraminifera, implying there was no or minimal contribution of foraminiferal shells from resuspended sediments. We do not expect a large effect concerning the difference in deployment depth, since planktonic foraminifera sink relatively fast (Takahashi & Bé, 1984). The collection area of the sediment trap increases with deployment depth, and the deeper trap could intercept foraminifera from a larger surface area (Siegel & Deuser, 1997). However, since the traps had the same opening, and were both located below the production depth of planktonic foraminifera, they should be recording the export flux in the same way and there should be no systematic bias towards collecting more specimens in the deeper trap (Figure 3). We can therefore assume that the effect of variable deployment depth is minor compared to interannual variability in the foraminifera flux. There is also no indication of a stable and sharp oceanographic front near the sediment trap that could cause a systematic difference in foraminifera species composition (and hence shell mass) between the two years (Baker et al., 1988; Fischer et al., 2016).

Deployment	Lat [N]	Long [W]	Water depth [m]	Deployment depth [m]	Sampling start [date/time]	Sampling end [date/time]	Number of samples
CB-3 upper	21.1380	-20.6720	4094	730	08-04-1990 11:00:00	30-04-1991 11:00:00	18
CB-18 upper	21.2862	-20.8037	4168	1222	25-03-2007 00:01:00	05-04-2008 00:01:00	20

Table 1. Cape Blanc time series location, water and sampling depth, sampling period and number of collected samples.

The sediment trap sample bottles were poisoned (1 mL HgCl2 per 100 mL filtered seawater) prior to deployment to ensure preservation of the intercepted material. The collection bottles were not buffered, although the high abundance of pteropods in the samples indicates that post-collection dissolution is unlikely to affect the flux estimates. After recovery of the traps, samples were wet sieved over a 1 mm mesh sieve to eliminate the presence of macrozooplankton (swimmers), and the size fraction < 1 mm was used for flux estimates. The residues were then wet-split using a McLane splitter system, and the aliquots were stored at 4 °C and bulk carbonate flux data for both time series were determined (Fischer et al., 2016). A different aliquot was

used to quantify the relative contribution of foraminifera to this flux. These aliquots were sieved through 63 μm and 150 μm mesh sieves. The 63-150 μm fraction was first weighed and then assumed to consist mainly of planktonic foraminifera. In the > 150 μm fraction, planktonic foraminifera and pteropods were separated and the pteropods were weighed; their weight was assumed to represent the total aragonite flux. Since the amount of foraminifera calcite in the fraction < 150 μm is small (see results), the analysis of factors affecting planktonic foraminiferal calcite flux was carried out on shells in the > 150 μm fraction. In this fraction, all shells of planktonic foraminifera were identified to species level, separated, and counted in 1/64 (CB-3) or 1/5 (CB-18) aliquots using a Zeiss Stemi 2000 binocular microscope. Both time series yielded perfectly preserved planktonic foraminifera shells without any signs of dissolution. The identification is based on the taxonomic concept of Schiebel & Hemleben (2017) as amended by Spezzaferri et al. (2015) and Morard et al. (2019). Following Spezzaferri et al. (2015), we grouped specimens of *Trilobatus sacculifer* with and without the terminal sac-shaped chamber into one category. To facilitate comparison with previous work, as well as achieve consistency between the counts from the two years (which had been carried out by different persons), we did not distinguish between *Globigerinoides ruber albus* and *Globigerinoides elongatus*. Furthermore, we decided to lump *Globorotalia menardii* with *Globorotalia ungulata* and *Globigerinella siphonifera* with *Globigerinella calida*. All shells were assigned to one of the resulting 27 taxonomic categories.

Afterwards, shell size was determined using a Keyence VHX-S650E digital microscope. The shells of each species were uniformly oriented with their aperture facing upwards on custom-made micropaleontological slides with a flat surface and blue background and photographed under 200-300x magnification, yielding a resolution of 1.0086-1.4663 μm per pixel. The digital microscope Keyence 3D Shape Measurement Software v. 1.00 allows automated identification of the foraminifera by creating a digital elevation model of the scanned slide surface at 5 μm resolution, as well as by combining the elevation information with colour images of the surface of the slide. The identified objects are characterised by a suite of parameters, among which we selected surface area (μm^2) as the representation of shell size. This parameter is highly correlated with other typically-used size parameters, such as maximum diameter, because it captures differences in shape between objects of similar diameter better, which is important when different species are compared (Brombacher et al., 2018; Moller et al., 2013).

Following size analysis, all specimens from one cup belonging to the same taxonomic category were placed in three-times, pre-weighed, aluminium weighing boats. The samples were then left for 24 hours in the weighing laboratory to acclimate with the room moisture before being weighed with a Sartorius SE2 ultra-micro analytical balance with a nominal resolution of 0.1 µg. The weighing was done in a random sequence, each sample five times, following Weinkauf et al. (2016). Unlike specimens extracted from the sediment, sediment-trap-derived foraminifera shells are translucent and empty; thus, the measured weight reflects only the weight of the shell without a contribution from (sedimentary) infill. The average weight of the specimens in each cup was used to determine the mean weight of the shells of the given species, which was then used to calculate the weight/size ratio for each species in each cup as a representation of its calcification intensity (see Beer et al., 2010).

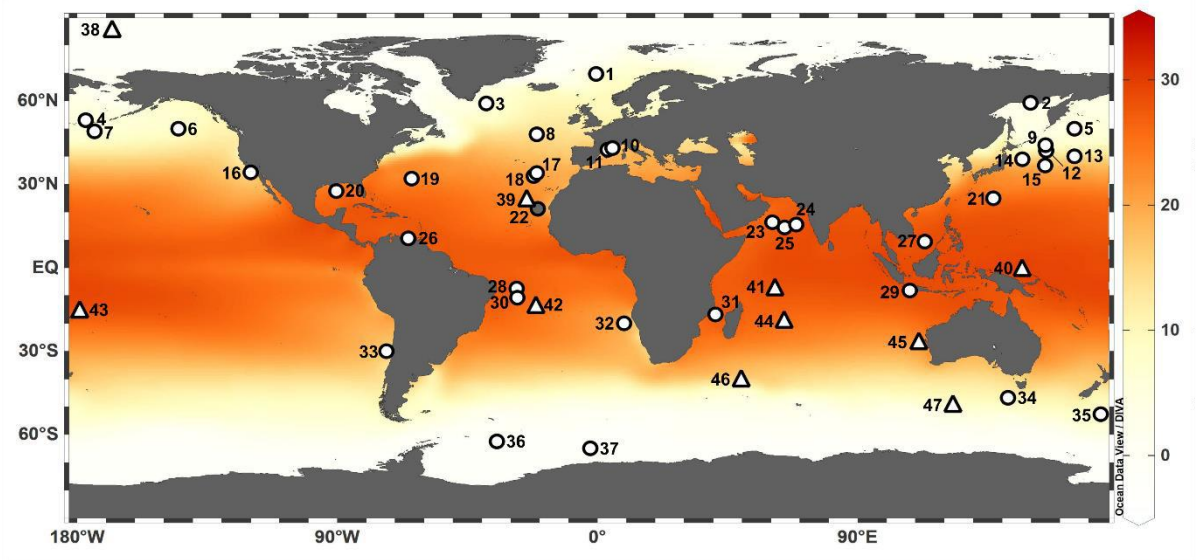

Figure 3. Position of the sediment trap mooring off Cape Blanc (22, filled symbol) used in this study, and the location of other sediment trap time series (open symbols, listed in Table 2) discussed, including the 10 locations of samples used by Rillo et al. (2019) for shell size measurements (open triangles). Background colours show the average annual sea-surface temperature taken from Locarnini et al. (2019) and plotted with Ocean Data View v. 5.2.0 (Schlitzer, 2019).

Site nr.	Lat [N]	Long [E]	Deployment depth [m]	Duration [days]	Size [µm]	References
1	69.7	-0.5	500	780	63–500	Jensen (1998)
2	59.3	149.8	258	365	> 150	Alderman (1996)
3	59.0	-38.5	2750	988	150–315	Jonkers et al. (2010; 2013)
4	53.1	-177.0	3198	2926	> 125	Asahi & Takahashi (2007)
5	50.0	165.0	3260	1141	> 125	Kuroyanagi et al. (2002)
6	50.0	-145.0	3800	1128	> 125	Sautter & Thunell (1989)
7	49.0	-174.0	4812	2803	> 125	Asahi & Takahashi (2007)
8	48.0	-21.0	2000-3700	378	> 150	Wolfteich (1994)
9	44.0	155.0	2957	851	> 125	Kuroyanagi et al. (2002)
10	43.0	5.2	500	3338	> 150	Rigual-Hernández et al. (2012)
11	42.4	3.5	500	3552	> 150	Rigual-Hernández et al. (2012)
12	42.0	155.2	1091	380	> 125	Mohiuddin et al. (2005)
13	40.0	165.0	2986	768	> 125	Kuroyanagi et al. (2002)
14	39.0	147.0	1371-1586	608	> 125	Mohiuddin et al. (2002)
15	36.7	154.9	5034	376	> 125	Mohiuddin et al. (2004)
16	34.3	-120.0	590; 470	1108	> 125	Darling et al. (2003)
17	34.0	-21.0	2000	378	> 150	Wolfteich (1994)
18	33.0	-22.0	3000	764	> 125	Storz et al. (2009)
19	32.1	-64.3	3200	1848	> 125	Deuser & Ross (1989); Deuser et al. (1981)
20	27.5	-90.3	700	1563	> 150	Poore et al. (2013); Reynolds et al. (2013)
21	25.0	137.0	917-1388	573	> 125	Mohiuddin et al. (2002)
22	21.1	-20.7	3500	718	> 150	Fischer et al. (1996); Žarić et al. (2005)
23	16.3	60.5	3020	508	> 125	Curry et al. (1992)
24	15.5	68.8	2790	482	> 125	Curry et al. (1992)
25	14.5	64.8	732	486	> 125	Curry et al. (1992)
26	10.5	-65.5	Not reported	1002	> 125	Tedesco & Thunell (2003)
27	9.4	113.2	720	662	> 154	Wan et al. (2010)
28	-7.5	-28.0	671	500	> 150	Žarić et al. (2005)
29	-8.3	108.0	1370-1860	963	> 150	Mohtadi et al. (2009)
30	-11.6	-28.5	710	944	> 150	Žarić et al. (2005)
31	-16.8	40.8	2250	863	250–315	Fallet et al. (2010; 2011)
32	-20.0	9.2	1648	524	> 150	Žarić et al. (2005)
33	-30.0	-73.0	2300-2500	1563	> 150	Marchant et al. (2004; 1998)
34	-46.8	142.0	3800	464	> 150	King & Howard (2003)
35	-52.6	174.2	442; 362	410	> 150	Northcote & Neil (2005)
36	-62.5	-34.8	863	418	> 125	Donner & Wefer (1994)
37	-64.9	-2.5	360	745	> 125	Donner & Wefer (1994)

Table 2. Sediment trap time series and their location with sampling details (deployment location, depth, sampling duration and size) used in the compilation of annual mean shell fluxes of planktonic foraminifera. Site numbers refer to Figure 3.

To facilitate the visualization and statistical analyses of the log-normally distributed flux data, the data were loge transformed, with zero values substituted by half of the lowest observed positive value of the given variable. Intra-and interannual variability was assessed using the geometric coefficient of variation. For this, we first determined the standard deviation (s) of the log-transformed values of each parameter, weighted by the sampling duration of each cup, and calculated the geometric coefficient of variation as:

$$\widehat{C_v} = \sqrt{e^{s^2} - 1}$$

To place the locally observed species-specific shell flux variability in a global context, we used shell flux data from 37 globally distributed time series (Figure 3 and Table 2) compiled by Jonkers & Kučera (2015). We used the periodic mean estimated using periodic regression of shell fluxes of the analysed species in order to characterise the global range of their mean annual flux variability, and then compared these to the intra-annual shell flux variability observed at Cape Blanc. This comparison is used to assess whether our observations in the time series can be extrapolated to space.

3. Results

The planktonic foraminifera calcite flux in the > 150 µm size fraction varied between a minimum in April, 1990 (0.14 mg/m^2/day) and maximum in April, 1991 (36 mg/m^2/day) and was on average 8.28 mg/m^2/day. Foraminifera calcite made up 2 to 80 (mean 19) % of the total calcite flux (Figure 4a and Table S1). Shells > 150 µm dominated the planktonic foraminifera calcite flux making up 62 to nearly 100 (mean 88) % of the overall foraminifera calcite flux in the size fraction > 63 µm. The low to negligible contribution to the calcite flux by foraminifera between 63 and 150 µm means that it is sufficient to investigate the factors modulating planktonic foraminifera calcite flux in the > 150 µm size fraction. The contribution of the individual planktonic foraminifera species (or taxonomic categories) to the shell and calcite flux varied intra-annually and showed a clear seasonal pattern with different species groups being present in summer and winter (Figure 4b and 4d). The total shell flux varied considerably between the two years, amounting to 834 #/m^2/day in 1990-1991 and being 33 % lower (562 #/m^2/day) in 2007-2008 (Figure 4c). However, the difference in the planktonic foraminifera calcite flux between the two years was smaller (15 %) and converse (7.6 vs. 9.0 mg/m^2/day), reflecting the fact that shells deposited in 2007-2008 were on average larger and more heavily

calcified than in 1990-1991 (Figure 4e and 4f). The mean foraminifera size varied between 31.56 * 10^3 μm^2 in March, 1991 and 187.17 * 10^3 μm^2 in January, 2008 and showed a marked difference between the two years with foraminifera shells being 36 % smaller on average in 1990-1991 than in 2007-2008 (71.23 * 10^3 μm^2 vs 111.85 * 10^3 μm^2; Figure 4e). The size of the individual species also showed large variability (Figure 5 and Table S2), with 15 out of 20 species for which mean size could be determined in both years as being smaller on average, as well as in 1990-1991, indicating that the variability in mean foraminifera shell size is not due to changes in the assemblage composition alone. The calcification intensity showed a smaller difference between the two years, indicating higher average calcification intensity in the 2007-2008 time series (Figure 4f). As for the size variability, differences in calcification intensity also occurred within individual species; however, the pattern was less consistent between the years (12 out of 20 species had higher calcification intensity in 2007-2008; Table S2), indicating that the variability in mean foraminifera calcification intensity reflects changes in the calcification intensity of individual species, as well as in the assemblage composition.

Many species show low shell fluxes, as well as low contributions to the calcite flux so that only ten species are responsible for > 90 % of shell and calcite flux (Figure 6). In the following investigation, we thus restrict our analysis to the factors that determine the planktonic foraminifera calcite flux to those ten species. In order to assess the importance of variability in shell flux, shell size, and calcification intensity on intra-annual timescales, we first compared the coefficient of variation of these parameters to that of the planktonic foraminifera calcite flux. We found that within each time series, shell size and calcification intensity vary quite little, and that only shell flux shows variability that is comparable to that of calcite flux (Figure 5a, b and c). This pattern also appears when the species are analysed individually (Table S3). Since similarity in the amount of variation alone does not necessarily imply predictability, we have determined in the next step how much of the variability in the calcite flux can be explained by each factor individually. We performed this analysis at species level, as well as for all foraminifera together. These analyses reveal that on intra-annual timescales, shell flux is consistently the best predictor of calcite flux; both for the total planktonic foraminifera flux and for the individual species (Figure 7 and 8, Table S3). In contrast, when interannual variability is assessed, variability in all four parameters is lower, and a markedly different picture emerges with regard to the partitioning of variance among the three factors. Shell flux still shows

variability that is comparable to the calcite flux; however, on the interannual timescales, shell size and calcification intensity show comparable variability (Figure 5d), and when all foraminifera are considered together, shell size variability even exceeds shell flux variability.

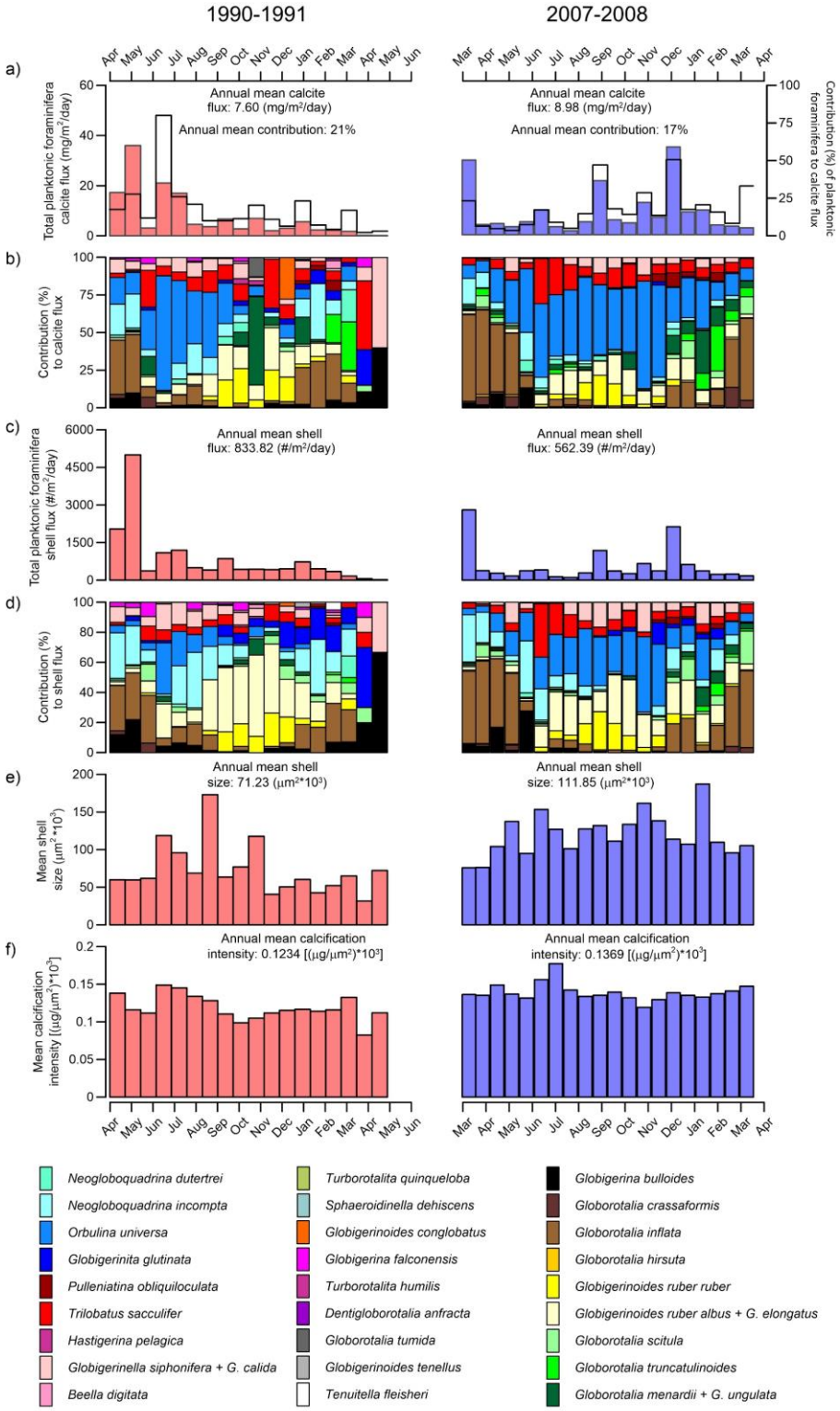

Figure 4. The Cape Blanc planktonic foraminifera time series. (a): total planktonic foraminifera calcite flux (coloured bars) with the relative contribution of planktonic foraminifera to calcite flux (black line); (b): contribution of the individual species to the total planktonic foraminifera calcite flux; (c): total planktonic foraminifera shell flux; (d): contribution of the individual species to the total shell flux; (e): mean shell size and (f): mean calcification intensity. Colours in (a, c, e) and (f) denote different years and in (b) and (d) the individual species, which are always shown in the same order, species legend below. Flux-weighted annual mean values are indicated where appropriate. All data refer to foraminifera > 150 µm. Individual species contributed differently to the shell and calcite fluxes, indicating that shell mass is not equal among different species. The comparison of the two years reveals compensatory dynamics among the factors influencing planktonic foraminifera calcite flux. Even though the shell flux in 2007-2008 was lower than in 1990-1991, the calcite flux was higher because average shell mass (size and calcification intensity) was higher in 2007-2008.

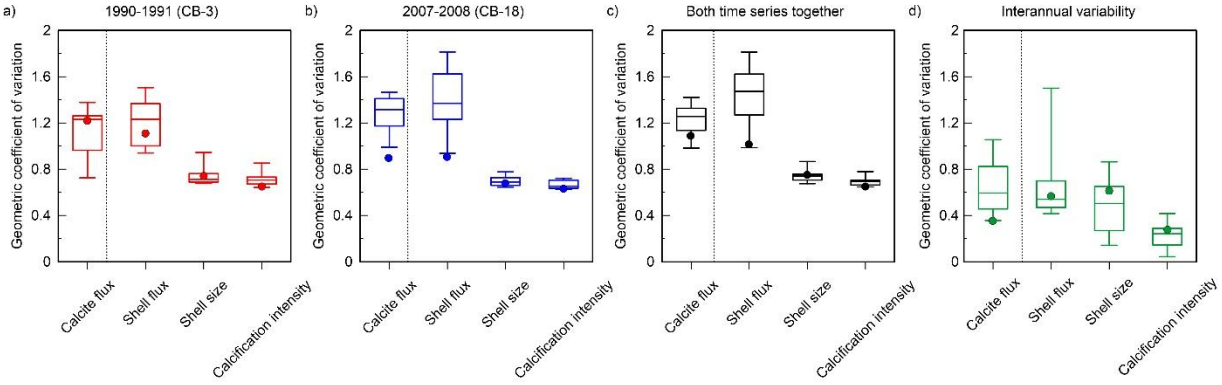

Figure 5. Intra-and interannual variance of planktonic foraminifera calcite flux, shell flux, mean size and mean calcification intensity (weight/size) among the ten most abundant and heaviest species (Figure 6 and Table S3), expressed as geometric coefficient of variation, plotted for 1990-1991 (red), 2007-2008 (blue), both time series together (black) and their interannual differences (green). Boxes extend from the lower to upper quartile values and whiskers to the maximum and minimum value. The horizontal line denotes the median. Solid circles show the geometric coefficient of variation in the same parameters for all foraminifera (without distinguishing species). On the intra-annual timescale, the variance in the planktonic foraminifera calcite flux was only matched by variance in the shell flux and shell size and calcification intensity varied much less, suggesting that shell flux variability dominates variability in planktonic foraminifera calcite flux. Compared to intra-annual variability, interannual variability is smaller for all parameters and both shell flux and shell size vary at a comparable magnitude with calcite flux.

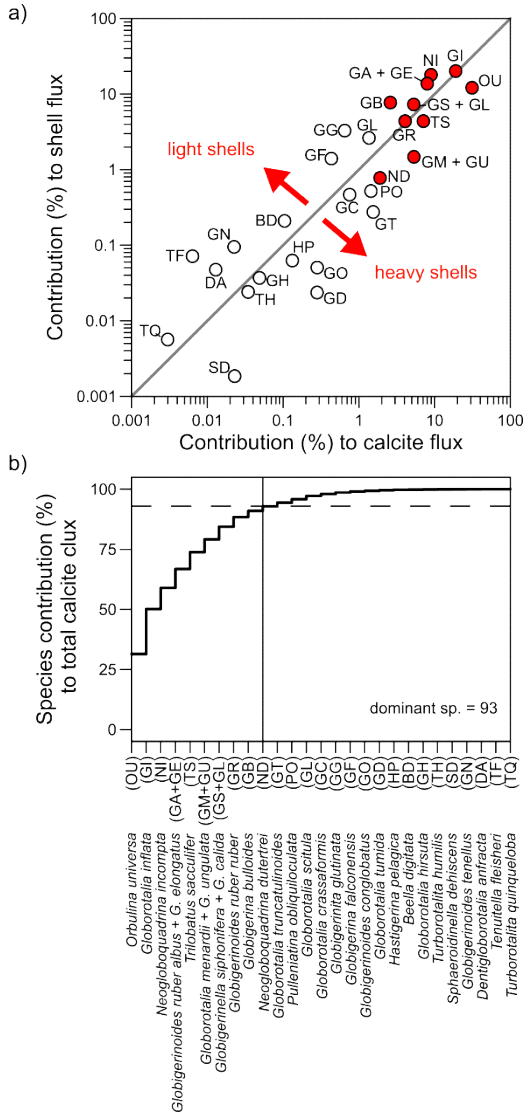

Figure 6. (a): relationship between the species shell flux and calcite flux. Black line denotes the 1:1 relationship that allows distinction between lightly and heavily calcified species. The ten most abundant species (red filled symbols in a) in the two time series combined account for more than 91 % of the planktonic foraminifera shell flux and more than 92 % of the planktonic foraminifera calcite flux (b).

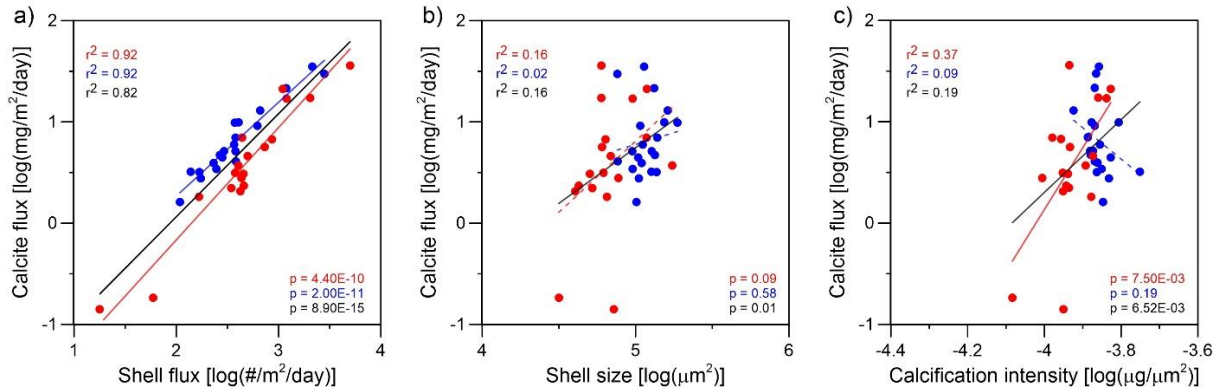

Figure 7. Predictors of planktonic foraminifera calcite flux. Linear regression between the planktonic foraminifera calcite flux, shell flux, mean shell size, and mean calcification intensity (weight/size), shown separately for the 1990-1991 (red) and 2007-2008 (blue) time series, as well as for both years together (black). Summary statistics are given for each regression and significant ($p \leq 0.05$) relations are shown as solid lines, whereas non-significant are shown as dashed lines. On intra-annual timescales, shell flux explains most of the variance in the planktonic foraminifera calcite flux (note that this not only holds for all foraminifera combined, but also on species level - see Table S3).

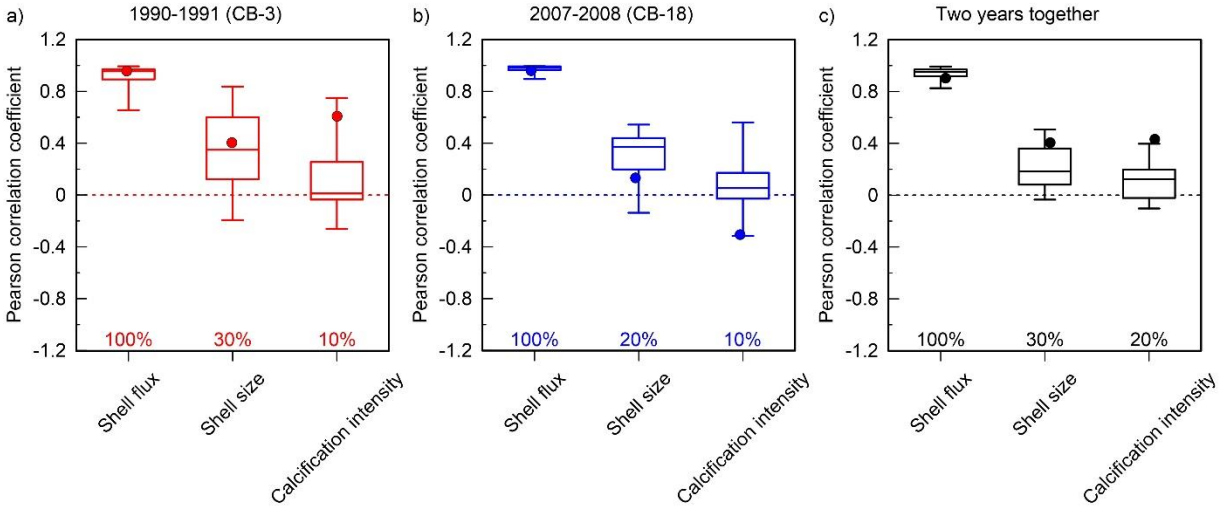

Figure 8. Pearson correlation coefficients between the calcite flux and shell flux, mean size, and mean calcification intensity (weight/size) for the ten most abundant species (Figure 6 and Table S3) plotted for 1990-1991 (red) and 2007-2008 (blue), both individually and jointly for the two time series (black). Boxes encompass the interquartile range values and whiskers to the maximum and minimum value. The horizontal line denotes the median. Solid circles show correlation coefficients calculated for the entire assemblage without distinguishing species. Also shown is the percentage of relationships between the calcite flux and each of the studied parameters that was significant at $p \leq 0.05$.

4. Discussion

4.1 Foraminifera contribution to the total calcite flux

The low proportion of foraminifera shells in the size range between 63 and 150 µm that are inferred in this study is consistent with earlier studies (Salmon et al., 2015; Schiebel, 2002; Schiebel et al., 2007). Since the calcite flux < 63 µm is largely dominated by other organisms (e.g. calcareous dinoflagellates and coccoliths) rather than planktonic foraminifera (Frenz et al., 2005), the largest portion of the contribution of planktonic foraminifera to the calcite flux thus consistently appears to be derived from the flux of shells > 150 µm. For both time series together, the planktonic foraminifera calcite flux > 63 µm measured in the two size fractions combined (63-150 µm and > 150 µm in the size fraction > 63 µm together) made up ca. 21 % of the total calcite flux. This is at the lower end of the estimate for the global contribution of planktonic foraminifera to the total calcite flux (20-50 %), which is mainly based on observations from plankton tows that do not directly provide export flux (Schiebel et al., 2007). A similar contribution of planktonic foraminifera (from 20 to 30 %) to the calcite flux was reported elsewhere (Rembauville et al., 2016; Salmon et al., 2015; Salter et al., 2014), which indicates the importance of coccolithophores in the total calcite flux.

The mean value above, however, masks marked intra-annual variability in the contribution of planktonic foraminifera to the total calcite flux. In our time series, it ranged between 2 and 80 % (Figure 4a and Table S1). Similar intra-annual variability in the contribution of foraminifera to the total calcite flux was observed elsewhere as well. In the Sargasso Sea (North Atlantic Ocean), it varied between 10 and 40 % (Salmon et al., 2015) and between 30 and 50 % in the Southern Ocean (Rigual Hernández et al., 2020; Salter et al., 2014). At the central Kerguelen Plateau (Indian Ocean), planktonic foraminifera made up between 10 and 20 % of the total calcite flux (Rembauville et al., 2016). The contribution to the total calcite flux in the Cape Blanc time series correlates positively with the shell flux ($r = 0.70$, $p < 0.01$), implying that its variability reflects changes in the shell flux. This pronounced variability in the contribution of planktonic foraminifera to the total calcite flux contrasts with the common assumption of a constant 50-50 partitioning of the biogenic calcite flux between planktonic foraminifera and coccolithophores, which is often applied in modelling studies (e. g., Berg et al., 2019; Horner et al., 2011). This large variability in the flux of foraminifera shells and in their contribution to the

total calcite flux could potentially imply seasonally varying ballasting properties of plankton-derived biominerals (Fischer et al., 2016; Romero et al., 2020), as well as seasonally different buffering of calcite undersaturation during settling and on the seafloor (Schiebel, 2002; Schiebel et al., 2007) (and hence the efficiency of the carbon pump).

4.2 Predictors of intra-annual variability in planktonic foraminifera calcite flux

Shell fluxes varied on intra-and interannual timescales (Figure 4c); however, our measurements show that the variability in the shell fluxes at population level was higher within, rather than between the years by a factor of 280 (Figure 5a, b c and 9). This pattern is in line with previous observations at the same location (Romero et al., 2020) and consistent with observations elsewhere in seasonally variable environments (Jonkers & Kučera, 2015; Žarić et al., 2006). The large seasonal variability in the shell flux reflects the interplay between the environmental variability and the ecological niches of the individual species (Žarić et al., 2005), where seasonal changes in environmental conditions sequentially open suitable habitat space that is quickly occupied and utilised by species adapted to conditions at a given time of the annual cycle (Jonkers et al., 2019; Jonkers & Kučera, 2015). The variability in shell flux on a population level is lower than on species level (Figure 5a, b and c), indicating that the niches of the individual species are indeed separated along the seasonal environmental gradient, and that the resulting seasonal species succession dampens the large shell flux variability at the population level.

On intra-annual timescales, shell size and calcification intensity displayed much less variability than shell fluxes and varied only by a factor of 6 and 2 respectively (Figure 5a, b and c, Table S3). Although there are only a few existing studies that report intra-annual shell size and calcification intensity variability, the pattern of larger intra-annual variability in the shell flux compared to shell size and calcification appears typical for seasonally variable settings. For instance, in the Madeira Basin, planktonic foraminifera shell flux varies by almost two orders of magnitude (Storz et al., 2009), whereas shell size varies by a factor of 1.9 and calcification intensity by a factor 1.8 (Weinkauf et al., 2016). Similarly, in the Sargasso Sea, cold water species show shell flux variability of over two orders of magnitude, yet shell size variability with a factor of only 3.8 (Deuser et al., 1981). All studies of planktonic foraminifera in sediment traps ignore small shells (below 0.15 or 0.063 mm), which may lead to an underestimation of

the size variability, but as we show here, the contribution of these small shells to the planktonic foraminifera calcite flux is low (12 %). Also, planktonic foraminifera begin to calcify at a stage where the shell is at least 0.002 mm (size of the proloculus), and the smallest adult specimens are around 0.05 mm. Therefore, variable contributions of specimens in the smaller fractions could not increase in the variability in mean sizes as much as variable contributions of large specimens, which we capture in the studied size spectrum. Among the studied larger specimens, the lower intra-annual variability in size and calcification intensity likely reflects intrinsic growth limitations that set limits on the maximum sizes of adult shells and the maximum calcification intensity of the shells.

On intra-annual timescales, shell flux is not only consistently the most variable component of the planktonic foraminifera calcite flux, but also its best predictor (Figure 7 and 8). Shell size only explained a small fraction of the calcite flux variability, but did so in a way that was consistent with expectations within the years (larger shells equal heavier shells), as well as between the two years. The influence of calcification intensity, on the other hand, varied in sign and importance between the two years (Figure 7c), probably because it showed low variability in the 2007-2008 period (Figure 5b). Most importantly, the intra-annual variability in shell fluxes of individual planktonic foraminifera species at Cape Blanc is comparable to the global range of annual mean shell flux and size for most species (Figure 9a). This implies that our observations in the temporal domain can be extrapolated to the spatial domain. In other words, as long as the flux of individual species varies substantially and the species distribution (or succession) reflects niche separation, in time, our results can be taken to indicate that for a steady-state estimate of the global flux in space, the key variable required to predict calcite flux is shell flux, whereas shell mass can be treated as an invariable parameter. Indeed, the observed intra-annual magnitude of planktonic foraminifera calcite flux variability can be predicted with 14 % (root mean square error normalised to range; NRMSE) accuracy based on shell flux alone (Table 3) and knowledge of the variability in shell size and calcification intensity would reduce the prediction error only to 4 and 11 %, respectively.

		Assuming the same size and calcification intensity among species	Assuming the same size, but variable calcification intensity among species	Assuming variable size, but the same calcification intensity among species	Assuming same shell flux and same calcification intensity between the year, but variable size
Intra-annual	RMSE [mg/m²/day]	4.95	4.08	1.56	
	NRMSE [%]	14	11	4	
Interannual	RMSE [mg/m²/day]	2.26	1.86	0.53	1.21
	NRMSE [%]	164	135	44	83

Table 3. Prediction accuracy of planktonic foraminifera calcite flux based on the knowledge of different parameters on intra-and interannual timescales. Mean residuals (root mean square error, RMSE) and RMSE normalized to the range (NRMSE) between the observed calcite flux and the calculated hypothetical calcite flux is listed for each scenario, and the errors are shown as absolute numbers and percentages. On intra-annual timescales, the variability in planktonic foraminifera calcite flux can be effectively predicted by using shell flux alone (14 % NRMSE), whereas long-term (interannual) predictions of calcite flux require the knowledge of more variables.

Evidently, the importance of shell flux as a predictor for planktonic foraminifera calcite flux depends on the ratio of variance in the shell flux over variance in the shell mass, specifically shell size. The prediction of interannual changes in the calcite flux at sites where the shell flux varies little, e.g. at tropical sites (Jonkers & Kučera, 2015), may require both shell flux and shell size as input variables, particularly if shell size is highly variable. However, in the spatial domain, shell flux shows more variability than shell size (4 vs 2 orders of magnitude; Figure 9). Even though the data available to us are not perfect (e.g. we may not capture the full spectrum of variability), this difference suggests that our inferences, which are based on the observed temporal variability at a single site, can be extrapolated to the spatial domain, and that the calculations presented above are valid, at least to first-order.

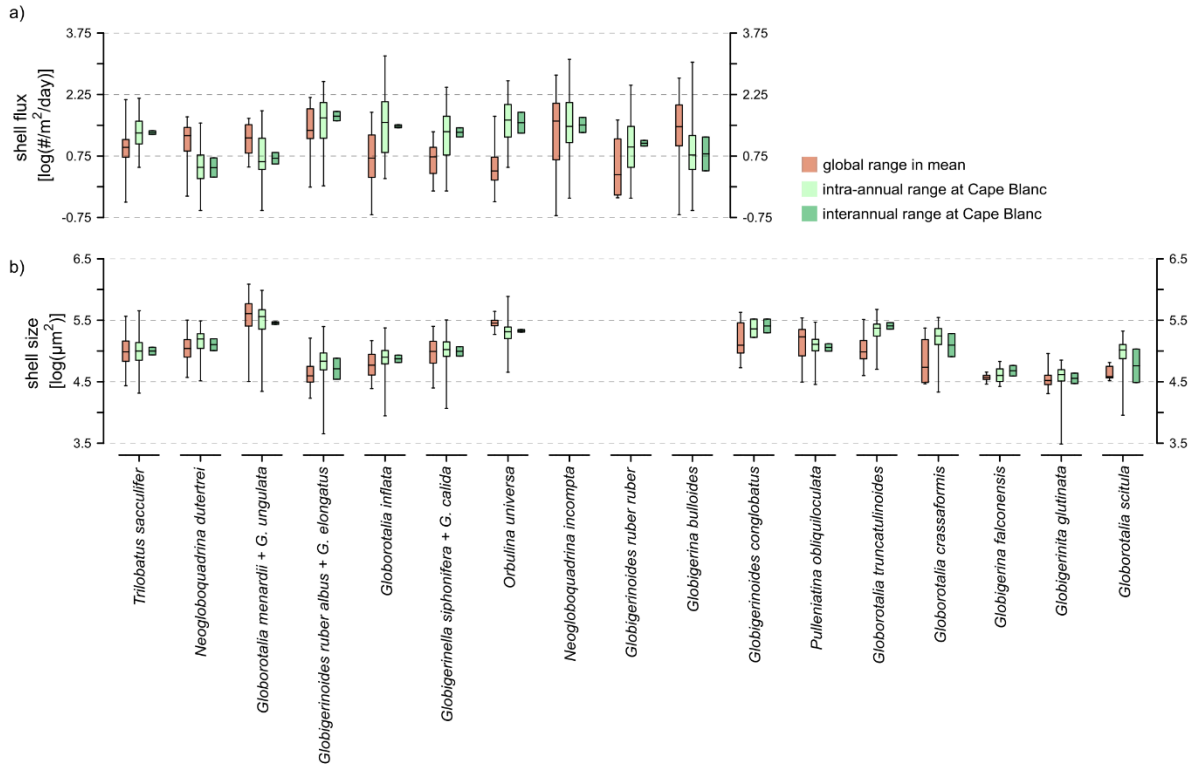

Figure 9. Intra-and interannual (light and dark green) variability in (a): shell flux and (b): shell size of the most dominant species at Cape Blanc compared to the global range of annual mean flux and size (brown) of those species. Flux data taken from Jonkers & Kučera (2015) and from time series listed in Table 2 and size data from Rillo et al., (2019; Figure 3). Boxes show the interquartile range and whiskers the maximum and minimum values. The horizontal line denotes the median. Annual mean shell fluxes for the global compilation are derived from periodic regression (Jonkers & Kučera, 2015). For most species the observed intra-annual shell flux variability at Cape Blanc shows a range that is comparable to, or larger than the global variability in annual mean fluxes, while the range of shell size variability is larger (b). This suggests that the insights from the Cape Blanc time series can be extrapolated in space. The comparison also shows that interannual variability in shell flux and size is comparably low, thus rendering their prediction more difficult.

4.3 Predictors of interannual variability in planktonic foraminifera calcite flux

In contrast to intra-annual variability, variability on interannual timescales is much more equally distributed among the factors potentially affecting the calcite flux (Figure 5d). Within species, shell flux, shell size, and calcification intensity all vary by less than a factor 2 between years, and indeed shell size variability is even larger than shell flux variability. Interestingly, on interannual timescales, shell flux and shell mass variability, which is mainly driven by size, appear to compensate each other, such that the calcite flux is less variable than shell flux or shell

size (Figure 5d). Whatever the exact cause of this compensatory behaviour is, its existence suggests that there is no simple positive linear relationship between the flux and size of planktonic foraminifera shells, at least at the population level. Planktonic foraminifera shell size decreases from oligotrophic subtropical gyres towards the polar waters of both hemispheres (Al-Sabouni et al., 2007; Schmidt et al., 2004), whereas their population density show the opposite pattern (Schiebel & Hemleben, 2005). Low population density but large size in lower latitudes, when translated to calcite flux, indicates that the difference in population density is counteracted by the pronounced latitudinal size gradient. Compared to intra-annual timescales, the two orders of magnitude smaller shell flux variability at interannual timescales and the comparable variability in shell size and calcification intensity within and between years, means that for the prediction of the interannual changes in planktonic foraminifera calcite flux, shell flux alone is not sufficient (Figure 5d). Indeed, when ignoring shell mass variability, predictions of temporal changes in planktonic foraminifera calcite flux at the studied site would be widely inaccurate (NRMSE: 164 %; Table 3). As with the prediction of intra-annual/large scale changes, the consideration of variable calcification intensity only leads to a relatively small improvement of the predictive skill (NRMSE: 135 %). Remarkably, a better prediction can be obtained using shell size variability alone and ignoring variability in shell flux and calcification intensity (NRMS: 83 %). The accuracy can be improved most when considering variability in shell flux as well as shell size. Nevertheless, even when including shell size as an additional predictor besides shell flux, interannual changes in planktonic foraminifera calcite flux cannot be predicted as accurately as intra-annual changes based on shell flux alone (NRMSE 44 vs 14 %; Table 3).

Our analyses thus yielded a clear ranking of the importance of the parameters controlling the planktonic foraminifera calcite flux. Irrespective of the (temporal) scale, calcification intensity consistently appears the least and shell flux the most important predictor of planktonic foraminifera calcite flux (Figure 7 and 8, Table 3). The importance of shell size varies with scale, and it can only be ignored in predictions of large-scale changes in planktonic foraminifera calcite flux. Naturally, these results prompt the question: which factors drive variability in foraminifera shell flux, size, and calcification intensity? Resolving the origin of this variability, however, was not the prime goal of our analyses; our goal was to guide setting research priorities. For instance, our analyses demonstrate that an accurate estimate of the global

planktonic foraminifera calcite budget can already be achieved with a simple model based on shell flux and average shell mass alone, and additional more complex parametrisation will likely lead to only marginal improvements (Table 3). At the same time, we highlight the difficulty of predicting interannual changes in planktonic foraminifera calcite flux, therefore implying that for this purpose, research efforts should concentrate on not only on modelling shell flux, but also on understanding which factors determine shell mass variability.

Empirical studies indicate a dominant (non-linear) effect of the general environmental conditions (often approximated by temperature) to explain shell flux variability on intra-annual and large spatial scales (Jonkers & Kučera, 2015; Žarić et al., 2005). Smaller scale changes in the shell flux, which ultimately translate into interannual variability, are likely to be driven by secondary biotic and/or abiotic factors. Similarly, variability in size and calcification intensity appears to be driven by complex combinations of environmental variables (Deuser et al., 1981; Weinkauf et al., 2016), rendering accurate prediction non-trivial. Mechanistic predictions of the planktonic foraminifera calcite flux on spatial-temporal scales will thus require more ecological insights into the environmental and biological factors controlling its variability (Langer, 2008; Schiebel, 2002; Schiebel et al., 2007).

Even though resolving the factors that drive variability in foraminifera shell flux and shell mass was not the prime aim of our study, the two years analysed in this work were not entirely identical, allowing a first-order assessment of the relationship between environmental conditions and planktonic foraminifera calcite fluxes. We observe that the higher mean planktonic foraminifera calcite flux in the slightly colder 2007-2008 period (Figure 4), is echoed by a similarly higher (~ 20 %) mean particle mass flux and mean opal mass flux during that year (Figure 2). Remarkably, the higher foraminifera calcite mass in 2007-2008 flux occurred despite lower mean shell flux (Figure 2). This could indicate that the overall productivity may be linked to planktonic foraminifera calcite flux in a different way than to their shell flux. Overall, it seems that even a modest difference in environmental conditions between the years can translate into a substantial interannual difference in mean planktonic foraminifera calcite fluxes.

Essentially, our results suggest that as long as the spatial or temporal magnitude of changes in the shell flux are large, constraining shell flux variability alone is sufficient to derive a reliable planktonic foraminifera calcite budget. The question at which temporal scale beyond interannual

planktonic foraminifera shell flux variability is sufficiently large to ignore shell mass variability in budget estimates still remains open. It is likely that at least up to multi-decadal scale, predictions of planktonic foraminifera calcite flux will require the knowledge of shell mass variability. This hypothesis can be tested using long-term sediment trap time series. Assessing the partitioning of factors modulating the planktonic foraminifera calcite flux at longer, geologically relevant timescales, would require detailed analysis of sedimentary time series of planktonic foraminifera flux, size, and calcification intensity. If our inferences hold, all three parameters are needed to predict the variability in planktonic foraminifera calcite flux on centennial to millennial timescales during climatically stable periods (such as during the Holocene). On longer timescales and across major climate transitions, the shell flux is likely to change dramatically, which implies that shell flux as a single parameter should be sufficient to predict the variability in calcite flux. Either way, understanding all the processes that are important to quantify planktonic foraminifera calcite flux on multi-decadal timescales will be essential for evaluation of the behaviour of this key component of the marine carbon cycle under future climate change scenarios.

5. Conclusions

Production and export flux of planktonic foraminifera represent a crucial component of the pelagic carbonate cycle. A detailed analysis of planktonic foraminifera assemblages using Cape Blanc sediment trap time series (from 1990-1991 and 2007-2008) allowed us to evaluate the species-specific intra-and interannual contribution of shell flux, shell size and calcification intensity to the observed variability in planktonic foraminifera calcite flux. Our results indicate that on intra-annual timescales, shell flux varies the most and appears to be the best predictor of seasonal changes in planktonic foraminifera calcite flux. Since shell flux varies seasonally at similar magnitude as mean annual flux does in space, constraining shell flux variability (either by measuring or modelling) is likely sufficient to derive a global steady-state planktonic foraminifera calcite budget. Including variability in shell size or calcification intensity in the calculations will only provide marginal improvements of the budget estimate.

In contrast, multiple mechanisms appear to act in concert to shape the variability in planktonic foraminifera calcite flux interannual timescales and our results imply that estimates of changes in mean annual calcite production also require constraints on the variability in shell mass. Since

temporal changes in calcification intensity appear less important, shell size is likely the most relevant predictor of planktonic foraminifera calcite flux, and its prediction is required next to the prediction of shell flux to model foraminifera calcite flux changes on timescales beyond the seasonal cycle.

Acknowledgments, Samples, and Data

We would like to thank two anonymous reviewers and Andrés Rigual-Hernández for their constructive comments on earlier versions of this manuscript. We thank Julie Meilland for valuable discussions and Michael Jerry Sabo for proofreading of the manuscript.

This work was only possible due to the long-term funding by the German Research Foundation (DFG) through the Research Center Ocean Margins (RCOM), the Excellence Cluster "The Ocean in the Earth System" and the Cluster of Excellence "The Ocean Floor–Earth's Uncharted Interface".

P.K. was supported by the Collegium Talentum Programme of Hungary, by the Slovak Research and Development Agency under the contracts APVV 15-0575 and APVV 16-0121, by the German Academic Exchange Service (DAAD) Research Grant for Doctoral Candidates and Young Academic Scientists, by the German Academic Exchange Service (DAAD) STIBET Scholarship, by the National Scholarship Programme of the Slovak Republic and by the Erasmus+ Programme of the European Commission.

Bulk carbonate flux and opal flux data for the two studied sediment trap time series (CB-3 and CB-18) and for the time series from 1988 to 2012 (from CB-1 to CB-23) in the upwelling area off Cape Blanc were taken from Fischer et al. (2016). Sea-surface temperature data used in Figure 2 were taken from the National Centers for Environmental Information AVHRR Analysis and annual sea-surface temperature data used in Figure 3 were obtained from Locarnini et al. (2019). Data used in the compilation of annual mean shell fluxes of planktonic foraminifera were taken from Jonkers & Kučera (2015) and from the time series listed in Table 2; morphometric data used in Figure 9b were taken from Rillo et al. (2019). All data sources are cited in the references.

Table S1. Sample label, sampling period, sampling duration, bulk carbonate flux (calcite and aragonite) flux, total calcite flux, aragonite flux, planktonic foraminifera (PF) calcite flux and shell flux captured by Cape Blanc time series 1990-1991 (CB3) and 2007-2008 (CB-18).

Sample label	Sampling start [date/time]	Sampling end [date/time]	Duration [days]	Bulk carbonate flux [mg/m^2/day]	Total calcite flux [mg/m^2/day]	Aragonite flux [mg/m^2/day]	PF > 150 µm calcite flux [mg/m^2/day]	PF shell > 150 µm flux [#/m^2/day]
CB3-1	08-04-1990/11:00:00	29-04-1990/23:00:00	21.5	123.20	98.79	24.41	17.30	2042.05
CB3-2	29-04-1990/23:00:00	21-05-1990/11:00:00	21.5	199.30	129.64	69.66	36.00	5000.93
CB3-3	21-05-1990/11:00:00	11-06-1990/23:00:00	21.5	49.10	26.48	22.62	3.15	375.07
CB3-4	11-06-1990/23:00:00	03-07-1990/11:00:00	21.5	46.60	26.36	20.24	21.10	1095.44
CB3-5	03-07-1990/11:00:00	24-07-1990/23:00:00	21.5	113.70	65.48	48.22	17.03	1196.65
CB3-6	24-07-1990/23:00:00	15-08-1990/11:00:00	21.5	45.70	21.89	23.81	4.59	500.09
CB3-7	15-08-1990/11:00:00	05-09-1990/23:00:00	21.5	53.40	36.73	16.67	3.72	404.84
CB3-8	05-09-1990/23:00:00	27-09-1990/11:00:00	21.5	50.60	0.59	50.01	6.74	863.26
CB3-9	27-09-1990/11:00:00	18-10-1990/23:00:00	21.5	34.50	24.38	10.12	2.79	434.60
CB3-10	18-10-1990/23:00:00	09-11-1990/11:00:00	21.5	40.30	34.35	5.95	6.99	440.56
CB3-11	09-11-1990/11:00:00	30-11-1990/23:00:00	21.5	23.60	18.84	4.76	2.06	422.70
CB3-12	30-11-1990/23:00:00	22-12-1990/11:00:00	21.5	51.90	47.73	4.17	3.07	452.47
CB3-13	22-12-1990/11:00:00	12-01-1991/23:00:00	21.5	32.60	24.27	8.33	5.64	732.28
CB3-14	12-01-1991/23:00:00	03-02-1991/11:00:00	21.5	34.10	32.31	1.79	2.34	458.42
CB3-15	03-02-1991/11:00:00	24-02-1991/23:00:00	21.5	55.00	51.43	3.57	2.23	345.30
CB3-16	24-02-1991/23:00:00	18-03-1991/11:00:00	21.5	11.00	10.70	0.30	1.81	166.70
CB3-17	18-03-1991/11:00:00	08-04-1991/23:00:00	21.5	8.40	8.10	0.30	0.18	59.53
CB3-18	08-04-1991/23:00:00	30-04-1991/11:00:00	21.5	5.20	4.90	0.30	0.14	17.86
CB18-1	25-03-2007/00:01:00	10-04-2007/00:01:00	16	158.01	127.80	30.21	29.82	2804.38
CB18-2	10-04-2007/00:01:00	29-04-2007/00:01:00	19	129.16	63.49	65.68	4.07	381.58
CB18-3	29-04-2007/00:01:00	18-05-2007/00:01:00	19	166.88	92.11	74.76	4.45	281.05
CB18-4	18-05-2007/00:01:00	06-06-2007/00:01:00	19	127.83	90.35	37.48	3.19	167.89
CB18-5	06-06-2007/00:01:00	25-06-2007/00:01:00	19	82.90	69.25	13.66	5.15	378.95
CB18-6	25-06-2007/00:01:00	14-07-2007/00:01:00	19	62.89	57.41	5.47	9.91	406.84
CB18-7	14-07-2007/00:01:00	02-08-2007/00:01:00	19	37.32	35.49	1.84	3.21	137.89
CB18-8	02-08-2007/00:01:00	21-08-2007/00:01:00	19	36.72	32.23	4.49	1.61	108.42
CB18-9	21-08-2007/00:01:00	09-09-2007/00:01:00	19	40.48	34.91	5.57	5.15	292.11
CB18-10	09-09-2007/00:01:00	28-09-2007/00:01:00	19	65.49	45.88	19.62	21.59	1187.89
CB18-11	28-09-2007/00:01:00	17-10-2007/00:01:00	19	39.29	33.12	6.17	5.95	366.84
CB18-12	17-10-2007/00:01:00	05-11-2007/00:01:00	19	40.88	33.01	7.87	4.71	265.79
CB18-13	05-11-2007/00:01:00	24-11-2007/00:01:00	19	48.23	45.04	3.19	12.94	663.16
CB18-14	24-11-2007/00:01:00	13-12-2007/00:01:00	19	54.90	51.37	3.53	7.01	377.89
CB18-15	13-12-2007/00:01:00	01-01-2008/00:01:00	19	79.39	69.27	10.12	35.05	2133.16

Table S1. continued

CB18-16	01-01-2008/00:01:00	20-01-2008/00:01:00	19	58.32	52.20	6.12	9.12	621.05
CB18-17	20-01-2008/00:01:00	08-02-2008/00:01:00	19	51.05	47.78	3.27	9.86	374.74
CB18-18	08-02-2008/00:01:00	27-02-2008/00:01:00	19	31.89	24.93	6.96	3.93	231.58
CB18-19	27-02-2008/00:01:00	17-03-2008/00:01:00	19	47.22	41.25	5.97	3.42	247.37
CB18-20	17-03-2008/00:01:00	05-04-2008/00:01:00	19	13.74	8.38	5.35	2.76	173.16

Table S2. Individual species mean size, mean shell weight and mean calcification intensity (weight/size) listed separately for 1990-1991 (CB-3), 2007-2008 (CB-18) and for both time series together. The last row refers to the total mean values calculated among all foraminifera combined without distinguishing species.

Species name	Mean size (µm²)			Mean shell weight (µg)			Mean calcification intensity (µm²/µg)		
	CB-3	CB-18	Together	CB-3	CB-18	Together	CB-3	CB-18	Together
Globigerina bulloides	40864	69119	46031	3.6	6.6	4.1	8.82E-05	9.59E-05	8.96E-05
Globigerinella siphonifera + G. calida	82736	117780	96288	8.0	11.1	9.2	9.64E-05	9.41E-05	9.55E-05
Globorotalia crassaformis	80667	192102	121599	8.8	38.2	17.3	1.09E-04	1.99E-04	1.42E-04
Globorotalia hirsuta	42286	184471	98402	4.4	32.9	13.2	1.05E-04	1.78E-04	1.34E-04
Globorotalia inflata	65113	85431	74735	8.8	12.9	10.6	1.34E-04	1.50E-04	1.42E-04
Globigerinoides ruber ruber	59541	98212	82234	7.8	12.8	10.7	1.31E-04	1.30E-04	1.31E-04
Globigerinoides ruber albus + G. elongatus	34740	76388	52159	4.3	10.3	6.7	1.25E-04	1.35E-04	1.29E-04
Trilobatus sacculifer	86274	114941	103051	15.4	21.1	18.7	1.79E-04	1.84E-04	1.82E-04
Globorotalia scitula	30666	107572	66835	1.7	11.1	5.2	5.58E-05	1.03E-04	7.81E-05
Globorotalia truncatulinoides	289400	226907	236554	84.6	59.8	63.4	2.92E-04	2.64E-04	2.68E-04
Globorotalia menardii + G. ungulata	270433	298442	287332	35.0	40.7	38.4	1.29E-04	1.36E-04	1.34E-04
Neogloboquadrina dutertrei	101648	158305	127771	19.3	37.5	27.0	1.90E-04	2.37E-04	2.12E-04
Neogloboquadrina incompta	56140	54593	55588	7.6	6.4	7.2	1.36E-04	1.17E-04	1.29E-04
Orbulina universa	223477	202775	210271	34.4	28.5	30.6	1.54E-04	1.41E-04	1.46E-04
Globigerinita glutinata	29496	43554	32715	2.3	3.0	2.5	7.67E-05	7.00E-05	7.51E-05
Pulleniatina obliquiloculata	99252	130981	127110	19.6	33.1	31.3	1.97E-04	2.53E-04	2.46E-04
Hastigerina pelagica	561836	471469	538228	26.2	28.0	26.9	4.66E-05	5.94E-05	5.00E-05

Table S2. continued

Beella digitata	104429	211377	114103	7.3	13.3	7.9	7.00E-05	6.30E-05	6.94E-05
Globigerinoides conglobatus	330211	197983	319471	71.6	45.1	69.5	2.17E-04	2.28E-04	2.18E-04
Turborotalita quinqueloba	NA	61463	61463	NA	6.0	6.0	NA	9.81E-05	9.81E-05
Sphaeroidinella dehiscens	NA	264252	264252	NA	139.1	139.1	NA	5.27E-04	5.27E-04
Globigerina falconensis	39123	58019	39294	4.0	5.9	4.0	1.01E-04	1.01E-04	1.01E-04
Turborotalita humilis	173401	NA	173401	18.4	NA	18.4	1.06E-04	NA	1.06E-04
Dentigloborotalia anfracta	17963	NA	17963	3.5	NA	3.5	1.93E-04	NA	1.93E-04
Globorotalia tumida	336146	NA	336146	150.8	NA	150.8	4.49E-04	NA	4.49E-04
Globigerinoides tenellus	31022	NA	31022	3.0	NA	3.0	9.82E-05	NA	9.82E-05
Tenuitella fleisheri	16845	NA	16845	1.1	NA	1.1	6.69E-05	NA	6.69E-05
Total	**71232**	**111855**	**88943**	**8.8**	**15.3**	**11.5**	**1.23E-04**	**1.37E-04**	**1.29E-04**

Table S3. Coefficient of determination (r^2), intercept (Int.), slope (Slp.), p-values (p-val.) and geometric coefficient of variations (geo. var.) calculated between individual species calcite flux, shell flux, mean shell size and mean calcification intensity (Calc. int.), for the ten most abundant species (Figure 6), listed individually and jointly for the two time series. Significant relations ($p \leq 0.05$) between calcite flux and the studied parameters are marked with an asterisk.

		1990-1991 (CB-3)			2007-2008 (CB-18)			Two years together		
		Shell flux	**Size**	**Calc. int.**	**Shell flux**	**Size**	**Calc. int.**	**Shell flux**	**Size**	**Calc. int.**
Globigerina bulloides	r^2	0.93	0.12	0.01	0.96	0.13	0.00	0.93	0.00	0.00
	Int.	0.67	-8.12	-0.33	0.83	-15.87	2.17	0.80	1.67	1.39
	Slp.	0.97	2.20	-0.59	1.00	3.64	0.13	0.93	0.04	-0.11
	p-val.	9.08E-11*	0.16	0.67	6.41E-13*	0.13	0.91	3.69E-22*	0.97	0.90
	geo. var.	1.29	0.68	0.69	1.62	0.66	0.72	1.81	0.71	0.70
Globigerinella siphonifera + G. calida	r^2	0.94	0.10	0.00	0.98	0.30	0.07	0.94	0.09	0.00
	Int.	0.77	-2.57	1.94	0.96	-18.99	-13.94	0.91	-3.04	0.74
	Slp.	1.04	1.01	-0.10	1.03	4.24	-4.04	1.01	1.08	-0.39
	p-val.	2.33E-11*	0.19	0.92	8.28E-17*	0.01*	0.24	1.13E-23*	0.07	0.67
	geo. var.	1.22	0.76	0.72	1.23	0.66	0.63	1.28	0.73	0.69
Globorotalia inflata	r^2	0.92	0.52	0.05	0.99	0.02	0.00	0.92	0.03	0.01
	Int.	0.63	-15.16	9.48	1.16	10.71	6.13	1.06	-1.49	6.89
	Slp.	1.10	3.79	1.76	0.98	-1.64	0.93	0.97	0.85	1.11
	p-val.	3.40E-09*	1.59E-03*	0.42	1.00E-19*	0.56	0.89	2.72E-21*	0.27	0.55
	geo. var.	1.50	0.71	0.67	1.43	0.65	0.62	1.65	0.73	0.66
Globigerinoides ruber ruber	r^2	0.80	0.17	0.07	0.96	0.01	0.01	0.88	0.01	0.02
	Int.	0.76	-5.48	4.04	1.10	-0.44	7.79	1.04	0.69	4.12
	Slp.	1.04	1.63	0.49	0.98	0.50	1.48	0.94	0.29	0.52
	p-val.	7.76E-06*	0.13	0.36	4.14E-14*	0.72	0.75	7.15E-18*	0.63	0.39
	geo. var.	1.16	0.71	0.85	1.41	0.70	0.63	1.62	0.76	0.76

Table S3. continued

Globigerinoides ruber albus + G. elongatus	r^2	0.85	0.04	0.00	0.99	0.04	0.01	0.84	0.00	0.00
	Int.	1.05	5.34	2.48	0.98	-7.55	9.88	1.14	3.03	2.70
	Slp.	0.80	-0.60	-0.04	1.01	2.08	1.88	0.83	-0.09	0.02
	p-val.	3.79E-07*	0.47	0.96	3.82E-18*	0.40	0.69	6.39E-16*	0.84	0.97
	geo. var.	1.25	0.70	0.73	1.14	0.64	0.63	1.23	0.75	0.69
Trilobatus sacculifer	r^2	0.90	0.36	0.00	0.93	0.19	0.08	0.89	0.26	0.04
	Int.	1.05	-8.21	3.66	1.21	-7.27	10.35	1.14	-5.99	8.15
	Slp.	1.09	2.19	0.30	1.08	1.97	2.05	1.08	1.72	1.48
	p-val.	5.56E-09*	0.01*	0.89	7.84E-12*	0.05	0.22	8.47E-19*	1.14E-03*	0.24
	geo. var.	1.00	0.69	0.64	0.94	0.68	0.65	0.99	0.70	0.65
Globorotalia menardii + G. ungulata	r^2	0.45	0.70	0.56	0.85	0.13	0.03	0.68	0.23	0.14
	Int.	0.86	-5.21	14.44	1.53	-4.19	7.38	1.46	-3.70	10.48
	Slp.	1.35	1.45	3.08	0.98	1.18	1.35	0.95	1.11	2.12
	p-val.	1.19E-02*	3.62E-04*	3.26E-03*	6.01E-09*	0.12	0.47	3.11E-10*	2.39E-03*	0.02*
	geo. var.	0.95	0.94	0.73	1.35	0.78	0.67	1.50	0.87	0.70
Neogloboquadrina dutertrei	r^2	0.43	0.02	0.07	0.80	0.15	0.31	0.79	0.01	0.16
	Int.	2.14	3.12	0.01	1.52	-5.74	10.67	1.56	0.56	8.80
	Slp.	0.34	-0.11	-0.69	1.04	1.48	2.38	0.89	0.30	1.82
	p-val.	5.90E-03*	0.61	0.33	1.03E-07*	0.09	0.01*	8.43E-14*	0.58	0.01*
	geo. var.	0.94	0.75	0.65	1.23	0.73	0.72	1.44	0.75	0.70
Neogloboquadrina incompta	r^2	0.99	0.01	0.00	0.99	0.20	0.10	0.99	0.03	0.01
	Int.	0.66	1.35	2.26	0.71	-8.02	-6.67	0.72	-0.24	1.05
	Slp.	1.03	0.26	-0.08	1.04	2.17	-2.26	1.02	0.56	-0.33
	p-val.	1.61E-14*	0.65	0.90	4.14E-19*	0.05*	0.18	6.04E-35*	0.27	0.54
	geo. var.	1.40	0.85	0.85	1.39	0.71	0.68	1.56	0.79	0.78

Table S3. continued

Orbulina universa	r^2	0.96	0.12	0.10	0.96	0.18	0.00	0.96	0.13	0.04
	Int.	1.33	-7.39	10.83	1.39	-10.54	2.29	1.36	-8.00	8.66
	Slp.	1.08	1.97	2.01	1.03	2.61	-0.25	1.05	2.11	1.42
	p-val.	7.16E-11*	0.18	0.22	2.50E-14*	0.06	0.91	1.26E-26*	0.03*	0.23
	geo. var.	1.37	0.69	0.68	1.01	0.66	0.64	1.27	0.67	0.66

Chapter 2

Mechanisms modulating the temporal variability of the planktonic foraminifera calcite flux across Termination I in the tropical Atlantic

This work is in preparation for submission.

P. Kiss[1,2*], L. Jonkers[2], N. Hudáčková[1] and M. Kučera[2]

[1]Department of Geology and Paleontology, Comenius University in Bratislava, Bratislava, Slovakia.

[2]MARUM - Center for Marine Environmental Sciences, University of Bremen, Bremen, Germany.

*Corresponding author: Peter Kiss (pkiss@marum.de)

Data availability: data generated in this study will be available on PANGAEA Data Publisher after acceptance of the manuscript.

Abstract

The planktonic foraminifera calcite flux is a key component of the pelagic carbon cycle. Due to its relevance for the pelagic calcite budget and the pelagic carbonate counter pump, in terms of oceanic capacity of CO_2 uptake, it is important to understand the mechanisms modulating the variable export of foraminifera calcite. In theory, the individual species calcite flux reflects changes in 1) shell flux and 2) shell mass, being the product of i) shell size and ii) calcification intensity, and in assemblages where shell mass differs among species also in 3) species composition. To determine how these mechanisms modulated the planktonic foraminifera calcite flux during periods of different environmental forcing across the last deglaciation, we generated a record of species-resolved shell flux, shell size and calcification intensity data from a well-dated sediment core (GeoB3104-1) with exceptional preservation of planktonic foraminifera in the tropical Atlantic. Our results reveal that ~95 % of the long-term (centennial and millennial) variability in the planktonic foraminifera calcite flux can be explained by shell flux, which is the most variable component of the planktonic foraminifera calcite flux. On the other hand, shell size and calcification intensity varied negligible on the millennial timescale, and they were also poor predictors of the variability in the planktonic foraminifera calcite flux. Therefore, our analyses of variability in shell flux, shell size and calcification intensity in the context of the resulting calcite flux revealed that in order to model the long-term global foraminifera calcite budget, at first the environmental background of shell flux variability needs to be constrained.

1. Introduction

Planktonic foraminifera are fundamental components of the pelagic carbon cycle. They fix dissolved inorganic carbon in their shells through the production of calcite, which is after the death of the organisms exported by the planktonic foraminifera calcite flux to the deep ocean. A considerable amount of the initially produced shell calcite is dissolved while settling through the water column (Schiebel et al., 2007), whilst shells reaching the seafloor are being buried in the sediment on geologically relevant timescales (Milliman, 1993; Schiebel, 2002; Schiebel et al., 2007). Furthermore, the process of calcite precipitation by planktonic foraminifera counteracts the efficiency of the marine biological pump. During biomineralization, carbon

dioxide is released into the ambient seawater, which partly offsets the oceanic capacity of carbon dioxide sequestration from the atmosphere (Frankignoulle & Canon, 1994). The planktonic foraminifera calcite flux is a key component of the global calcite flux. It is assumed that it constitutes up to half of the global calcite flux (Langer, 2008; Schiebel, 2002; Schiebel et al., 2007), while the rest is created by coccoliths (Baumann et al., 2004; Milliman, 1993; Rigual Hernández et al., 2020). The contribution of planktonic foraminifera calcite flux to the global calcite flux varies in space and time, for instance in the Sargasso Sea (North Atlantic Ocean) it was ~ 40 % (Salmon et al., 2015), in the Southern Ocean it was ~ 45-50 % (Rigual Hernández et al., 2020; Salter et al., 2014) and in the Indian Ocean it was ~ 15 % (Rembauville et al., 2016).

The planktonic foraminifera calcite flux is made by the individual species calcite fluxes, which variable contribution to the total planktonic foraminifera calcite flux may reflect changes in the population or individual growth. On the population level, changes in the planktonic foraminifera calcite flux arise from shell flux, which is the number of exported foraminifera shells. On the individual level, changes in the calcite flux emerge from shell mass, which is the product of the species shell size and calcification intensity. In assemblages where shell mass differs among the species, the species composition in the planktonic foraminifera calcite flux is also a relevant mechanism, since some heavily calcified species can have considerable influence on the calcite flux (Salmon et al., 2015). The partitioning of mechanisms responsible for the variability in the planktonic foraminifera calcite flux depend on the temporal scale. A detailed analysis of the candidate mechanisms modulating the planktonic foraminifera calcite flux in the Cape Blanc upwelling area (Atlantic Ocean) revealed that the intra-annual or seasonal changes are caused by shell flux, which alone explains 82 % of the variability in the planktonic foraminifera calcite flux, while the combination of shell flux with shell mass shape the variability in the planktonic foraminifera calcite flux between the years (Kiss et al., 2021). However, these outcomes were made by using modern foraminifera assemblages obtained by sediment trap times series under seasonally varying sea-surface temperature, carbon dioxide concentration and ocean carbonate chemistry. Thus, previous research has not investigated how the contribution of the modulating mechanisms (shell flux, shell size and calcification intensity) and the planktonic foraminifera calcite flux responded to environmental changes that far exceed the magnitude of modern intra- and interannual environmental changes.

To resolve this issue, we study the relative contribution of variability in shell flux, shell size, and calcification intensity in individual species to the total planktonic foraminifera calcite flux during the period of the last deglaciation. The targeted time-interval covers the period from the Last Glacial Maximum (LGM, ~ 22.000 years ago) to the last ice age termination (appr. 9.000 years ago; Clark et al., 2012; Denton et al., 2010). The deglacial climate transition is characterized by major changes in sea-surface temperature, atmospheric carbon dioxide concentration as well as ocean carbonate chemistry (Shakun et al., 2012; Fig. 1). Specifically, a warming in southern-hemisphere temperature occurred during the Heinrich Stadial I. (~ 18 to 14.7 ka), and another warming is recognized during the Younger Dryas (~12.9 to 11.7). Whilst these two temperature steps were of similar magnitude, the associated levels and changes of atmospheric and ocean carbon dioxide concentration were different (Monnin et al., 2001; Shakun et al., 2012), which provide us an excellent opportunity to investigate the changes in shell flux and shell mass in individual species and in the total planktonic foraminifera community under variable climatic conditions.

Here, we generated a species-resolved shell flux and shell mass data from the period of the Last Glacial Maximum, Heinrich Stadial I., Younger Dryas, and Holocene. We investigated the relative contribution of their variability in the context of the resulting planktonic foraminifera calcite flux by using a well-dated sedimentary time series from the western tropical Atlantic (GeoB3104-1). With this approach we provide novel insight into the long-term evolution of the planktonic foraminifera calcite flux as well as we resolve the partitioning of mechanisms shaping the planktonic foraminifera calcite flux during climatically unstable periods.

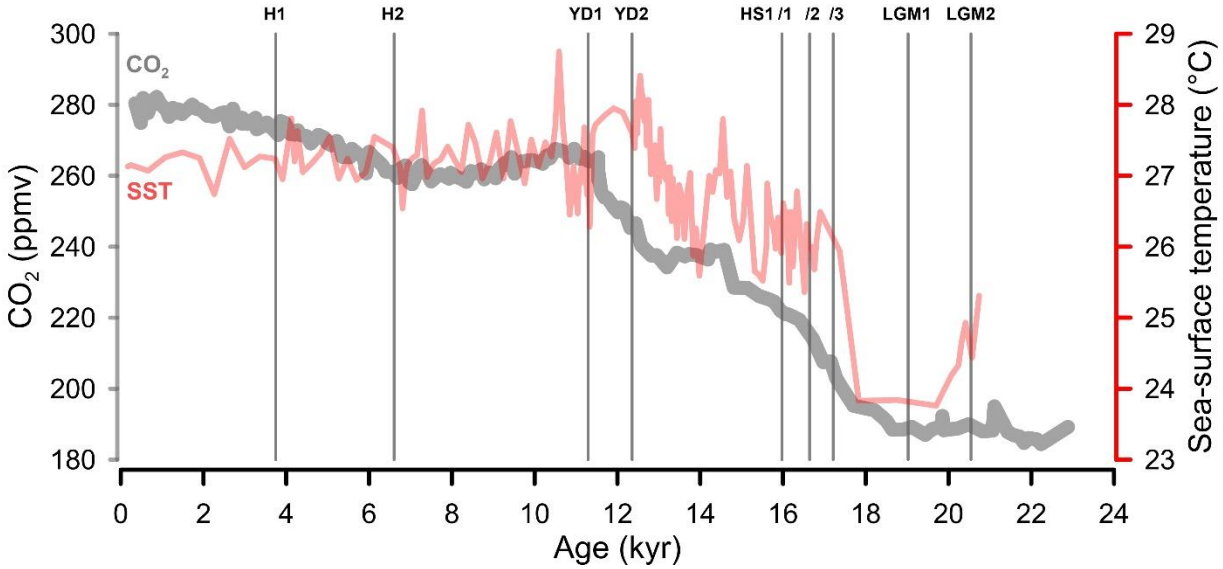

Figure 1. Changes in the atmospheric carbon dioxide (grey line) concentration and global mean sea-surface temperature (red line) during the last ~ 24.000 years. Grid lines on the X-axes indicate the age of the studied samples (H1 – Holocene sample 1; H2 – Holocene sample 2; YD1 – Younger Dryas 1; YD2 – Younger Dryas 2; HS1/1, 2 , 3 – Heinrich Stadial I. sample 1, 2 and 3; LGM1 – Last Glacial Maximum sample 1; LGM2 – Last Glacial Maximum sample 2). Sea-surface temperature data were taken from Weldeab et al. (2006). This figure shows the large amplitude environmental changes associated with the last deglaciation and carbon dioxide reconstruction from Bazin et al. (2013).

2. Material and methods

The partitioning of mechanisms (shell flux, shell size, and calcification intensity) shaping the long-term variability in the planktonic foraminifera calcite flux in response to large amplitude environmental changes can be the best studied by analyzing sedimentary time series. Here, we focus on the last deglacial transition that contains key periods of sea-surface temperature and ocean carbon dioxide changes within ~22.000 years, thus we can investigate how the planktonic foraminifera calcite flux with its regulating mechanisms responded to those dramatic environmental changes. The most important prerequisite of our analyses was the spectacular preservation of the foraminifera community, so we selected a site with shallow water depth (700 m), where foraminifera shells are not affected by dissolution. The perfect preservation of foraminifera shells was also necessary for the applied shell-weighing method that is used for interpreting the calcification intensity of the specimens. Using the shell-weighing method to determine calcification is difficult from contamination by adhering sediment inside the

chambers. However, before applying the shell-weighing method, we carefully assessed the preservation of foraminifera shells in each sample, and we concluded that the specimens are spectacularly preserved and empty, reflecting no signs of lithogenic infill.

Here, we use a gravity core (GeoB3104-1), which was taken from the western tropical Atlantic, localized ~70 km from the North-eastern coast of Brazil (Fig. 2). The selected sedimentary time series contains an exceptionally preserved and thick deglacial transition with high resolution (sedimentation rate ~13 cm kyr-1), which has been explicitly used for characterizing the environmental changes through this period since the mid 90's (Arz et al., 1999; Voigt et al., 2017). The age model used in this study was adapted from Arz et al. (1998b). The upper 2.1 m of the total 5.2 m long gravity core was sampled in the core repository of MARUM (Germany), where in 10 cm intervals about 5 g of material was taken. Thus, in overall 21 samples were taken, covering the period from the last deglaciation to the Holocene. Each sample was wet-weighted and about 2 grams of material from each section was wet sieved over 63 μm and 150 μm mesh sieves. The residues (63-150 μm and >150 μm) were then dried at 40°C for 24 hours and in dry condition, five times in a random sequence weighed, with a Sartorius SE2 ultra-micro analytical balance with a nominal resolution of 0.1 μg. From the available 21 we selected 9 samples, from four important periods of the last 22.000 years: i) Last Glacial Maximum, ii) Heinrich Stadial I, iii) Younger Dryas and iv) Holocene. From each period, we used 2 samples, except for a sample from Heinrich Stadial I., where three samples were used. After the sample selection, both size fractions from each period were split into different representative aliquots. The LGM samples were split to 1/2 and 1/8 aliquots, the Younger Dryas samples to 1/2 and 1/8 aliquots, the Holocene samples to 1/4 and 1/16, while the entire sample has been used for the Heinrich Stadial I.

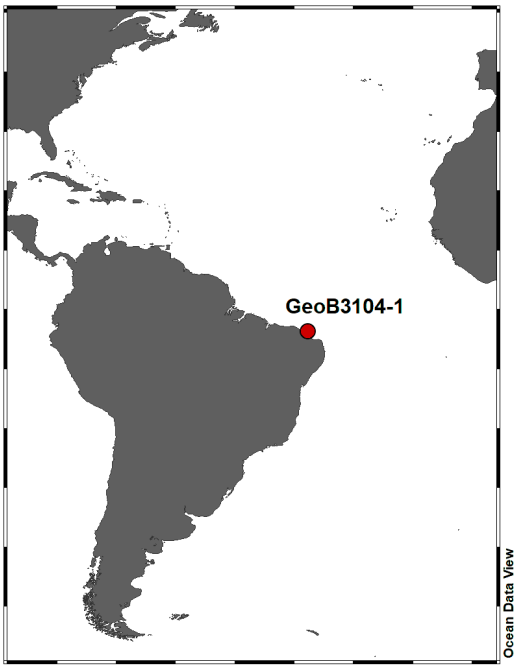

Figure 2. Location of sedimentary time series (GeoB3104-1) used in this study. The map was created by using software Ocean Data View v. 5.2.0 (Schlitzer, 2019).

In the 63-150 µm size fraction all foraminifera, without distinguishing species, were picked and weighed together. In the > 150 µm aliquots, all planktonic foraminifera shells were identified on species level based on the taxonomic concept of Schiebel & Hemleben (2017), Spezzaferri et al. (2015), Morard et al. (2019), and counted by using a Zeiss Stemi 2000 binocular microscope. All samples yielded spectacularly preserved foraminifera shells, but to facilitate the shell-weighing method we separated the perfectly preserved shells unfilled shells from those which showed signs of contamination or dissolution. Therefore, within each taxonomic category we distinguished between filled and unfilled specimens. We used only shells categorized as unfilled for the shell-weighing method, while for the shell flux and shell size interpretation we used a merged group involving filled and unfilled specimens.

For the size measurements, we used the filled and unfilled shells since sedimentary infill do not affect shell size. Foraminifera shells obtained from the 9 samples were mounted with their apertures facing upwards on custom-made micropaleontological slides with blue background. The measurements were done by using a Keyence VHX-S650E digital microscope. In overall, we measured the surface area (μm^2) of 7468 specimens assignable to 31 species. The

measurements include information about the surface area, maximum diameter, minimum diameter and perimeter of the shells. Here, we use the surface area as it highly correlates with other morphometric parameters, and it better captures the differences in shape, which is crucial for comparing size among different species (Brombacher et al., 2018; Moller et al., 2013).

The size measurements were followed by the shell-weighing method. For this approach, we used only the unfilled category of shells in order to exclude shells that are perhaps contaminated or affected by dissolution. The weighing was done in a random sequence as introduced by Weinkauf et al. (2016). The obtained average weight of species was further used for calculating the calcification intensity as the ratio of surface area and weight (see Beer et al., 2010).

The planktonic foraminifera shell fluxes were interpreted based on the ratio of the foraminifera shells number and sample volume (calculated as the ratio of wet weight of the sample and wet bulk density), multiplied by the accumulation rate. Following the minimum, median and maximum accumulation rates we determined the minimum and maximum possible shell flux. The planktonic foraminifera calcite fluxes were calculated based on the ratio of total mass of planktonic foraminifera (measured here) and the sample volume, multiplied by the accumulation rate. For the estimation of contribution of planktonic foraminifera to the calcium carbonate we used the dry bulk density measured by Müller, P. J. (2004) and measurements of calcium carbonate content of Arz et al. (1998a). Using these data, we calculated the mass accumulation of calcite by multiplying the dry bulk density by the mass of calcite and by the accumulation rate.

To facilitate the statistical analyses and visualization of the measurements, the data were loge transformed. The variability of shell flux, size, and calcification intensity in each sample was assessed using the geometric coefficient of variation (Kiss et al. 2021).

3. Results

The planktonic foraminifera calcite flux in the > 150 μm size fraction was the highest during the Last Glacial Maximum (Fig. 3A), when it ranged in the two samples together between a minimum 2.07 and 3.70 log(mg/cm^2/kyr). We documented the lowest calcite flux during the Heinrich Stadial I., ranging in the three samples together between 0.58 and 2.46 log(mg/cm^2/kyr). The planktonic foraminifera calcite fluxes in the Younger Dryas and the

Holocene samples were of similar magnitude, with calcite flux varying between a minimum 1.88 and maximum 3.48 log(mg/cm^2/kyr). The contribution of the individual planktonic foraminifera species to the shell and planktonic foraminifera calcite flux was variable in each sample (Fig. 3B, C). The total planktonic foraminifera shell flux in the > 150 µm showed large variability (Fig. 3C and 4) and a similar pattern across the four studied periods as observed in the planktonic foraminifera calcite flux (Fig. 3A), being the highest during the Last Glacial Maximum, ranging in the two samples together between a minimum 3.99 and 5.59 log(#/cm^2/kyr), slightly lower during the Holocene and Younger Dryas (Fig. 3C). The low planktonic foraminifera calcite flux during the Heinrich Stadial I. was also associated with lowest shell flux (Fig. 3), which ranged in the three samples together between a minimum 2.46 and maximum 4.64 log(#/cm^2/kyr). The planktonic foraminifera mean shell size and calcification intensity showed notable variability in the samples (Fig. 3E and Table S1), with the largest mean size difference between the Last Glacial Maximum and the Heinrich Stadial I., with foraminifera shells being 26 % smaller on average in the Heinrich Stadial I. samples than during the Last Glacial Maximum (80.41 vs 59.65 * 10^3 µm^2; Fig. 3E). We found the most heavily calcified shells also during in the Last Glacial maximum samples and the most lightly calcified shells in the Younger Dryas (Fig. 3F), with shells being 23 % less heavily calcified on average in the Younger Dryas than during the Last Glacial Maximum (15.68 vs 12.11 ([µg/µm^2])/10^5).

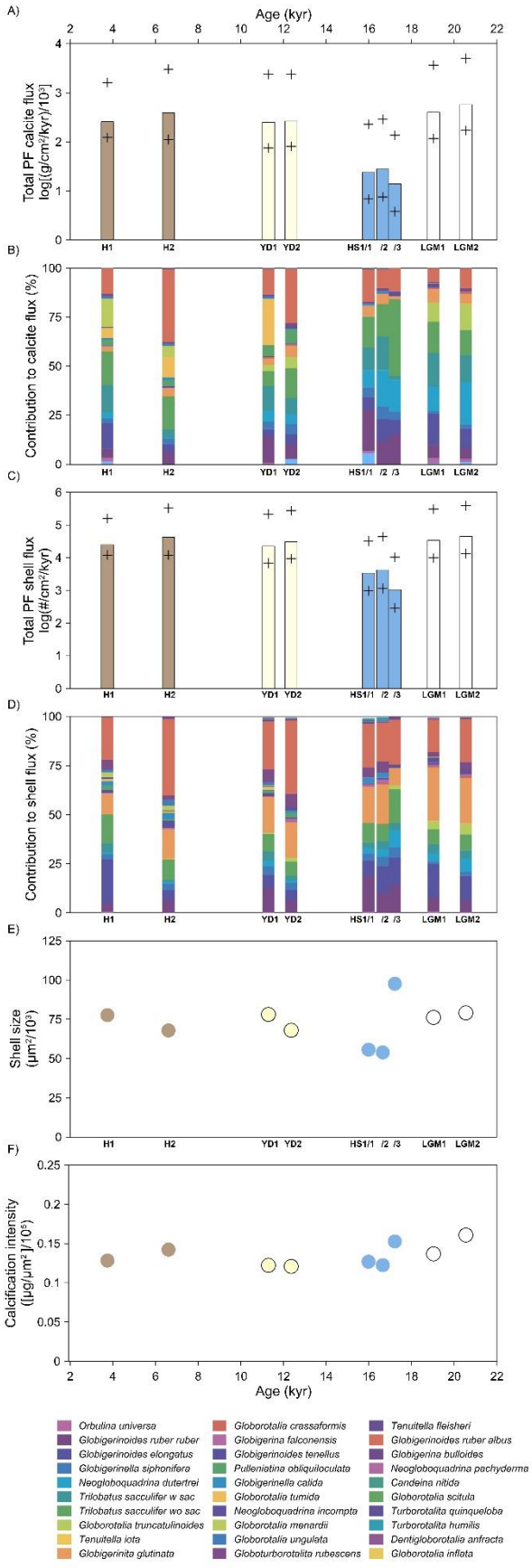

Figure 3. The planktonic foraminifera (A): total calcite flux (coloured bars); (B): contribution of the individual species to the total planktonic foraminifera calcite flux; (C): total planktonic foraminifera shell flux; (D): contribution of the individual species to the total shell flux; (E): mean shell size and (F): mean calcification intensity. Colours in (A, C, E) and (F) denote different samples (H1 – Holocene sample 1; H2 – Holocene sample 2; YD1 – Younger Dryas 1; YD2 – Younger Dryas 2; HS1/1, 2 , 3 – Heinrich Stadial I. sample 1, 2 and 3; LGM1 – Last Glacial Maximum sample 1; LGM2 – Last Glacial Maximum sample 2) and in (B) and (D) the individual species, which are always shown in the same order, species legend below. All data refer to foraminifera > 150 µm. The calcite and shell flux (A and C) indicate major changes across the last deglaciation, whereas shell size (E) and calcification intensity (F) remained relatively stable across the time.

Some species display low shell flux and are lightly calcified, thus their contribution to the calcite flux is lower than the contribution of some dominant species which have high shell flux of heavily calcified shells. The dominant group involves 11 species, which amount for more than 86 % of the variability in shell flux and more than 92 % of the variability in calcite flux (Fig. 5). In the next step we determined the coefficient of variations in each sample. The geometric coefficient of variation among the mechanisms displayed in each sample the highest variability in the shell flux and the lowest variability in shell size and calcification intensity (Fig. 4). After this, we tested the predictability of calcite flux by the modulating mechanisms with linear regression (Fig. 6), where the outcomes show a significant (p-value = <0.01) and very high positive correlation (r = 0.99) between the calcite flux and shell flux. In fact, the ~95 % of the variability in the calcite flux can be explained by shell flux.

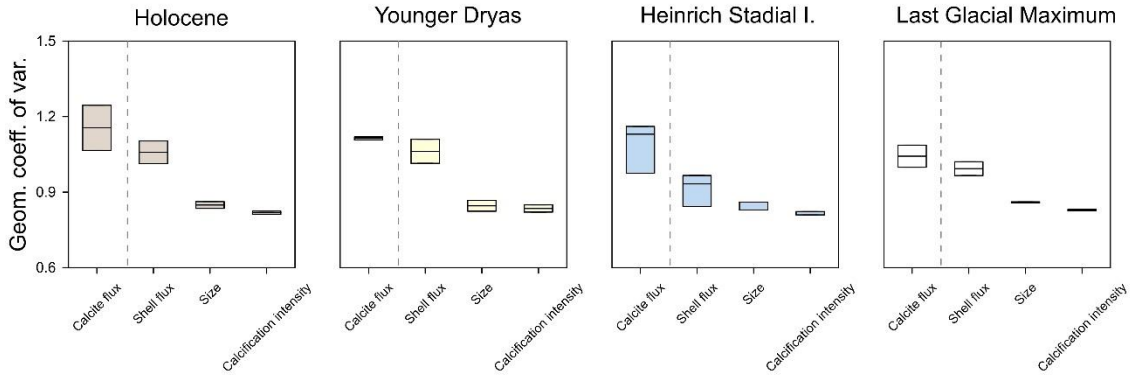

Figure 4. Variance of planktonic foraminifera calcite flux, shell flux, mean size and mean calcification intensity (weight/size), expressed as geometric coefficient of variation (geom. coeff. of var), plotted for the Holocene samples together, Younger Dryas samples together, Heinrich Stadial I. samples together and Last Glacial Maximum samples together. Boxes extend from the minimum to the maximum values and the horizontal line denotes the median. On the millennial timescales, the variance in the planktonic foraminifera calcite flux was only matched by the variance in the shell.

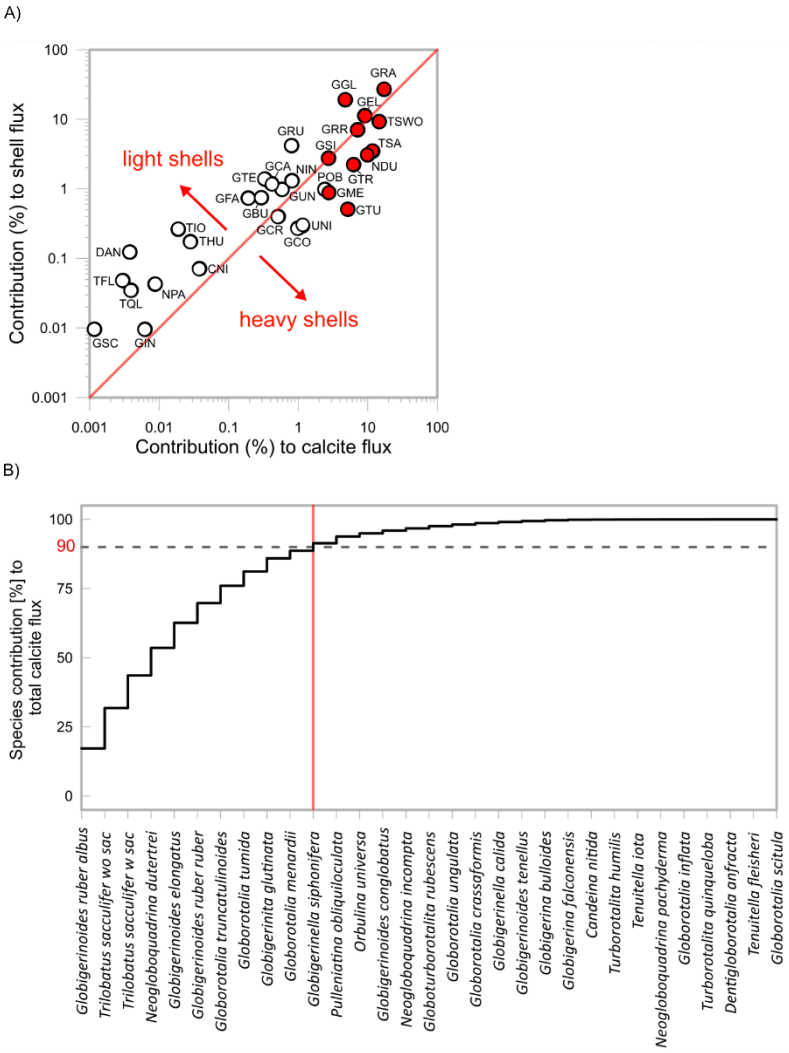

Figure 5. (A): relationship between the individual species shell flux and calcite flux. Red line in the background denotes the 1:1 relationship that allows distinction between lightly and heavily calcified species. The most abundant species (red filled symbols in A) from all samples combined account for more than 91 % of the total planktonic foraminifera calcite flux and more than 86 % of the shell flux (B).

Since shell flux appears the most relevant predictor, in the next step we focused on its composition. We analyzed the contribution of individual species shell fluxes to the total shell flux throughout the studied time-periods. The principal component analyses displayed that the species contribution across the studied time period changed (Fig. 7).

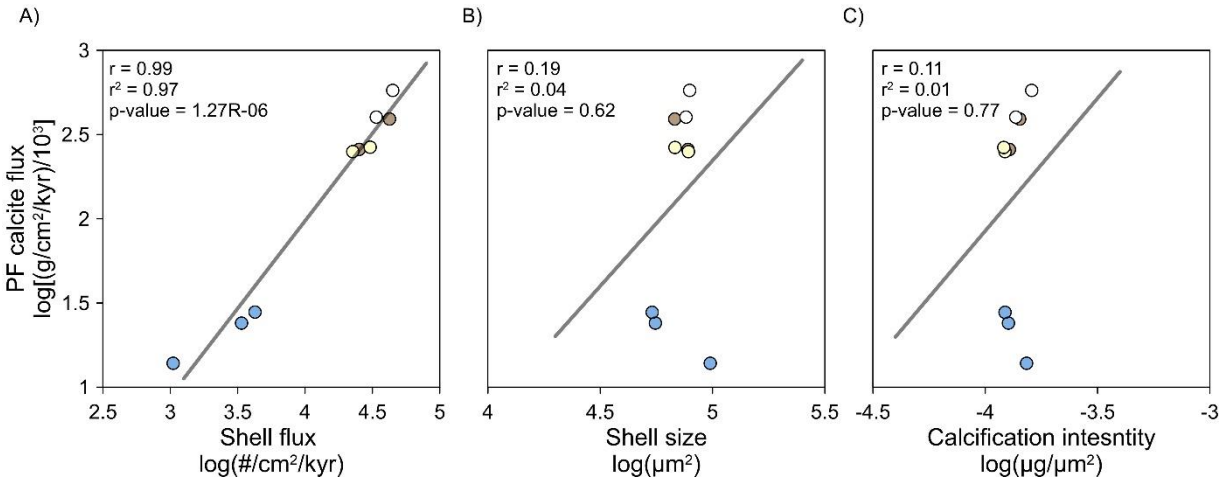

Figure 6. Predictability of the planktonic foraminifera calcite flux by using linear regression between the planktonic foraminifera calcite flux, shell flux (A), mean shell size (B) and mean calcification intensity (C), for the Holocene samples (brown filled symbols), the Younger Dryas samples (yellow filled symbols), the Heinrich Stadial I. samples (blue filled symbols) and the Last Glacial Maximum samples (open symbols). Summary statistics are given for each regression. On the millennial timescales, the shell flux appears as the most relevant predictor of planktonic foraminifera calcite flux.

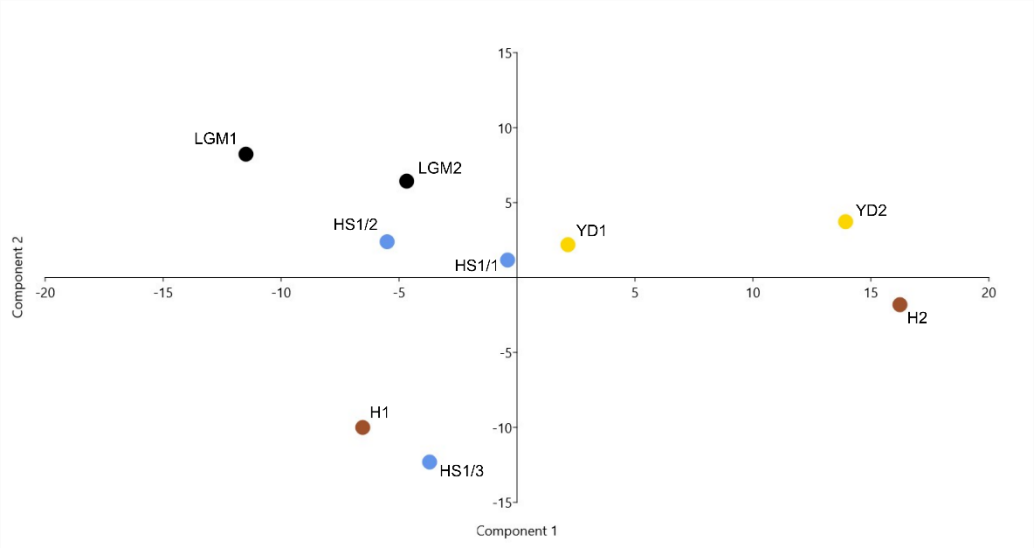

Figure 7. Principal component analyses of the individual species contribution to the total shell flux, calculated for each sample. Filled dots indicate different samples: Holocene samples (brown filled symbols), Younger Dryas samples (yellow filled symbols), the Heinrich Stadial I. samples (blue filled symbols) and the Last Glacial Maximum samples (open symbols). This analysis revealed that the individual species contribution to the total planktonic foraminifera shell flux varies between the samples as well as between the samples from the same time-period.

4. Discussion

4.1 Contribution of planktonic foraminifera to the total calcite flux

The contribution of planktonic foraminifera shells in the size fraction 63-150 µm to the total calcite flux ranged between 2.1 and 6 % (Fig. 8A). In contrast, the contribution of planktonic foraminifera in the > 150 µm size fraction to the total calcite flux varied from 1.7 to 19.1 % (Fig. 8A). The relatively high proportion of planktonic foraminifera in the 63-150 µm size fraction during the Heinrich Stadial I. is similar to the contribution of planktonic foraminifera in the > 150 µm size fraction (2.4 %), which highlights the importance of planktonic foraminifera in the 63-150 µm size range that contribution is often insignificant compared to the > 150 µm size fraction (Salmon et al., 2015; Schiebel, 2002; Schiebel et al., 2007). However, there is a possibility that the high contribution of planktonic foraminifera shells in the 63-150 µm size fractions are biased, since the foraminifera shells in this size fraction are impossible to categorize into filled and unfilled groups. Therefore, all shells were weighed together, and we cannot rule out the chance that the foraminifera shells in the 63-150 size fractions were contaminated, which explain their higher shell weight and high contribution to the total calcite flux. In the remaining samples, the contribution of foraminifera shells in the > 150 µm size fraction were at least three-times higher than the contribution of foraminifera shells in the 63-150 µm size fraction, which implies that the > 150 µm size fraction is sufficient to investigate the mechanisms modulating the planktonic foraminifera calcite flux.

In overall, the planktonic foraminifera shells in the > 63 µm size fraction (63-150 µm and > 150 µm in the size fraction > 63 µm together) made up during the Last Glacial Maximum 24 %, Heinrich Stadial I. 4.5 % and Holocene 17.4 % of the total calcite flux (Fig. 8B), which is at the lower end of the estimated global contribution of planktonic foraminifera to the total calcite flux ranging between 20-50 % (Schiebel et al., 2007). The low contribution of planktonic foraminifera to the total calcite flux highlights the importance of other calcifying organisms in terms of their contribution to the total calcite flux (Baumann et al., 2004; Schiebel et al., 2007). The fact that the contribution of planktonic foraminifera in the > 150 µm size fraction display high positive correlation with the total calcite flux ($r = 0.93$, p-value = 2.42E-04; Fig. 8B) indicate that the variability in the calcite flux reflects changes in the shell flux.

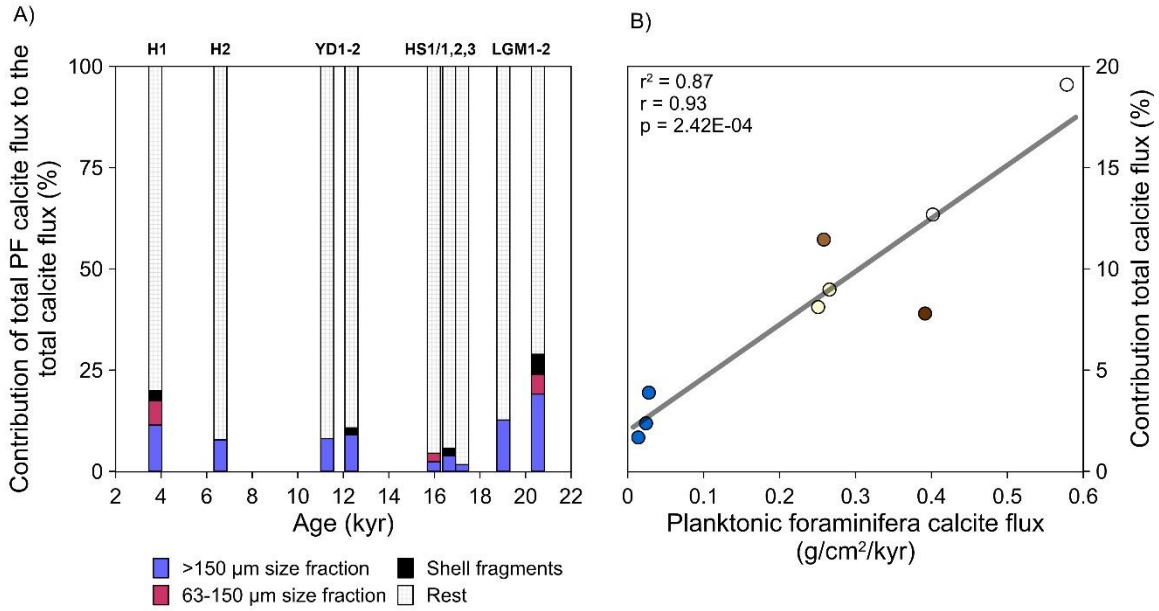

Figure 8. (A): bar charts are showing the contribution of planktonic foraminifera > 150 µm size fraction, planktonic foraminifera 63-150 µm size fraction and the planktonic foraminifera shell fragments to the total calcite flux across the studied time periods (H1 – Holocene sample 1; H2 – Holocene sample 2; YD1-2 – Younger Dryas sample 1 and sample 2; HS1/1, 2 ,3 – Heinrich Stadial I. sample 1, sample 2 and sample 3; LGM1-2 – Last Glacial Maximum sample 1 and sample 2). (B): linear regression between the planktonic foraminifera calcite flux and the contribution of planktonic foraminifera > 150 µm size fraction to the total planktonic foraminifera calcite flux shown for the Holocene samples (brown filled symbols), Younger Dryas samples (yellow filled symbols), the Heinrich Stadial I. samples (blue filled symbols) and the Last Glacial Maximum samples (open symbols). Summary statistics is given for the regression. The high positive correlation between the calcite flux and the contribution of planktonic foraminifera in the > 150 µm size fraction, indicates that the variability in the planktonic foraminifera calcite flux reflects changes in the shell flux.

4.2 Predictors of long-term variability in planktonic foraminifera calcite flux

The highest drop in the efficiency of the planktonic foraminifera calcite flux is observed between the Last Glacial Maximum and the Heinrich Stadial I. (Fig 3.). This decrease in calcite flux is echoed by low shell flux, which plausible explain that the changes in the calcite flux during the Heinrich Stadial I. were driven by shell flux. However, we do not know which mechanisms drove the changes in the calcite flux in the remaining time-periods.

On the millennial timescale, shell flux showed constantly the highest variability in each sample. Considering all samples together, shell flux at population level varied by a factor of 43 (Fig. 4). The fact that the shell flux matched the variability in calcite flux (factor of 42) across the last deglaciation indicates that shell flux likely changed dramatically across major climate transitions with the calcite flux. Shell flux on the millennial timescale displayed considerably lower variability than on the intra-and interannual timescales (factor of 43 vs ~280; Jonkers & Kučera, 2015; Žarić et al., 2006; Kiss et al., 2021), which could result from the fact that short-term variability in shell flux is influenced by seasonal changes in environmental conditions, which is masked in the long-term shell flux variability.

Shell size and calcification intensity showed much lower variability than shell flux, while on the population level shell size varied by a factor 1.8 and calcification intensity by a factor 1.3 (Fig. 4). The low variability in shell size and calcification intensity is in line with previous observations, although there are only a few observations documenting their variability on a population level. However, on species level the literature review revealed similar variability, for instances, in the North Atlantic, shell size of *Globigerina bulloides* varied by a factor of 1.3 and calcification intensity by a factor of 1.9 during the past 45.000 years (Barker & Elderfield, 2002). Similarly, calcification intensity of species *Pulleniatina obliquiloculata* varied by a factor 1.4 throughout the past 250 kyr (Qin et al., 2020) and in the Mediterranean Sea, shell size varied by a factor of 1.5 and calcification intensity by factor of 3.4 among four species of planktonic foraminifera between 126–121 kyr (Weinkauf et al., 2013). In contrast, the variability in shell size and calcification intensity in modern assemblages captured by sediment trap time series is slightly higher, for example shell size varies by a factor between 2 to 6 (Deuser et al., 1981; Weinkauf et al., 2016). Values above thus indicate that shell size and calcification intensity in terms of the long-term variability in calcite flux are not so significant as shell flux.

This can be potentially the results of intrinsic growth limitations of foraminifera shells constructed by sequentially arranged chambers (Raup, 1966) that sets minimum and maximum limits on adult shell mass, whereas the high variability in shell flux reflects the connection between the species habitat and the environmental conditions (Žarić et al., 2005).

On the millennial timescale, shell flux was constantly the most variable component of the planktonic foraminifera calcite flux and also its best predictor (Fig. 4 and 6). Shell size explained only a small proportion of the calcite flux variability and calcification intensity was the least variable (Fig. 4) and the least important mechanism for predicting the long-term variability in calcite flux (Fig. 6). These inferences imply that on the long-term timescales, by knowing the shell size and mean shell flux combined with mean calcification intensity, the magnitude of planktonic foraminifera calcite flux variability can be predicted with 32.2 % accuracy (root mean square error normalized to range; NRMSE; Table 1). A more accurate prediction can be achieved by the knowledge of shell flux and mean size and mean calcification intensity when the prediction accuracy could reduce the error to 9 %. By introducing shell size or calcification intensity into the models, only marginal improvement of the prediction accuracy can be made (NRMSE 6.2 – 6.4%; Table 1). Apparently, shell flux is the most important predictor, and slight improvements of the model accuracy can be achieved by involving shell size and calcification intensity, but these results show the outstanding importance of shell flux in predicting changes in the planktonic foraminifera calcite flux.

		Assuming same shell flux and same calcification intensity between the year, but variable size	Assuming the same size and calcification intensity among species	Assuming the same size, but variable calcification intensity among species	Assuming variable size, but the same calcification intensity among species
Millennial timescale	RMSE [mg/m²/day]	181.80	50.60	36.11	34.98
	NRMSE [%]	32.2	9	6.4	6.2

Table 1. Prediction accuracy of planktonic foraminifera calcite flux based on the knowledge of different modulating mechanisms on long-term (millennial) timescales. Mean residuals (root mean square error, RMSE) and RMSE normalized to the range (NRMSE) between the observed calcite flux and the calculated hypothetical calcite flux is listed for each scenario, and the errors are shown as absolute numbers and percentages. It appears that on the millennial timescales an

accurate prediction can be made by the knowledge of shell flux and mean size and calcification intensity (9 % NRMSE), while involving shell mass results only into marginal improvements (6.2 – 6.4 % NRMSE).

4. 3 The importance of species composition in the planktonic foraminifera calcite flux

The total planktonic foraminifera shell flux is the product of the individual species shell fluxes. On the millennial timescales we can determine that different species contributed variable to the calcite flux (Fig. 3 B and D). There are some species that contribution was larger than the others (Fig 5.), which emphasize the species composition as an important mechanism modulating the long-term variability in the planktonic foraminifera calcite flux. Since the changes in the individual species calcification intensity varied the least (factor of 1.3; Fig. 4) and are insignificant for predicting the variability in the calcite flux, we focused on the individual species shell size variability across the observed ~22.000 years. The ANOVA test revealed that the shell size did not change significantly through time, and that the observed changes in shell size are due to the individual species, which in fact explain 85 % (p-value = < 0.01) of the variability in the shell size variability. There are only a few species (4 out of 31 species), including *Dentigloborotalia anfracta*, *Globorotalia crassaformis*, *Globorotalia menardii* and *Globorotalia truncatulinoides*, which changes in size were significant through time (p-value = < 0.01), but these species cumulative comprise only ~9 % of the total planktonic foraminifera calcite flux (Fig. 5).

The principal component analyses revealed that the contribution of individual species to the shell flux and calcite flux was different in the studied samples. Some similarities between the samples could be observed, but we do not see a clear pattern allowing to group the samples based on the individual species contribution to calcite and/or shell fluxes (Fig. 7). It means that total planktonic foraminifera shell flux and calcite flux had different composition and variable contributions of individual fluxes throughout the studied periods. In fact, the moderate correlation between the planktonic foraminifera calcite flux and the first principal component scores indicate that the planktonic foraminifera calcite flux reflects changes in the individual species contribution (Fig. 9). For the final interpretation this still mean, that predictions of variability in the planktonic foraminifera calcite flux will require shell flux, which is the most variable component of the calcite flux and its best predictor. However, for instances the

Holocene assemblages, displayed that the individual species contribution and the assemblage composition can be a mechanism modulating the variability in the planktonic foraminifera calcite flux, but of course, to a lesser degree than the shell flux.

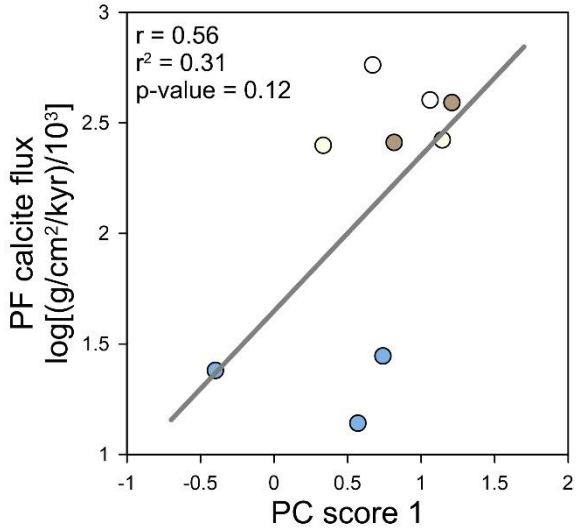

Figure 9. Linear regression between the planktonic foraminifera calcite flux and the first principal component scores (Fig. 7). Colours in denote different samples: Holocene samples (brown filled symbols), Younger Dryas samples (yellow filled symbols), the Heinrich Stadial I. samples (blue filled symbols) and the Last Glacial Maximum samples (open symbols). The moderate correlation between the two parameters imply that the planktonic foraminifera calcite flux reflects changes in the individual species contribution.

5. Conclusion

The planktonic foraminifera calcite flux is an important compound of the pelagic carbon cycle. A species-resolved shell flux, shell size and calcification intensity data of planktonic foraminifera obtained from sedimentary time series (GeoB3104-1) from the tropical Atlantic allowed us to assess the response of the planktonic foraminifera calcite flux and its modulating mechanisms (shell flux, shell size and calcification intensity) on large amplitude environmental changes during the last deglaciation. Our results indicate that the variability in the planktonic foraminifera calcite flux during the Last Glacial Maximum, Heinrich Stadial I., Younger Dryas and Holocene was driven by the shell flux. Shell flux appeared across the last deglaciation constantly the most variable component of the planktonic foraminifera calcite flux and its best predictor. Shell size and calcification intensity varied negligible; we did not determine the effect of Ice Age on planktonic foraminifera shell mass.

		Holocene sample 1	**Holocene sample 2**	**Younger Dryas sample 1**	**Younger Dryas sample 2**	**Heinrich Stadial sample 1**	**Heinrich Stadial sample 2**	**Heinrich Stadial sample 3**	**LGM sample 1**	**LGM sample 2**
Globigerinoides ruber albus	Shell flux	5501.7	16533.5	5486.2	11366.0	750.2	839.3	239.8	5660.4	9855.8
	Shell size	55.3	53.3	57.2	57.6	51.7	37.0	64.8	42.8	51.6
	Calc. int.	16.2	23.1	13.9	15.2	14.6	12.6	15.9	14.6	14.9
Trilobatus sacculifer wo sac	Shell flux	3681.4	4313.1	2001.7	2169.7	335.2	373.0	184.4	2623.1	3619.8
	Shell size	95.2	105.6	81.6	117.4	76.8	77.8	143.6	124.2	122.5
	Calc. int.	20.6	23.4	18.3	26.5	20.3	25.7	36.7	31.0	27.2
Trilobatus sacculifer w sac	Shell flux	1222.6	575.1	1037.9	736.5	95.8	167.9	36.9	1518.6	1845.7
	Shell size	177.9	219.9	200.9	164.3	131.2	166.6	54.1	221.8	206.8
	Calc. int.	30.6	15.2	26.0	31.1	46.9	28.9	20.1	32.7	31.9
Neogloboquadrina dutertrei	Shell flux	190.2	287.5	667.2	418.0	95.8	167.9	92.2	1380.6	3100.1
	Shell size	171.1	153.8	152.4	144.8	114.6	146.6	167.2	150.0	154.3
	Calc. int.	35.0	5.8	19.1	28.5	26.9	36.9	20.7	28.2	37.4
Globigerinoides elongatus	Shell flux	5610.3	2156.5	1482.8	1652.2	255.4	578.2	147.5	5867.5	5698.4
	Shell size	52.8	57.3	52.2	64.4	40.1	48.5	55.3	76.0	71.4
	Calc. int.	15.3	18.4	18.6	17.1	20.4	15.8	16.3	18.4	18.4
Globigerinoides ruber ruber	Shell flux	1100.3	2731.6	2817.2	1891.0	622.5	429.0	147.5	2347.0	2634.2
	Shell size	75.7	73.4	91.1	83.8	67.5	77.0	130.0	82.2	92.4
	Calc. int.	22.0	16.5	21.2	18.3	17.7	16.0	14.8	21.7	19.7
Globorotalia truncatulinoides	Shell flux	13.6	NA	222.4	617.1	NA	NA	18.4	1380.6	2401.2
	Shell size	65.4	NA	172.2	149.2	NA	NA	202.0	156.1	169.4
	Calc. int.	10.6	NA	25.3	24.3	NA	NA	NA	24.0	29.3
Globorotalia tumida	Shell flux	258.1	431.3	370.7	NA	NA	NA	NA	NA	NA
	Shell size	204.3	377.0	490.5	NA	NA	NA	NA	NA	NA
	Calc. int.	42.4	30.3	46.1	NA	NA	NA	NA	NA	NA
Globigerinita glutinata	Shell flux	2689.7	6325.9	4077.6	5533.7	622.5	857.9	92.2	9111.9	10411.3
	Shell size	35.2	35.0	35.8	41.2	26.9	26.6	40.3	39.0	40.9
	Calc. int.	8.5	8.8	7.3	7.9	10.4	9.3	7.2	8.7	8.3
Globorotalia menardii	Shell flux	624.9	1006.4	74.1	NA	NA	NA	NA	138.1	NA
	Shell size	366.3	197.0	133.1	NA	NA	NA	NA	56.2	NA
	Calc. int.	23.6	20.8	4.9	NA	NA	NA	NA	7.0	NA
Globigerinella siphonifera	Shell flux	679.2	1437.7	963.8	1035.1	127.7	205.2	55.3	414.2	824.3
	Shell size	102.7	90.2	80.3	123.8	86.3	80.0	101.4	109.9	125.2
	Calc. int.	12.3	11.9	16.8	14.3	14.0	17.8	14.5	14.6	15.1

Table S1. Mean size, mean shell weight and mean calcification intensity (weight/size; Calc. int.) of the most dominant planktonic foraminifera (Fig. 5), listed separately for each studied time-period and sample.

Chapter 3

Calcification intensity in the planktonic foraminifera *Globigerina bulloides* under different climatic conditions

This work is in preparation for submission.

P. Kiss[1,2*], L. Jonkers[2], N. Hudáčková[1], M. Golej[3] and M. Kučera[2]

[1]Department of Geology and Paleontology, Comenius University in Bratislava, Bratislava, Slovakia.

[2]MARUM - Center for Marine Environmental Sciences, University of Bremen, Bremen, Germany.

[3]Earth Science Institute, Slovak Academy of Sciences, Bratislava, Slovakia.

*Corresponding author: Peter Kiss (pkiss@marum.de)

Abstract

Through biomineralization of calcite, planktonic foraminifera fix large amounts of dissolved inorganic carbon in their shells, which is after the death of the organisms exported to the sea floor. The production of planktonic foraminifera calcite, releases carbon dioxide into the ambient seawater, which offsets the oceanic capacity of carbon dioxide sequestration. Therefore, a better understanding of how the different calcification aspects of planktonic foraminifera responded to distinct sea-surface temperature and carbon dioxide forcing in the past is crucial, and also required for more accurate predictions of planktonic foraminifera calcification under future climate change. To assess the calcification aspects of planktonic foraminifera in the geological past, we generated a record of shell size, calcification intensity (shell weight/size) and shell wall thickness data of well-preserved *Globigerina bulloides* specimens from mid-Miocene sediments in the Devínska Nová Ves (DNV, Slovakia) area. The investigated specimens were obtained from the period of the Middle Miocene Climate Transition (13.6-12.7 Ma years), when they calcified under a climatic setting immediately postdating the prominent Miocene climatic optimum with high carbon dioxide content. We compared the inferences with the calcification intensity of *Globigerina bulloides* from modern assemblages collected by sediment trap times series (from 1990-1991 and 2007-2008) from the Cape Blanc upwelling area (Atlantic Ocean), representing an environment with generally warm climate and elevated atmospheric carbon dioxide concentration (> 350 ppm). Our results indicate negligible shell size difference between the modern and mid-Miocene specimens, since the mean shell size of *Globigerina bulloides* was only 3 % larger in the modern assemblages than in the mid-Miocene samples. However, we found a larger difference in the calcification intensity, with *Globigerina bulloides* shells being 30 % more heavily calcified in the mid-Miocene than in the modern assemblages. Therefore, this implies that the long-term evolution of *Globigerina bulloides* under a generally warmer climate and elevated atmospheric carbon dioxide concentration, did not translate to substantial shell size or to a pronounced calcification intensity difference.

1. Introduction

The past 17 million years contain key periods of changes in sea-surface temperature and carbon cycle (Herbert et al., 2016; You et al., 2009). The climate proxies indicate a warm global climate

occurring during the Miocene Climatic Optimum (MCO, from 17 to 14.5 Ma) due to strong carbon dioxide forcing causing approximately 15°C higher sea-surface temperatures compared to present (Super et al., 2018). In the Serravallian (Late Badenian), the MCO was followed by the Middle Miocene Climate Transition (MMCT), when sea-surface temperature cooled down and the atmospheric concentration of carbon dioxide decreased below 290 ppmv (Fig. 1). Thus, in terms of the atmospheric carbon dioxide concentration, the MMCT was similar to the pre-industrial CO_2 levels (Wigley, 1983). Across the past 200 years we observe a continuous increase of atmospheric carbon dioxide concentration, culminating into levels > 400 ppmv at present due to strong industrial activities (Tans & Keeling, 2020). As atmospheric carbon dioxide dissolves into the global ocean, it is altering the marine ecosystems by lowering the sea water's pH and thus the ocean becomes more acidic. In addition, ocean acidification lowers the carbonate ion concentration required for calcite shell production (Comeau et al., 2009; Riebesell et al., 2000). The climate transition since the Serravallian marks a major step towards the present icehouse climate, which provides us an opportunity to assess the response of calcification aspects of marine calcifiers under different environmental forcing and to model future global climate change scenarios.

Planktonic foraminifera are marine calcifiers that represent a crucial component of the global carbon cycle. Through the formation of calcite, they fix large amounts of dissolved inorganic carbon in their shells which is then exported to the seafloor. The resulting calcite flux represents up to half of the pelagic calcite flux (Schiebel, 2002; Schiebel et al., 2007), while the rest is created by coccoliths (Baumann et al., 2004; Milliman, 1993). The production of calcite reduces the oceanic alkalinity, since the biomineralization of calcite releases carbon dioxide into the ambient seawater (Frankignoulle & Canon, 1994; Zeebe & Wolf-Gladrow, 2001) that counterbalances the strength of carbon dioxide sequestration by the biological pump. The calcification of planktonic foraminifera and coccoliths display changes in response to different climate conditions over the geological past. For example, a recent work shows a decreasing trend of coccoliths calcification intensity since the mid-Miocene to the Holocene (Bolton et al., 2016). Considering the results by Barker & Elderfield (2002), the observed (de Moel et al., 2009; Zarkogiannis et al., 2019), and anticipated changes (Lombard et al., 2011) concerning planktonic foraminifera calcification under different climate conditions, we could expect

enhanced calcification under colder climatic conditions, thus more heavily calcified specimens in the mid-Miocene.

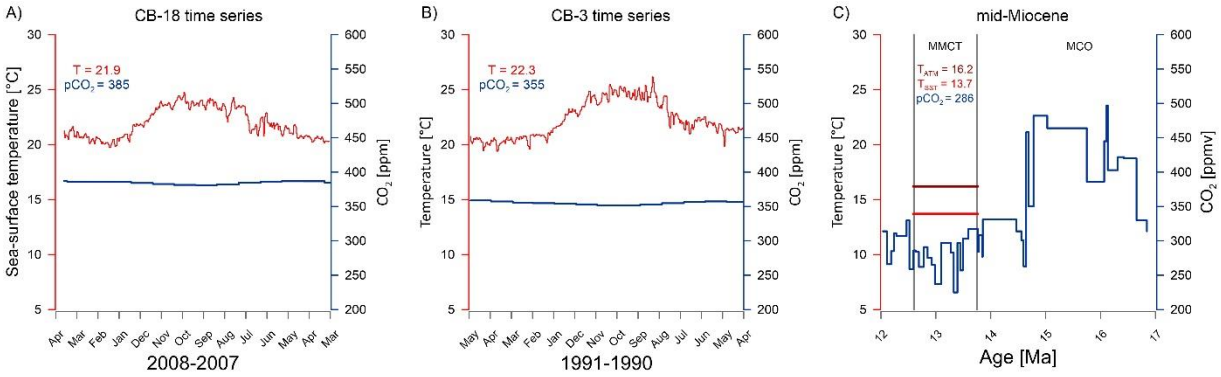

Figure 1. Sea-surface temperature (red line) and CO_2 (blue line) and their variability during (A): Cape Blanc time series 2007-2008 (CB-18); (B): Cape Blanc time series 1990-1991 (CB-3); (C): the mid-Miocene, throughout the Middle Miocene Climatic Transition (MMCT) and the Miocene Climatic Optimum (MCO), grid lines on the X axis indicate the age of the Devínska Nová Ves samples. Mean CO_2 and annual mean sea-surface temperature for each studied period is shown with red, in addition atmospheric temperature (T_{ATM}) for mid-Miocene is shown with dark red (C). Sea-surface temperature data for CB time series were taken from Reynolds et al. (2007), CO_2 data for CB time series were taken from the NOAA CO_2 monitoring program, while CO_2 data for the mid-Miocene was taken from Super et al. (2018). Sea-surface temperature estimations for mid-Miocene were taken from Kováčová and Hudáčková (2009; T_{SST}) and atmospheric temperature from Doláková et al. (2020).

The degree of calcification in planktonic foraminifera is reflected by their shell wall thickness. Species that are more heavily calcified possess thicker shell walls, while lightly calcified species have thinner shell walls (de Moel et al., 2009). In general, deeper-dwelling species have thicker shell walls and they usually bear a crust, which increases their shell mass (Salmon et al., 2015). The shell wall thickness varies in space and time, between the species and also within the species (Lombard et al., 2010; Moy et al., 2009; Weinkauf et al., 2016). It can be determined based on the species shell weight and size ratio, which provides information about the amount of calcite in a shell in relation to its size (Beer et al., 2010; Henehan et al., 2017). However, the shell weighing method requires perfectly preserved foraminifera shells with empty chambers and thus determining calcification with the shell-weighing method is mostly suitable among Holocene specimens. At present, several studies exist that investigated the connection between the

environmental parameters and calcification intensity. Most of them found that changes in the calcification intensity are caused by changes in the carbonate system (Barker & Elderfield, 2002; Bijma, J. et al., 2002; Lombard et al., 2010; Marshall et al., 2013), temperature (Qin et al., 2020), salinity (Allen et al., 2016) or nutrient availability (Aldridge et al., 2012). Since some of these factors are connected, such as temperature and atmospheric carbon dioxide concentration, it makes it difficult to find a singular parameter responsible for various calcification intensity among planktonic foraminifera. Planktonic foraminifera species *Globigerina bulloides* are often used in paleoceanographic and climate studies (e. g., Davis et al., 2013). These species during periods when seawater carbonate saturations are higher, calcify more intensively (Barker & Elderfield, 2002; Moy et al., 2009) and thus possess thicker shell walls. Since calcification intensity of planktonic foraminifera could have an extensive impact on the oceans carbon dioxide sequestration, it is crucial to understand its variability under different climatic conditions for predicting its behaviour under future climate change scenarios.

Here, we measured the size, calcification intensity and shell wall thickness of *Globigerina bulloides* from mid-Miocene sedimentary samples collected in the area of Devínska Nová Ves (Slovakia, Fig. 2 and 3). These specimens archive in their shells the degree of calcification under low sea-surface temperature and low atmospheric (and oceanic) carbon dioxide concentration. We compare this data with the calcification aspects of *Globigerina bulloides* obtained from modern assemblages captured by sediment trap time series moored in the Atlantic Ocean (1990-1991 and 2007-2008), which specimens represent the degree of calcification of *Globigerina bulloides* under generally warmer climate and elevated atmospheric and oceanic carbon dioxide concentration. In this way, we compare how the long-term evolution of *Globigerina bulloides* under different climatic conditions and carbonate chemistry translated to different shell size, calcification intensity and shell wall thickness.

2. Material and Methods

The most important prerequisite for assessing the calcification intensity of planktonic foraminifera by using the shell-weighing method is the spectacular preservation of foraminifera shells. This means that the shells must be empty and translucent, allowing to obtain only the weight of the shells without any contribution from sedimentary infill. Thus, we use well-preserved specimens of *Globigerina bulloides* from the sediment trap mooring array off Cape

Blanc (CB, Atlantic Ocean), for assessing the calcification intensity of specimens from modern assemblages, which calcification underwent under generally warm sea-surface temperature and constantly rising atmospheric carbon dioxide concentration. From the available long-term time series record off Cape Blanc, we selected 1990-1991 (CB-3) and 2007-2008 (CB-18), which is reported to yield foraminifera suitable for shell weighing. Sample treatment of CB samples is given by Kiss et al. (2021).

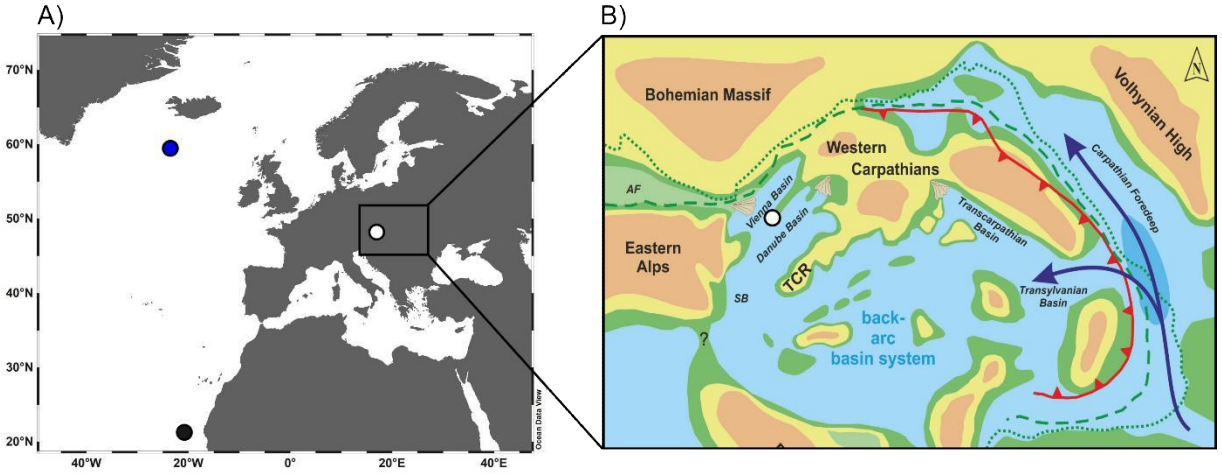

Figure 2. (A): Position of the sediment trap mooring off Cape Blanc (filled symbol), Devínska Nová Ves site (open symbol) and the location of NEAP 8K sediment core (Barker & Elderfield, 2002) discussed in this study (blue symbol); (B): mid-Miocene paleogeography of the Central Paratethys with the location of DNV site (open symbol). The map in (A) was plotted with Ocean Data View v. 5.2.0 (Schlitzer, 2019), whilst the paleogeographic reconstruction of mid-Miocene Central Paratethys was taken from Kováč et al. (2017).

The geological past contains key periods of changes in sea-surface temperature and atmospheric carbon dioxide concentration, which allow us to study the response of foraminifera calcification under such conditions. The Serravallian (Late Badenian, 13.6-12.7 Ma years) climate is characterized by a transition and simultaneous atmospheric carbon dioxide decrease, with similar sea-surface temperature to the present Black Sea (Shapiro et al., 2010). To obtain well-preserved planktonic foraminifera specimens from this period, we use samples from the Devínska Nová Ves outcrop that is situated in the Vienna Basin (Slovakia, Fig. 2 and 3). The 15 m long DNV profile covers several stages of the Serravallian, but we focused on the upper 2.8 m long sequence covering the period of the MMCT during the Serravallian. We selected 5 out of the 23 available samples, which sample treatment is given by Kováčová & Hudáčková (2009). Specimens of *Globigerina bulloides* were picked from >125 μm size fractions and

counted in 1/16 or 1/32 aliquots using a Zeiss Stemi 2000 binocular microscope. The identification is based on the taxonomic concept of Schiebel & Hemleben (2017) and Kennett & Srinivasan (1983). Despite the samples yielded perfectly preserved shells of *Globigerina bulloides*, we separated filled from unfilled specimens. This was important to ensure that only specimens with unfilled shells are used for the shell-weighing method, since the determination of calcification intensity in this way in "old" material (= pre-Quaternary) from consolidated sediments is difficult because of invariable contamination by adhering sediment inside the shell.

To prove that we correctly separated the unfilled and filled shells of *Globigerina bulloides*, as well as to measure the specimens shell wall thickness, we randomly selected two specimens from the unfilled category from each DNV sample and from 7 cups of the 2007-2008 (CB-18) time series and observed them in polished thin sections. The selected two specimens from the CB and DNV samples were placed uniformly, with their aperture facing upwards, on a double-sided tape. After the shell fixation, a cylinder-shaped silicone holder was placed on the tape with the shells in the centre to create a barrier for the liquid epoxy rexin. After the preparation of the epoxy mixture the silicone holder was filled with it and left to harden for 24 hours at room temperature (22°C). Afterwards, the samples were hand grinded on a glass plate using SiC powder F800 to reach the required level (in order to perform a cut of the last three chambers). In cases where empty/unfilled chambers occurred, the grinding process was stopped, and the shell chambers were filled again with epoxy resin to avoid shell damage during the next grinding. The process of grinding was repeated after the hardening in the same process finished with SiC powder F1200. The samples were then cleaned in ultrasonic cleaner and polished using 1micron diamond solution for approximately 20-25 min under low pressure. The processed thin sections were afterwards imaged using a Zeiss Stemi 508 stereo microscope and ZEN 3.3 (blue edition) software at a resolution of 0.22 µm x 0.22 µm per pixel. The wall thickness of the penultimate and ultimate chambers was then extracted from the processed two-dimensional cross-sectional images (Fig. 3b).

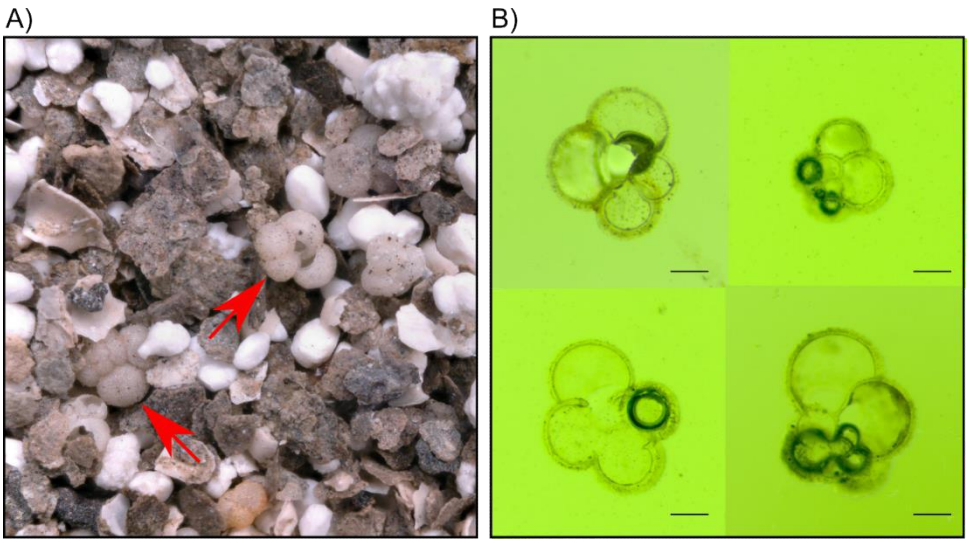

Figure 3. (A): Preservation of *Globigerina bulloides* specimens at the Devínska Nová Ves site. Arrows point towards well-preserved and empty individuals suitable for the shell-weighing method, (B): Polished thin sections of *Globigerina bulloides* picked from the DNV samples. Scale bar 100 μm. This method proves the excellent preservation of specimens that do not show sedimentary infill inside the chambers influencing their shell weight. The thick and round-shaped infills that are visible in the interior of each specimen are air bubbles, which are created during the preparation of polished thin sections.

Afterwards, the shell size of *Globigerina bulloides* was measured by using a Keyence VHX-S650E digital microscope. The filled and unfilled shells of *Globigerina bulloides* were uniformly oriented with their aperture facing upwards on micropaleontological slides and photographed under 300x magnification, yielding a resolution of 1.4663 μm per pixel. The images created with the digital microscope were segmented with the Keyence 3D Shape Measurement Software v. 1.00, which automatically identifies the foraminifera shells by combining elevation information with colour images of the surface of the slide and an elevation model at 5 μm resolution. After this, the segmented foraminifera shells were characterized with maximum size, minimum size, perimeter and surface area. From the suite of these parameters, we use surface area, as it captures the most effectively the differences in shape (Brombacher et al., 2018; Moller et al., 2013).

The size measurements were followed by the shell-weighing method, for which we used only the unfilled category of *Globigerina bulloides*. These unfilled shells from each DNV sample were placed in three-times, pre-weighed, aluminium weighing boats. The samples in the weighing boats were then left for 24 hours in the weighing laboratory to acclimate with the room

moisture. The weighing of specimens was performed in a random sequence, each sample five times, following Weinkauf et al. (2016) with a Sartorius SE2 ultra-micro analytical balance with a nominal resolution of 0.1 µg. After weighing, the average shell weight of the specimens was determined, which was further used to calculate the specimen's calcification intensity (see Beer et al., 2010). We calculated the calcification intensity as the ratio of shell weight divided with the specimen's surface area.

To facilitate the statistical comparison of size measurements, which were picked from different CB (> 150 µm) and DNV (> 125 µm) size fractions, we harmonized the obtained size data. This was done by filtering the size measurements of DNV samples based on the minimum maximum shell size measured in the CB samples. In this way we excluded shells smaller than > 150 µm from the DNV samples and used the obtained data for further analyses.

3. Results

At first, we compared the environmental conditions during the studied time periods (Fig. 1). The mean sea-surface temperature during the 1990-1991 and 2007-2008 time series was slightly over 22 °C (Reynolds, R. W. et al., 2007) and both time series were associated with generally high atmospheric CO_2 concentrations that exceeded 350 ppmv (Tans & Keeling, 2020). On the other hand, the DNV samples were deposited between 13.6 and 12.7 Ma years, when the mean sea-surface temperature was lower than 14 °C (Kováčová & Hudáčková, 2009) and the atmospheric CO_2 concentration was < 290 ppmv (Super et al., 2018). Therefore, we have an excellent opportunity to analyse the calcification intensity of *Globigerina bulloides* under different carbon dioxide levels.

After establishing the environmental background of the studied samples, we compared the mean size of *Globigerina bulloides* between the CB time series and the DNV samples. The mean size in the Cape Blanc 1990-1991 time series was 40.86 * 10^3 µm^2, while the mean size in 2007-2008 time series was 69.12 * 10^3 µm^2, meaning that the mean size in the two-time series together was 46.03 * 10^3 µm^2 (Fig. 4). The mean size in the DNV samples was 44.87 * 10^3 µm^2. These values above indicate negligible mean size difference between the two sites, with shells being 2.6 % larger in the CB time series compared to the DNV samples. The similar mean shell sizes, however, masks notable size variability. In the 1990-1991 time series, the size ranged between

a minimum 18.16 and maximum 94.11 * 10^3 μm^2, in the 2007-2008 time series from 23.61 to 198.92 * 10^3 μm^2 and in the DNV samples between 16.37 and 138.28 * 10^3 μm^2 (Fig. 4).

After we documented the mean size and its variability between the CB and DNV samples, we analysed the calcification intensity of *Globigerina bulloides*. The mean calcification intensity of *Globigerina bulloides* in the Cape Blanc 1990-1991 time series was 8.82 * 10^5 $\mu g/\mu m^2$, while the mean calcification intensity in 2007-2008 time series was 9.59 * 10^5 $\mu g/\mu m^2$, thus making the mean calcification intensity in the two-time series together 8.96 * 10^5 $\mu g/\mu m^2$ (Fig. 4). The mean calcification intensity in the DNV samples was 11.61 * 10^5 $\mu g/\mu m^2$, being 30 % more heavily calcified compared to the mean calcification intensity of CB time series. The calcification intensity of *Globigerina bulloides* in the 1990-1991 (CB-3) time series ranged between a minimum 3.43 to maximum 27.24 * 10^5 $\mu g/\mu m^2$, in the 2007-2008 (CB-18) time series varied from 3 to 36.8 * 10^5 $\mu g/\mu m^2$, and in the DNV samples ranged from 2.95 to 29.40 * 10^5 $\mu g/\mu m^2$.

In the next step we observed *Globigerina bulloides* in polished thin sections in order to measure their shell wall thickness. These measurements show in the 2007-2008 time series (CB-18) that the wall thickness of the penultimate chamber varied between a minimum 2.14 and maximum 8.03 µm (mean = 5.48 µm, median = 5.45), while the thickness of the ultimate chamber ranged from 2.39 to 7.24 µm (mean = 4.57 µm, median = 4.73). On the other hand, we found specimens with thicker penultimate and ultimate chambers in the DNV samples. Here we documented that the thickness of the penultimate chamber ranged between a minimum 4.17 and maximum 8.34 µm (mean = 6.26 µm, median = 6.02), and the thickness of the ultimate chamber varied between 3.78 to 7.57 µm (mean = 5.78 µm, median = 6.15). Nevertheless, the polished thin sections provided an excellent opportunity to report the specimen's preservation and proved their suitability for the shell-weighing method, since the specimens did not yield lithogenic infill inside their chambers.

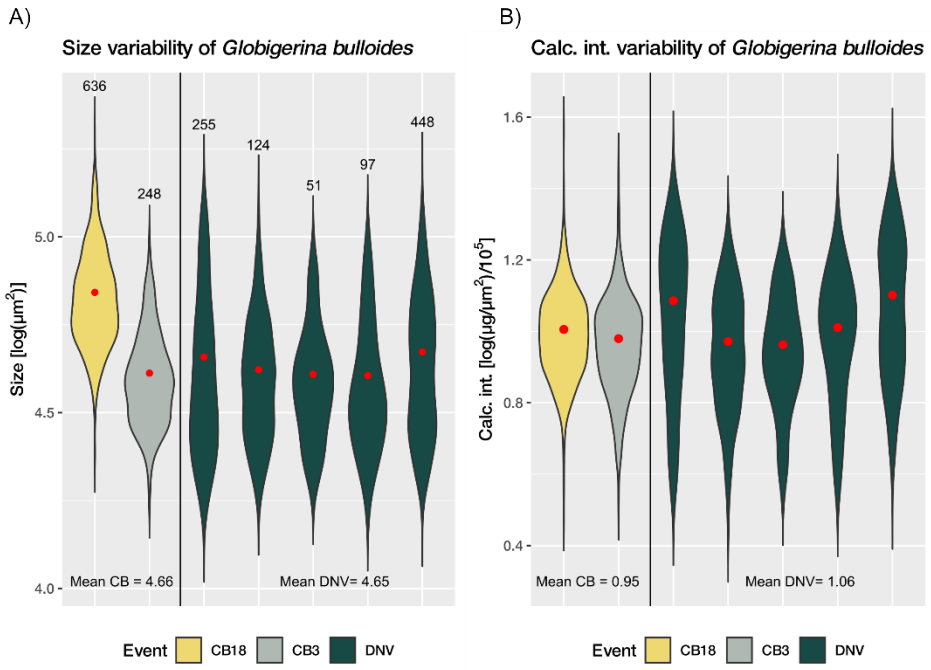

Figure 4. Variability of (A): size and (B): calcification intensity of *Globigerina bulloides* (> 150 µm) in the time series 2007-2008 (CB-18, yellow), time series 1990-1991 (CB-3, grey) and DNV samples (13.6-12.7 Ma years, green). Red circles denote the mean for each assemblage. In (A) numbers above the violins indicate the number of measured individuals.

4. Discussion

The mean size of *Globigerina bulloides* showed little difference between the Cape Blanc time series and the mid-Miocene sediment samples, with shells being on average only 2.6 % larger in the modern assemblages than in the mid-Miocene DNV samples (Fig. 4). The largest specimens occurred in the Cape Blanc 2007-2008 time series (CB-18), which was a slightly colder period with higher dissolved inorganic carbon concentration in the seawater (mean = 2208.81 µmol kg^{-1}) compared to the Cape Blanc 1990-1991 time series (CB-3) when the sea-surface temperature was higher, and the dissolved inorganic carbon concentration was the seawater was lower (mean = 2141.91 µmol kg^{-1}). In fact, the 2007-2008 time series yielded specimens that were on average 69 % larger than in the 1990-1991 time series, and these specimens were on average 9 % more heavily calcified than specimens from the 1990-1991 time series. The outcomes of the sediment trap time series analyses are in line with previous observations documenting intensified calcification under conditions with more dissolved inorganic carbon in the seawater (Baker et al., 1988; Bijma, J. et al., 2002; Lombard et al., 2010; Marshall et al., 2013). The shell wall thickness measurements followed the same pattern as

observed in the calcification intensity. We found that the shell wall thickness of the penultimate and ultimate chambers was thicker during the mid-Miocene, whilst the modern representatives of *Globigerina bulloides* had thinner shell walls.

The mean size of the specimens in the mid-Miocene DNV samples is 3 % smaller than the average shell size in the two Cape Blanc time series together (44.87 vs 46.03 * 10^3 μm^2; Fig. 4). In terms of the calcification intensity, the specimens from the mid-Miocene are 30 % more heavily calcified. Indeed, the difference in the mean size and mean calcification intensity between the modern and mid-Miocene samples are negligible, which is unlikely to the long-term evolution of *Globigerina bulloides* under warmer climatic conditions and different carbonate concentration of the sea water. In fact, we found that the mean calcification intensity was higher in only three out of five mid-Miocene samples than the calcification intensity in the sediment trap time series (Fig. 5 and 6). The remaining two mid-Miocene samples fall between the mean modern calcification intensity range, meaning that 2007-2008 time series (CB-18) were more heavily calcified than the mid-Miocene samples (Fig. 5). The lack of substantial changes in the mean calcification intensity under distinct climatic conditions challenge the assumption of enhanced calcification of *Globigerina bulloides* during periods of atmospheric CO_2 decrease, which is associated with increased carbonate saturation in the seawater (Barker & Elderfield, 2002; Zarkogiannis et al., 2019). Overall, it seems that even the notable difference in the atmospheric carbon dioxide concentration and the modest difference in sea-surface temperature (Fig. 1) between the two sites did not translate into a substantial difference in mean calcification intensity (Fig. 4, 5 and 6).

In order to extend the observed differences in the mean calcification intensity between modern and mid-Miocene samples to glacial-interglacial cycles, we take advantage of data produced by Barker & Elderfield (2002). Their data comprises measurements of *Globigerina bulloides* calcification intensity during the past 50.000 years in the North Atlantic (NEAP 8K sediment core; Fig. 2A), which reflects higher calcification intensity across the last glacial period (Fig. 5C). This comparison revealed that specimens during the last glacial-interglacial period in the North Atlantic were 17 % more heavily calcified than specimens during the mid-Miocene at the DNV site. However, the most pronounced difference in the mean calcification intensity of *Globigerina bulloides* appeared between the Cape Blanc time series and the North Atlantic

samples. The North Atlantic specimens from the NEP 8K sediment are on average 54 % more heavily calcified than specimens in the 1990-1991 time series (CB-3) and 41 % more heavily calcified than in the 2007-2008 time-series (CB-18; Fig. 5 and 6).

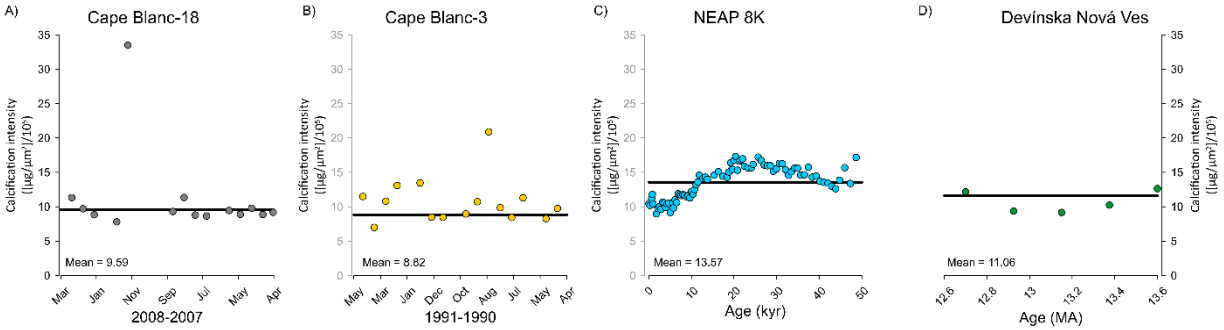

Figure 5. Mean calcification intensity of *Globigerina bulloides* during (A): time series 2007-2008 (Cape Blanc-18); (B): time series 1990-1991 (Cape Blanc-3); (C): in the North Atlantic NEAP 8K samples, data taken from Barker & Elderfield (2002) and (D): at the Devínska Nová Ves site. Mean values are indicated for each sample with the black grid lines. It appears that the specimens of *Globigerina bulloides* in the North Atlantic (NEAP 8K, (C)) were much more heavily calcified compared to modern (A, B) and mid-Miocene specimens (D).

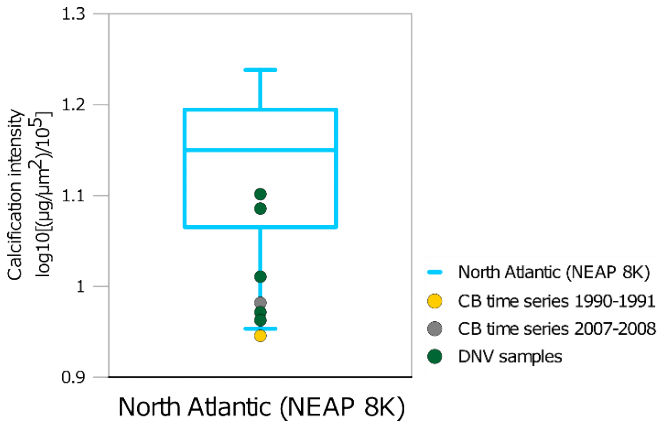

Figure 6. Comparison of mean calcification intensity of *Globigerina bulloides*. The boxplot indicates the calcification intensity data measured in the sediment core from the North Atlantic (NEAP 8K), data taken from Barker & Elderfield (2002). Dots imply the mean values obtained from the studied samples, see legends next to the boxplot. This comparison shows marked difference in the mean calcification intensity of *Globigerina bulloides* in the North Atlantic, while these specimens occur much more heavily calcified as the mid-Miocene or the Holocene specimens from the Cape Blanc time series.

Such differences in the mean calcification intensity across the studied sites could emerge from several possible reasons. At first, we do not know how calcification intensity relates to shell size. We can for instance assume that calcification intensity is independent of shell size, which would mean that in an assemblage the most heavily calcified specimens occur irrespective of size. Another assumption could be that the largest shells in an assemblage are the most heavily calcified ones, which would also indicate a strong relationship between these two parameters. In order to bring novel insights into the understanding of calcification intensity and shell size, we tested with linear correlation the relationship between mean calcification intensity and mean shell size of *Globigerina bulloides* in the mid-Miocene DNV samples, Cape Blanc time series and among the specimens from the North Atlantic (Fig. 7). These analyses revealed a positive and significant correlation between calcification intensity and size in the DNV samples ($r = 0.89$, $p = 0.05$), suggesting that larger shells are also more heavily calcified. This simple relationship does not hold in the Cape Blanc time series, where size and calcification intensity appear with no relationship ($r = 0.02$, $p = 0.91$). This could emerge due to the fact that the 2007-2008 (CB-18) time series is yielding specimens, which despite their large size are disproportionately lightly calcified (Fig. 4). The relationship between size and calcification intensity in the North Atlantic specimens is further complicated, since the parameters appear with a weak negative correlation ($r = -0.22$, $p = 0.05$). Thus, the inferences of the presented correlation test suggest that the notable differences in the mean calcification intensity between the North Atlantic and Cape Blanc samples is not due to shell size differences.

Clearly, the mean calcification intensity is the highest in the North Atlantic samples and the lowest in the Cape Blanc time series (Fig. 4 and 5). Another explanation of this difference could be given based on the specimens SSU rRNA analyses. In the subpolar and transitional zones of the North Atlantic two genotypes (type IIa and IIb) of *Globigerina bulloides* occur, while in the warmer waters of the Mediterranean and the Canary Islands, where the Cape Blanc samples were obtained, one genotype (type I) is recognized (Darling & Wade, 2008). Despite the genotype's distinct ecological preferences, they are not distinguished in paleoceanographic studies. In theory, the differences in the habitat between the North Atlantic and Canarian genotypes may induce variable calcification intensity, which could plausibly explain why the North Atlantic specimens are so much more heavily calcified compared with the specimens from the Cape Blanc area (Fig. 5 and 6). We do not know if the calcification intensity of the

different genotypes would remain constant under the same environmental conditions. This unresolved issue is further complicated with a possibility that perhaps genotypes II could bear more crust in the North Atlantic than elsewhere. Generally, deeper dwelling species have thicker shell walls and bear crust that constitute the majority of their shell mass (Salmon et al., 2015) and it is suspected that crusting in foraminifera changes their calcification. The origin of crust in *Globigerina bulloides* is less clear, although its formation may be caused due to temperature or deeper depth (de Villiers, 2003). Overall, the crust effect on the interpretation of calcification intensity between the North Atlantic and the Cape Blanc area is hard to explain, but we cannot rule out that different genotypes of *Globigerina bulloides* were measured by Barker & Elderfield (2002), perhaps more encrusted ones that display higher calcification intensity, compared to specimens measured by us from the Cape Blanc area.

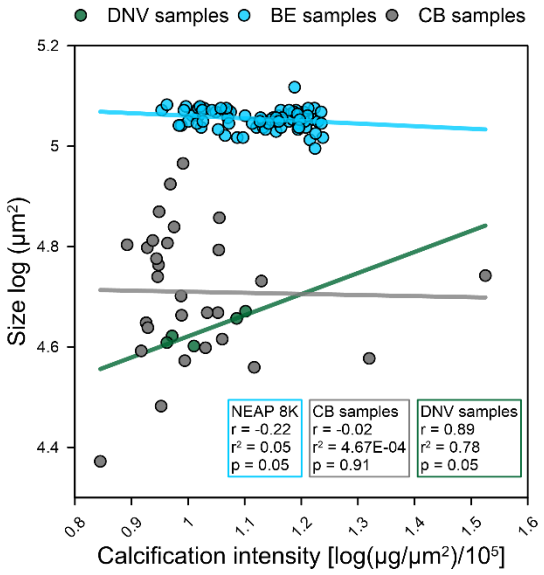

Figure 7. The relationship between *Globigerina bulloides* mean calcification intensity and mean size, shown for the mid-Miocene DNV samples (green filled circles), Cape Blanc 1990-1990 and 2007-2008 time series together (grey filled circles), and for specimens obtained from the North Atlantic (NEAP 8K sediment core, red filled circles), data taken from Barker & Elderfield (2002). Linear regression is shown for each sample, legends see above, and summary statistics are given for each regression. It appears that there is no constant relationship between size and calcification intensity, hence the large difference in the calcification across the samples (Fig. 6) cannot be explained by shell size even if the specimens in the North Atlantic are clearly larger.

Preservation of planktonic foraminifera shells in an assemblage appears to be the most important prerequisite for determining calcification intensity by using the shell-weighing method. Shells are variable preserved across different sites and the determination of their shell weights in sedimentary samples (Barker & Elderfield, 2002; Zarkogiannis et al., 2019), could be challenged from invariable contamination by adhering sediment inside the chambers. In this way, the measured weight does not directly provide the real weight of the shell, but the shell with its sedimentary infill, which could, at the end, reflect higher calcification intensity. Since moored sediment traps capture foraminifera shells at a certain depth before the shells reach the seafloor, we consider sediment trap material as the most suitable choice for shell weighing, reflecting the most accurate weight of the specimens. The filled shell preservation of specimens from the North Atlantic sediment core remains unanswered but may help for future studies setting priorities for sample choice in order to determine shell weight.

5. Conclusions

Planktonic foraminifera precipitate calcareous shells, which represent a key component of the pelagic carbon cycle. A detailed analysis of shell size, shell wall thickness, and calcification intensity of *Globigerina bulloides* obtained from two years of sedimentation (1990-1991 and 2007-2008) from the Cape Blanc upwelling area (Atlantic Ocean) and from mid-Miocene sediments of Devínska Nová Ves site (Slovakia), allowed us to quantify the changes in their calcification aspects in response to different climatic conditions. Our results indicate a marked difference in size between the two Cape Blanc time series with shells being on average 69 % larger during 2007-2008 compared to 1990-1991, while mean size of the modern specimens is only 3 % larger on average than their mean size during the mid-Miocene. The differences in the mean calcification intensity (weight/size) between the two-time series are negligible (being 8 % less in time series 1990-1991 than in 2007-2008), whereas the mid-Miocene representatives of *Globigerina bulloides* are 30 % more heavily calcified than the modern specimens. Our data also suggest that the documented difference in calcification intensity did not emerge from the variable shell size among the individuals. We can conclude that the long-term evolution of *Globigerina bulloides* under generally warmer climate and elevated carbon dioxide conditions translated only into a minor difference in shell size and caused slight difference in calcification

intensity between modern and mid-Miocene specimens, thus we did no observe substantial differences in the calcification aspects under different climatic conditions.

Appendix chapter 1

An Ontogenetic Description of *Orbulina suturalis* (Foraminifera) from the Danube Basin (Slovakia)

This work has been published in the journal *Acta Geologica Slovaca*.

Peter Kiss[1], Natália Hudáčková[1], Andrej Ruman[1] & Zuzana Heřmanová[2]

[1]Department of Geology and Paleontology, Faculty of Natural Sciences, Comenius University in Bratislava, Mlynská dolina, Ilkovičova 6, 842 15 Bratislava, Slovakia.

[2]National Museum, Prague, Cirkusová 1740, 193 00 Praha – Horní Počernice; Charles University, Institute of Geology and Palaeontology, Albertov 6, 128 43 Prague 2, Czech Republic.

*Corresponding author: Peter Kiss (pkiss@marum.de)

Abstract

Orbulina suturalis (Brönnimann, 1951) is a planktic foraminifera species that occurred in the Central Paratethys during the Middle Miocene, throughout the Badenian (Langhian, Serravallian) stage. Despite the stratigraphic and paleoecologic significance, the ontogeny of the species remained seldom explored. In this study the inner shell morphology was observed by using a tomographic microscope to identify the ontogenetic stages. The entire shell development of *Orbulina suturalis*, from the monothalamous prolocular stage to the polythalamous terminal stage, was interpreted. Each stage is described by its general morphological features, such as the dimensions of the shell, the shape and number of the chambers, the position of the aperture, the peripheral outline, the texture of the wall and the coiling direction. The constructed ontogenetic model of *Orbulina suturalis* was correlated with the „five stage concept" of *Globigerinoides sacculifer* introduced by Brummer et al. (1987).

Key words: Orbulina suturalis; tomographic microscope; Badenian; Western Carpathians

1. Introduction

Orbulina suturalis (Brönnimann, 1951) is an abundant polythalamous planktic foraminifera in Badenian sediments of the Central Paratethys. The first appearance of *Orbulina suturalis* in the Western Carpathians was accepted as a marker of biostratigraphic zonation to define the base of the local CPN 7 or the global M6 Planktic Foraminifera Zone (Cicha et al., 1975; Wade et al., 2011). In spite of their biostratigraphic application, the ontogeny and ecological demands of the species have been a subject of much speculation since their first description by d'Orbigny (1839).

Ontogenetic investigations of planktic foraminifera are often limited by a lack of preservation of non-adult individuals in fossil records (Caromel et al., 2015; Gerber et al., 2008). Thin-walled juvenile individuals are easily destroyed by taphonomic factors of the environment. In some cases, when younger individuals of genus *Orbulina* are preserved, they may be incorrectly classified (Hemleben et al., 1989). The shell morphology during the earlier development stages could morphologically resemble the adult morphology of different species or genus (Brummer et al., 1986, 1987; Hemleben et al., 1989).

The shell construction of *Orbulina suturalis* is a continuous biological process, characterised by the sequential growth of calcite chambers during the entire life of the specimen (Huang, 1981). In fact, each morphological feature remains an integral part of the growing foraminifera shell, providing a unique possibility to reconstruct the complete ontogeny from the first calcified chamber (proloculus) to the last (terminal) chamber (Huang, 1981). According to the five-stage model of growth in the globigerinids proposed by (Brummer et al., 1987), the development of fossils and recent spinose planktic foraminifera is ongoing throughout the prolocular, juvenile, neanic, adult and terminal stages.

The aim of the presented investigation was to analyse the general ontogenetic stages of *Orbulina suturalis* by tomographic microscope and to correlate them with the „five stage concept" (*sensu* Brummer et al., 1987) of *Globigerinoides sacculifer*. This observation could contribute to the correct taxonomic classification of species from genus *Orbulina*, as well as in identification of evolutionary processes within the phylogenetic lineages of Badenian planktic foraminifera.

2. Materials and methods

Our studied material was obtained from Middle Miocene deposits of the Danube Basin (Slovakia) which presented a part of the Central Paratethys (Fig. 1). The settling of this intermountain basin was affected by several eustatic changes during the Badenian and Sarmatian (Hudáčková & Kováč, 1993; Kováč et al., 2007). A bulk sample was taken from the Modrany-1 borehole (Kováč et al., 2018). To separate foraminiferal tests, the traditional wet sieving method was used (Kováčová & Hudáčková, 2009). A foraminiferal assemblage containing the studied specimen was rich in planktic foraminiferal tests. Age was given as NN5 Zone accordingly to calcareous nannoplankton association from the same bulk sample (Kováč et al., 2018). For the purpose of this paper, 80 specimens of *Orbulina suturalis* were separated and transferred to a petri dish with water (∅ 15 cm, 2 dcl) due to their tests weight classification. Foraminifera shells filled with pyrite settled on the bottom (72 specimens), while the remaining 8 shells were isolated for further observation. Only one specimen was chosen with an unfilled shell and well-preserved wall for tomographic analyse.

The chosen specimen was small, about 0.5 mm, preserved as a three-dimensional fossil. Our specimen was studied using X-ray micro-tomography SkyScan 1172. The effective pixel size

was ca. 0.56 µm. Tube voltage was set to 40 kV and the current source was 250 µA. No filter was used. Random Movement was set to 5. Data were acquired with an angle slope of 0.120 degree. 180° rotation was used. The acquired data were processed using flat field correction and reconstructed by the supplied software NRecon (Bruker). Photographs and video visualizations were created by Avizo 9.1 software. Presented figures were designed by the graphic program CorelDRAW Graphics Suite X5, and for 3D visualization, Microsoft Paint 3D was used.

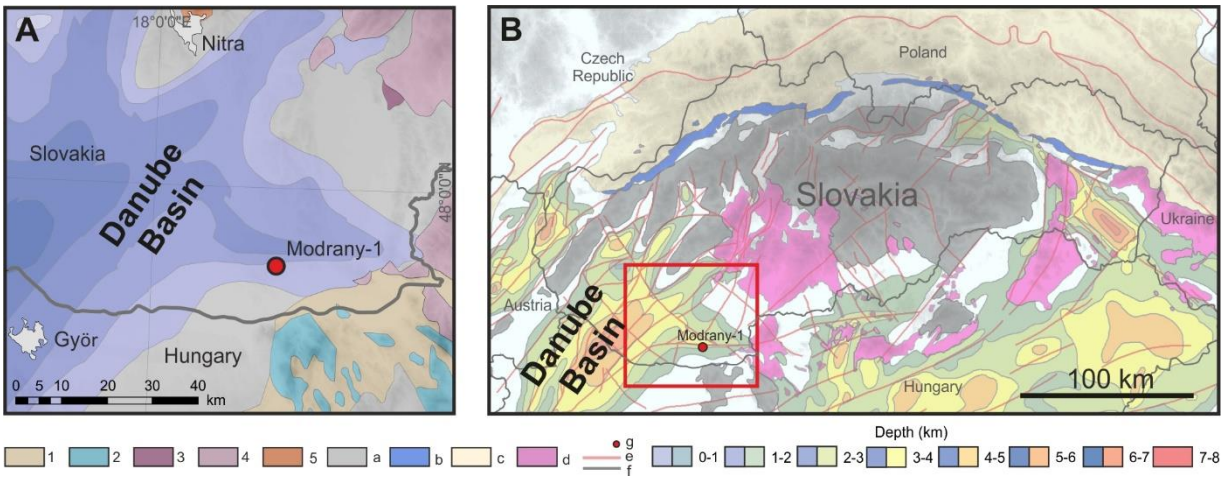

Fig. 1. (A) Map of the Southeastern Danube Basin; (B) Position of the study area in the Europe and in the Carpathian–Pannonian system. *Explanatory notes:* (1) Paleogene sediments of the Buda basin; (2) Bukkikum and the Pelsonia; (3) Silicicum; (4) Miocene volcanic fields; (5) Tatricum; (a) Inner Alpine, Carpathian and Dinaric mountains; (b) Klippen Belt; (c) Foredeep and Flysch belt; (d) Miocene volcanic fields; (e) Faults; (f) State boundaries; (g) Wells. Modified after Horváth et al. (2015) and Hók et al. (2014).

3. Results

On the studied shell of *Orbulina suturalis*, we managed to identify five ontogenetic stages: prolocular, juvenile, neanic, adult and terminal („five-stage model", sensu Brummer et al., 1987). The shell dimension of the studied *Orbulina suturalis* is 400 µm (average dimension was 390 µm) and it is made up of 12 chambers arranged in ± 2,5 trochospirally (dextrally) coiling whorls (Fig. 2A–E). The coiling of the first whorl is lower in comparison to the second whorl. The size of the chambers increases continuously from the deuteroconch to the terminal chamber. The number of chambers per whorl gradually decreases. The wall porosity tends to be higher during the adult and terminal stages than observed in the earlier phases of development. The

first stage of ontogeny (~ 17 µm), the prolocular stage, is marked by the establishment of the oldest chamber, which is the proloculus or protoconch (Figs. 2A–D and 3A, B). Tomographic analyses have enabled to determine this chamber in the centre of the first trochospiral whorl. Proloculus has a globular shape with the exception of a short and flattened area where the second chamber (deuteroconch) is added (Fig. 2B). The wall texture during this stage is sparsely perforated and the character and position of the primary aperture is unidentifiable.

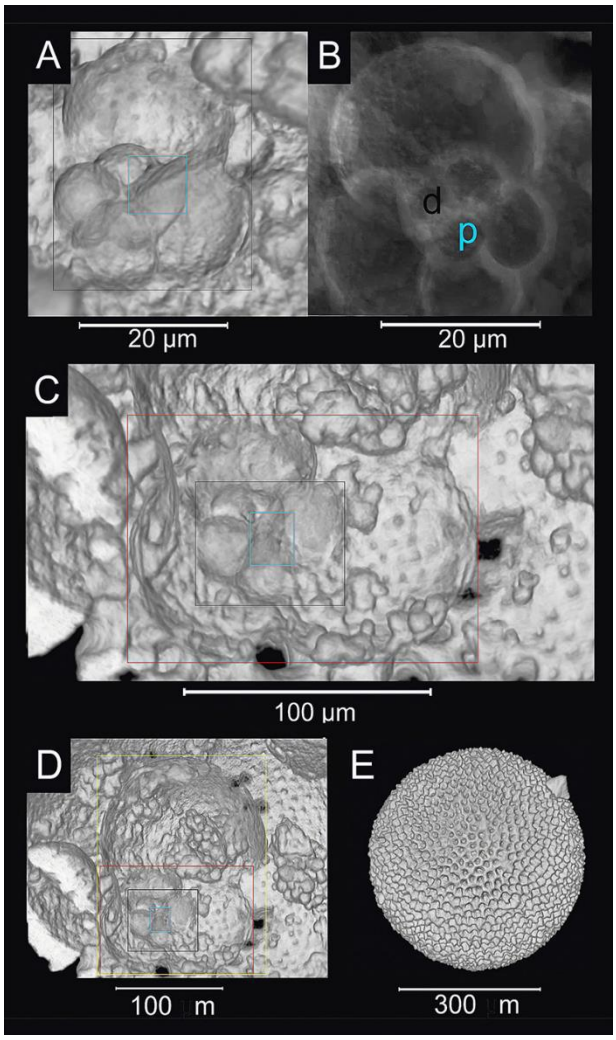

Fig. 2. Ontogenetic stages of *Orbulina suturalis* (A-E). *Explanatory notes:* (A) Prolocular and juvenile stages; (B) Position of the proloculus and deuteroconch inside the juvenile shell; (C) Neanic stage; (D) Adult stage; (E) Terminal stage. *Explanatory notes:* (p) Proloculus; (d) Deuteroconch; (blue square) Prolocular stage; (black square) Juvenile stage; (red square) Neanic stage; (yellow square) Adult stage

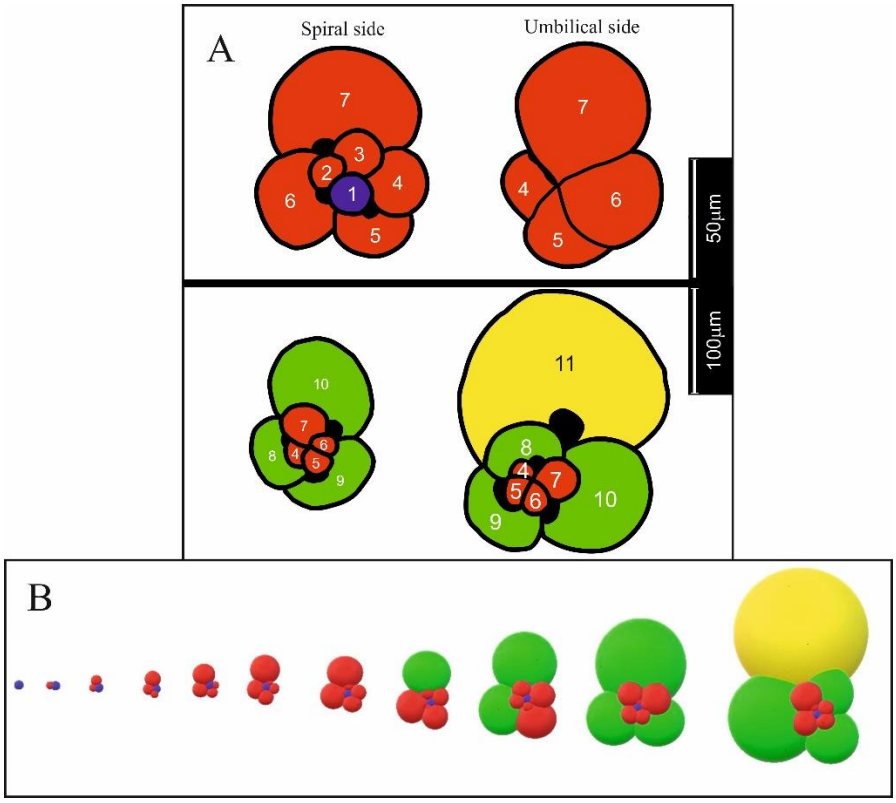

Fig. 3. (A) Position of the apertures and chambers arrangement during the juvenile, neanic and adult stages; (B) Development of the shell from the proloculus to the adult chamber of *Orbulina suturalis*. *Explanatory notes:* (1) Proloculus (blue colour); (2) Deuteroconch (red colour); (3–7) Juvenile chambers (red colour); (8–10) Neanic chambers (green colour); (11) Adult chamber (yellow colour).

The second stage of the imaged specimen, the juvenile stage, is composed of six juvenile chambers (Figs. 2A–D and 3A, B). The juvenile shell dimension is ~ 95 µm. Proloculus, together with the juvenile chambers, are arranged in ± 1,25 trochospirally, dextrally, coiling whorls (Fig. 2B). The coiling of the first whorl is more acute (~ 25°) than the subsequent whorls. The juvenile stage is initiated by the growth of the second chamber (~ 17 µm) which is the deuteroconch (Figs. 2B and 3A). The proloculus, together with the deuteroconch, forms the first polythalamous morphotype during the life cycle of *Orbulina suturalis*. The shape of the juvenile chambers is globular, apart from flattened areas, where the consecutive chambers are created (Fig. 2B). The size of the chambers gradually increases from the deuteroconch. The suture is depressed and the chamber walls are rounded (Fig. 2B). The primary aperture is open, ovoid and umbilical (Fig. 3A). The peripheral outline of the aperture could be secondarily modified

with an imperforated lip. The juvenile wall texture is sparsely perforated with rounded and small pores. Spine bases are detectable between the pores. The juvenile morphology of *Orbulina suturalis* is reminiscent of the morphology of genus *Turborotalita* (Figs. 2A and 3A). We managed to identify the juvenile stage according to the size of the shell, suture, chamber's perforation and number and aperture position.

The third stage of the studied specimen, the neanic stage, is made up of three globular neanic chambers (Figs. 2C, D and 3A, B). The size of the neanic shell reaches ~ 150 μm. Neanic chambers are situated on the second trochospiral whorl (Fig. 3A, B). Their shape is more inflated than the previously built chambers. The neanic shell is characterized by a lobate peripheral outline, a depressed suture and thicker shell walls. The wall texture is spinose and the entire shell becomes densely perforated with larger pores. The primary aperture remains open and umbilical (Fig. 3A). In general, the neanic stage of *Orbulina suturalis* has a globigerinoides-like morphology (Fig. 3A, B). This stage was documented based on coiling variations, the chambers' shape and their dimensions.

The fourth stage of the sample, the adult stage, is composed of one globular and inflated adult chamber (Figs. 2D and 3A, B). This chamber indicates the end of the trochospiral coiling. Due to its large size (120 μm), it occupies the first half of the last trochospiral whorl. The adult chamber has rounded wall instead of a flattened range, where the neanic chambers are localised. The peripheral outline is lobate and the suture is depressed (Fig. 3A, B). The wall texture is densely perforated with large pores. Spine bases appear among the pores. The primary aperture is open and umbilical with a high arch. The total length of the adult individual is ~ 250 μm (Fig. 3A). The adult shell is made up of 11 chambers arranged in 2,5 trochospirally (dextrally) coiling whorls (Figs. 2D and 3A, B). *Orbulina suturalis* during this stage is morphologically similar to *Globigerinoides sacculifer* (Fig. 3A). This stage was determined according to the wall texture, coiling direction, shell size and primary aperture.

The last stage of development, the terminal stage, is connected with the construction of the last globular, the so-called terminal chamber (Fig. 2E). It is unequivocally the largest chamber of the shell (~ 400 μm). The terminal chamber has rounded calcite wall of thickness being more than 5 μm. The terminal chamber envelopes the older chambers (prolocular, juvenile, neanic and adult) situated on the trochospiral whorls (Supplementary Fig. S1). The wall texture during

this stage is densely perforated with large pores (Fig. 2E). Numerous spine bases are visible among the pores. The terminal stage is marked by the formation of 30 sutural apertures along the peripheral outline of the neanic and adult chambers. Morphological features constructed throughout the stages older than the terminal are weakly visible from the spiral side of the terminal shell. This stage was recognised according to the globular terminal chamber (Fig. 2E) and its sutural apertures.

Morphological descriptions of the individual stages were correlated with the ontogenetic concept for spinose species („five stage concept") derived from *Globigerinoides sacculifer* by Brummer et al. (1987) (Fig. 4).

4. Discussion

We identified five ontogenetic stages in our studied sample (prolocular, juvenile, neanic, adult and terminal). The shell construction from the monothalamous protoconch to the polythalamous terminal stage fits the „five stage concept" documented by Brummer et al. (1987). Development was interpreted by tracing the individual stages backwards from the last chamber to the first two-chambered morphotype (proloculus+deuteroconch) (Figs. 2B and 3A). Changes in morphology, such as coiling direction, test diameter, wall texture, and primary aperture have enabled to detect each ontogenetic stage (Figs. 2A–E and 3A, B). Based on the drastic morphological variation and development pattern, the studied specimen belongs to the first group of planktic foraminifera described by Brummer et al. (1986).

The prolocular stage of growth is formed by the proloculus in both *Globigerinoides sacculifer* and *Orbulina suturalis*. Isolated proloculi in the studied bulk sample (Modrany-1 borehole) have not been found. This fact supports the idea that the proloculus has weakly or non-calcified walls (Brummer et al., 1986, 1987). The most important morphological differences were observed during the second, juvenile stage of ontogeny (Fig. 4). In the studied specimen, this stage was marked by the creation of six juvenile chambers arranged in ±1,25 trochospirally coiling whorls (Figs. 2A, B and 3A, B), while in *Globigerinoides sacculifer*, eight to thirteen chambers are created, which are situated in ±1,5 trochospiral whorls (Brummer et al., 1987) (Fig. 4). The aperture of the juvenile shell in both species is umbilical, however, the umbilicus of our studied sample is secondarily modified by an imperforated umbilical lip. One notable morphological difference between the neanic stages was documented in the diameter of the shell. The longer

diameter of the studied specimen during this stage is 150 µm (Fig. 2C), while *Globigerinoides sacculifer* reaches more than 200 µm in the neanic stage (Fig. 4). The neanic stage in *Orbulina suturalis* is made up of three (Figs. 2C and 3A, B) while in *Globigerinoides sacculifer* of 3-6 chambers (Fig. 4). The number of neanic chambers probably depends on the amount of juvenile chambers. According to Bé et al. (1985), as more juvenile chambers are present, less neanic chambers are necessary to reach the size of the adult stage. During the adult stage of the imaged *Orbulina suturalis*, the penultimate, adult, chamber formation was observed (Figs. 2D and 3A, B). Among species of *Globigerinoides sacculifer*, Brummer et al. (1987) documented the growth of 1 to 4 adult chambers (Fig. 4). The wall texture, the shell size, the umbilical aperture, the shape of the chambers and the chambers' arrangement of an adult *Orbulina suturalis* are morphologically reminiscent of the adult and terminal stages of *Globigerinoides sacculifer* (Figs. 2D and 3A, B). Major morphological changes are marked by the terminal stage. This stage of the studied specimen commences with the growth of the last, terminal chamber, which envelopes the older chambers (Figs. 2E), and by the transition of the umbilical aperture into 30 sutural apertures, located on the spiral side of the shell. Brummer et al. (1987) described 1 to 3 terminal chambers among species *Globigerinoides sacculifer*, as well as the growth of the kummerform chamber (Fig. 4), which is not typical for genus *Orbulina*.

Throughout the development of *Orbulina suturalis* and *Globigerinoides sacculifer*, major changes of the primary aperture are recognised. After the prolocular stage, growth of an umbilical aperture begins, which persists until the end of the adult stage (Fig. 3B). The most significant size variations of the aperture are documented between the neanic and the adult stages, when the umbilicus starts to shift towards its adult position (Brummer et al., 1986, 1987). According to Brummer et al. (1987), these aperture modifications are presumably generated due to trophic behavioural changes. Juvenile individuals with a small aperture usually feed on microplankton, while adult individuals with a massive umbilicus are largely carnivorous in diet (Hemleben et al., 1989) (Fig. 3A). Among species of genus *Orbulina*, the umbilicus is transformed into several sutural apertures after the adult stage.

	Orbulina suturalis				*Globigerinoides sacculifer*			
Ontogenetic stage	**SS (µm)**	**NoCC**	**NoW**	**PoPA**	**SS (µm)**	**NoCC**	**NoW**	**PoPA**
Prolocular stage	17	1	-	-	19	1	-	Interiomarginal, marginal
Juvenile stage	95	6	±1,25	Umbilical with lip	90	8-13	±1,5	Umbilical
Neanic stage	150	3	1	Umbilical	210	3-6	0,5-1	Umbilical
Adult stage	250	1	0,5	Umbilical with lip	>210	1-4	-	Umbilical + secondary
Terminal stage	400	1	-	Sutural apertures	350	1-3 + kummerform chamber	-	Umbilical + secondary

Fig. 4. Morphological differences between the ontogenetic stages of species *Orbulina suturalis* (Danube basin, Slovakia) and *Globigerinoides sacculifer* (*sensu* Brummer et al., 1987). *Explanatory notes:* (SS) Size of the shell; (NoCC) Number of created chambers; (NoW) Number of whorls; (PoPA) Position of the primary aperture.

5. Conclusion

Orbulina suturalis is among the most abundant planktic foraminifera in Badenian sediments of the Western Carpathians. This study confirmed the five-stage model of growth of spinose planktic foraminifera, documented by Brummer et al. (1987). In the studied shell of *Orbulina suturalis*, the prolocular, juvenile, neanic, adult and terminal stages have been shown by using a tomographic microscope SkyScan 1172. Throughout the visualised ontogenetic stages, major morphological changes were described. Chambers' number and size, coiling direction, wall texture and even aperture modifications have been visible during calcite shell development. Transitions, such as in the position of the apertures, could be interpreted as a result of changes in trophic demands, which can differ between the ontogenetic stages. The results confirm the disadvantages of recent classification of planktic foraminifera, which is based on the morphology of terminal stages. With the application of the current classification, ontogenetic stages of *Orbulina suturalis*, could be incorrectly classified into several species. *Orbulina*

suturalis during the juvenile stage is morphologically similar to the genus *Turborotalia*, the neanic stage has a globigerinoides-like morphology and the adult stage is reminiscent of the morphology of species *Globigerinoides sacculifer*. This investigation contributes to making a more effective classification of pre-adult Badenian (Langhian, Serravallian) planktic foraminifera.

Acknowledgements

The authors would like to express their gratitude to Katarína Holcová for valuable discussion and to Samuel Rybár. This work has been supported by research grants APVV 15-0575, APVV 14-0118, APVV 16-0121 and by Ministry of Culture of the Czech Republic (DKRVO 2017/05, 00023272). The authors are grateful to the reviewers, Katalin Báldi and Danuta Peryt, who provided constructive comments and suggestions. We thanks to Michael Sabo (Canadian Lecturer, Comenius University) for proofreading of the manuscript.

Appendix chapter 2

Convergent evolution of spherical shells in Miocene planktonic foraminifera documents the parallel emergence of a complex character in response to environmental forcing

This manuscript has been submitted for publication in the journal *Paleobiology*.

Peter Kiss[1,2], Natália Hudáčková[1], Zuzana Heřmanová[3], Michael Georg Siccha Rojas[2], Jürgen Titschack[2,4], Lóránd Silye[5], Andrej Ruman[1], Samuel Rybár[1] and Michal Kučera[2]

[1]Department of Geology and Paleontology, Faculty of Natural Sciences, Comenius University in Bratislava, Mlynská dolina, Ilkovičova 6, 842 15 Bratislava, Slovakia; kiss56@uniba.sk

[2]MARUM – Center for Marine Environmental Sciences, University of Bremen, Leobener Str. 8, D-28359 Bremen, Germany

[3]National Museum, Prague, Václavské náměstí 1700/68, 110 00 Praha 1, Czech Republic

[4]Senckenberg am Meer, Marine Research Department, D-26382 Wilhelmshaven, Germany

[5]Department of Geology, Babeș-Bolyai University, Str. Kogălniceanu 1, 400084, Cluj-Napoca, Romania

*Corresponding author: Peter Kiss (pkiss@marum.de)

Abstract

The spherical encompassing last chamber of the planktonic foraminifera *Orbulina universa* is a prime example of a complex character whose evolution has been documented by a sequence of intermediate forms. However, the mechanism that induced the evolution of the spherical chamber remained unclear. Here we show that in parallel with the emergence of *Orbulina* in the world ocean, a convergent evolutionary transition occurred in the semi-isolated Paratethys, leading to the emergence of the endemic *Velapertina*, occupying a similar niche in the surface waters as *Orbulina*. Using X-ray computed tomography we show that the evolution of the encompassing final chamber involved in both lineages the same sequence of steps, combining progressively spherical shell shape with changes in the position, number, and size of apertures. The similarity in the sequence of character acquisition indicates structural determinism given by the way foraminifera shells are constructed and the presence of natural selection favouring spherical morphology. Collectively, the observed synchronous parallel evolution of spherical chambers in the two lineages implies the emergence of a singular environmental driver of this spectacular complex character.

Keywords: foraminifera, phenotypic integration, shell architecture, ontogeny, evolution of complex characters, X-ray computed tomography

1. Introduction

The evolution of complex characters has been a contested ground since the first formulation of the theory of evolution by natural selection by Darwin (1859). In theory, the fossil record should allow direct assessment of the sequence of changes leading to the emergence of such traits, but because of the prevalence of speciation by punctuated equilibria (Gould & Eldredge, 1977; Gould & Eldredge, 1993; Kelley, 1983; Spanbauer et al., 2018), the fossil record often lacks the necessary resolution. A notable exception is the fossil record of marine plankton, such as planktonic foraminifera, which allows tracing of species transformations through time and in space with unparalleled continuity (Bicknell et al., 2018; Coxall et al., 2007; Malmgren et al., 1983; Pearson & Ezard, 2014).

An iconic example of gradual morphological transformation leading to the emergence of a complex character is the evolution of the spherical encompassing final chamber in the

planktonic foraminifera *Orbulina universa* (d'Orbigny, 1839), which is completely documented by a series of transitional forms leading from the ancestral *Trilobatus* to the descendant *Orbulina* (Blow, 1956; Jenkins, 1968; Pearson et al., 1997). This transition occurred in the open ocean and the transitional forms emerged throughout the cosmopolitan warm-water habitat of the evolving lineage within a very short time, providing several key biostratigraphic datums (Kennett & Srinivasan, 1983; Wade et al., 2011). The transition does not appear to be associated with a shift in the habitat of the evolving lineage (Pearson et al., 1997) and does not occur in association with any distinct global climatic event, making it difficult to speculate about the trigger for the emergence of the idiosyncratic shell form. However, a similar character evolved independently in an unrelated lineage of Paleogene foraminifera, culminating in the morphologically similar *Orbulinoides* (Cordey, 1968), implying that the spherical shape, minimising the surface to volume ratio of the adult shell, may represent a response to a specific lifestyle among planktonic foraminifera.

Indeed, there is abundant morphological (Norris, 1991), genetic (Weiner et al., 2015) and isotopic (Coxall et al., 2007) evidence for parallel or repeated evolution of specific chamber shapes and shell elements in planktonic foraminifera. Notable examples are the iterative evolution of compressed chambers with a keel (Norris, 1991), or of digitate or radially elongated chambers (Coxall et al., 2007; Weiner et al., 2015). The prevalence of iterative evolution among planktonic foraminifera can be explained by the presence of strong constructional constraints, imposing functional limits on the geometrical variability of shells constructed by sequential addition of interconnected chambers (Raup, 1966). Alternatively, the repeated evolution of similar traits may reflect phenotypic integration, resulting from the existence of a developmental and genetic network controlling the emergence of morphological traits in an organism (Pigliucci, 2003). Functional and developmental integration may both be heritable and interconnected, jointly shaping (or rather channeling) the phenotypic landscape of an evolving clade (Müller & Wagner, 1996).

In the case of the emergence of the spherical shell shape in planktonic foraminifera, it appears that the Paleogene *Orbulinoides* and the Neogene *Orbulina* followed a similar sequence of steps during their evolution, but it was only in *Orbulina*, where the evolutionary trend culminated in the emergence of a complex character, involving at the same time the enlargement of the final

chamber and the migration of the apertures over the entire chamber surface. This makes it difficult to speculate about the evolutionary mechanisms and potential drivers of the evolution of the complex character in *Orbulina*. However, next to these two well-known and globally distributed lineages, there also exists a third case of the evolution of a spherical shell shape in planktonic foraminifera: the enigmatic *Velapertina*. The genus *Velapertina* is endemic to the Central Paratethys, where it appears to have repeated the same sequence of transitional steps as *Orbulina*, culminating in the acceleration of chamber growth rate combined with aperture displacements. The existence of a potential endemic form with shell morphology similar to the *Orbulina* lineage was first formally acknowledged by Łuczkowska (1955), who described these forms from the Miocene of the Carpathian Foredeep as *Globigerinoides indigena*. The independent origin of this lineage from the *Orbulina lineage* was highlighted by Popescu (1969), who assigned this species to a new genus, *Velapertina*. Popescu (1969) described two new species of the genus, but these appear to be extreme morphologies with aberrant (kummerform) final chambers, otherwise identical with *Velapertina indigena*. A fourth species, *Velapertina sphaerica* (Popescu, 1987), has a morphology consistent with the *Orbulina* lineage. The origin of the idiosyncratic *Velapertina* remains unclear, but ever since its discovery, it has been only reported from Miocene deposits in the Paratethys.

Remarkably, the dating of the Miocene formations where the enigmatic *Velapertina* appears (NN6 Zone; e. g., Hohenegger et al., 2014) implies that the evolution of the final encompassing chamber in this lineage took place very shortly after the emergence of *Orbulina* (NN5 Zone). This coincidence cast doubts on the nature of *Velapertina*, and because there are only a few well documented cases of endemic evolution in planktonic foraminifera (e. g., Aurahs et al., 2009; Darling et al., 2007; Huber et al., 2020) and because it proved difficult to establish by external morphology alone whether it represents a variant of *Orbulina* (Łuczkowska, 1971; Szczechura, 1984) or an entirely independent lineage, the existence of *Velapertina* could so far not be used in arguments on evolutionary processes in planktonic foraminifera.

Here, we resolve the nature of *Velapertina* by revealing the interior shell architecture through CT (computed tomography) X-ray scanning of exceptionally well-preserved specimens and analysis of the full ontogenetic sequence leading to the development of its final encompassing chamber. We compare the ontogenetic trajectory of *Velapertina* with *Orbulina* and constrain

the habitat of the taxa by stable isotopic investigation of the shells and discuss the evolutionary consequences of the resulting findings.

2. Materials and methods

In order to constrain the spatio-temporal distribution of *Velapertina* throughout the Paratethys, and to resolve the degree of its co-occurrence with the *Orbulina* lineage, we carried out an extensive literature review, compiling all localities where either lineage has been reported (Fig. 1 and Table S1). Only localities which provide sufficient stratigraphic constraints to resolve the occurrences to the level of a planktonic foraminifera zone were considered. The search was carried out by querying the literature through Google Scholar, using combinations of taxonomic (Velapertina, Orbulina, Praeorbulina, indigena, suturalis, glomerosa, circularis) and geographic (Paratethys) keywords. The taxonomy has been harmonised across the papers to the genus level and in each case the occurrence and biozone has been recorded. In all cases where *Velapertina* was recorded as co-occurring with one of the other taxa, we made sure that the co-occurrence was reported from within the same sample in the sediment sequences described in each paper. Next to the canonical *Velapertina indigena* (Łuczkowska, 1955), three more species of the genus have been formally described (Popescu 1969, 1973, 1987), but these have been so far only recorded from single localities and in our opinion, it remains questionable whether the described morphologies represent distinct taxa or extreme forms within a variable species.

Since the terminal stage morphology, with the spherical encompassing final chamber with multiple small areal apertures is similar between the genera *Velapertina* and *Orbulina* (Fig. 2), we decided to study their relatedness by reconstructing the ontogenetic trajectory preserved in the sequence of chambers preceding the terminal spherical chamber. *Velapertina* is endemic to the Paratethys (Łuczkowska, 1971) and can be studied only on material from this realm. Thus, to resolve the relatedness of *Velapertina* and *Orbulina* we concentrated on specimens of the *Orbulina* lineages from the Paratethys assuming that these are representative of populations that could be potential ancestors or nearest relatives of *Velapertina*. In addition, we have also analysed one specimen of *Praeorbulina* from the Pacific, to make sure the morphology of the Paratethyan specimens is representative for the lineage at large. In the Paratethys, we concentrated on three middle Miocene localities (Fig. 1) of middle Miocene age (Badenian stage in the regional Paratethyan stratigraphy), representing the time shortly after the origin of

both lineages and exhibiting the best preservation of planktonic foraminifera, making it likely that the initial whorls inside the spherical shells of the studied species are preserved and suitable for CT scanning and 3D rendering.

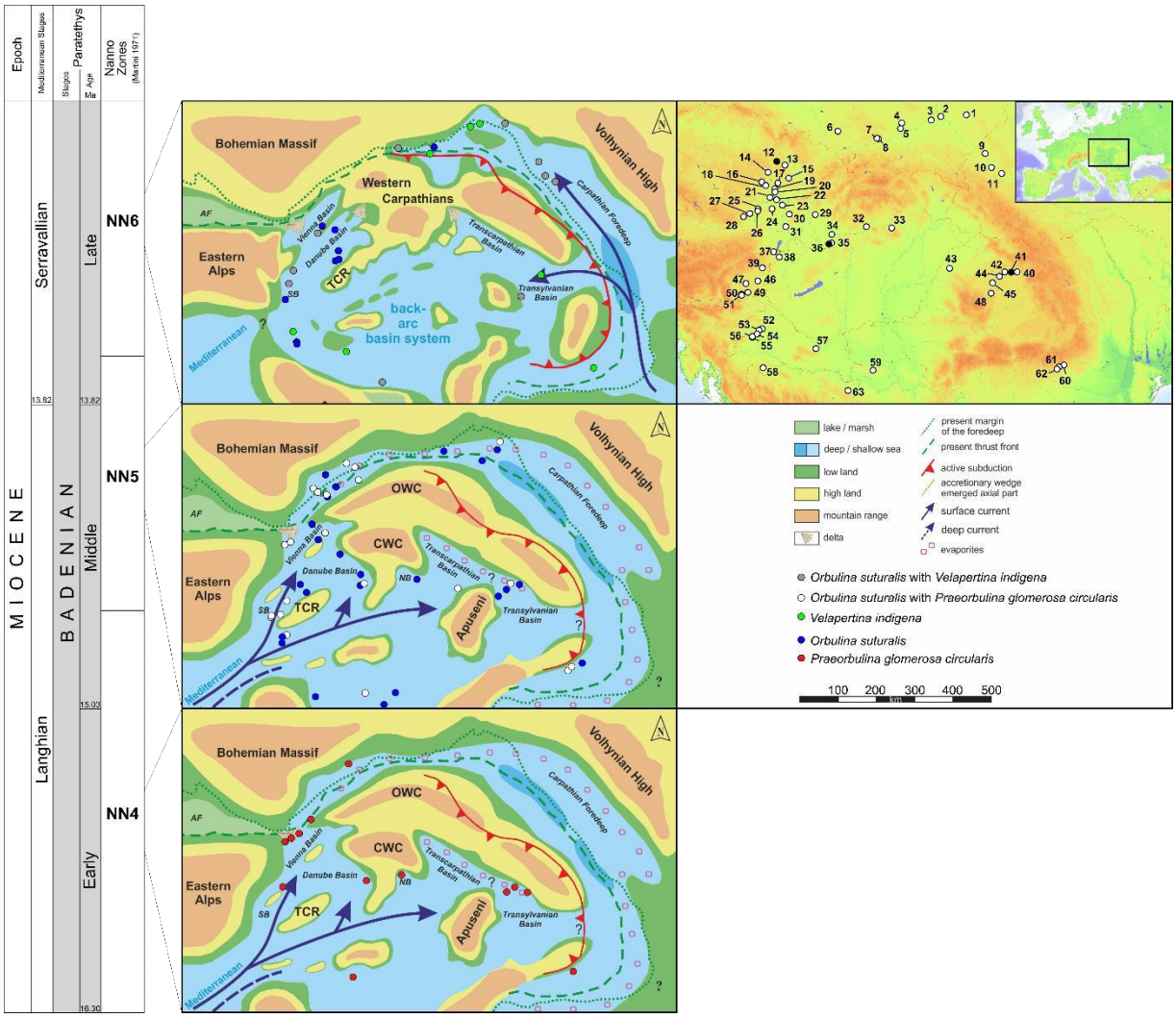

Figure 1. Distribution of *Praeorbulina glomerosa circularis*, *Orbulina suturalis* and *Velapertina indigena* throughout the Langhian and Serravallian (Badenian stage in the regional Paratethyan stratigraphy) Central Paratethys. Colours show the distinct species individual occurrence and co-occurrences, see legends. Paleogeographic reconstructions of the Paratethys were taken from Kováč et al. (2017), while locations used in the compilation of species distribution in space and time were collected following literature synthesis, site numbers refer to Supplementary table 1. The presented synthesis reveals that *Velapertina* and the *Orbulina* lineage were widespread throughout the middle Miocene Central Paratethys and that the representatives of the two lineages had overlapping distributions with well-documented co-occurrences.

One well preserved *Orbulina suturalis* specimen was obtained from a sample at 1303–1298 m in Modrany-1 well (N47°50058.51, E18°2208.42, Locality 36 in Fig. 1) from the south-eastern part of the Danube Basin (Slovak Republic), dated to M6 or NN5 Zone (Vlček et al., 2020). At this site, *Praeorbulina glomerosa circularis* was rare and did not yield specimens suitable for CT scanning. Further material was collected from an outcrop of Badenian (Langhian) clays also assigned to M6 or NN5 Zone at Jevíčko (N49°3815.6, E16°4113.3, Locality 12 in Fig. 1) in Moravia (Czech Republic) (Bubík, 2015; Reuss, 1854). At this locality, one well preserved specimen of *Praeorbulina g. circularis* and *Orbulina suturalis* was taken for CT scanning. The Pacific specimen of *Praeorbulina g. circularis* was selected from ODP Hole 872C, recovered in the vicinity of the Marshall Islands (Pacific Ocean). This sample is assignable to middle Miocene N10 Zone and the foraminifera were reported to be excellently preserved (Pearson, 1995). Finally, well-preserved *Velapertina indigena* specimens were retrieved from an outcrop at Chiuza (47° 14.610'N, 24° 14.863'E, Locality 41 in Fig. 1), located in the northern part of the Transylvanian Basin (Romania), dated to NN6 Zone, which corresponds to M7-M9 Zone (Filipescu, 1996).

At localities Jevíčko, Chiuza and from Modrany-1 core sample, about two hundred grams of sediment was collected. Samples were crushed into fragments of about 0.5 to 1 cm^3 size, soaked in tap water and diluted in 3% hydrogen peroxide (H_2O_2) until fully disintegrated and wet sieved over 63 μm and 150 μm mesh sieves. The residues were then dried and split at 40°C for 24 hours. Planktonic foraminifera were manually picked and determined from size fractions > 150 μm, except for a sample from Chiuza, where the fraction > 63 μm was used. The sample treatment of material obtained from Hole 872C, leg 144 is given by Pearson (1995). Planktonic foraminifera taxonomy follows the concepts of Blow (1956), Łuczkowska (1971) and Pearson et al. (1997). Initially, 80 individuals of *Orbulina suturalis* were isolated from the dried residue from Modrany-1, 80 individuals of *Praeorbulina g. circularis* and of *Orbulina suturalis* from Jevíčko and 80 individuals of *Velapertina indigena* from Chiuza. These specimens were subsequently transferred to a Petri dish filled with water to separate tests, which were not filled with sediment. Specimens with sediment-filled chambers sank to the bottom of the Petri dish, while those with empty shell interior remained floating. From among the presumably unfilled tests, we selected two individuals per species with particularly good preservation and well-developed terminal stage morphology for X-ray tomographic scanning.

The X-ray tomography was performed with the SkyScan 1172 high-resolution micro-CT device at the Natural Museum in Prague (Czech Republic). Tube voltage was set to 40 kV and the current source was 250 µA. No filter was used. Random Movement was set to 5. Data were acquired with an angle slope of 0.2° and 180° rotation. The acquired data were processed using flat field correction and reconstructed by the supplied software NRecon (Bruker), which resulted in an isotropic voxel size of 0.54 µm for the <0.5 mm large specimens. Each CT scan was visualized and morphometrically analysed with the software Amira ZIBE edition version 2019.04 (Stalling et al. 2005; http://amira.zib.de). The shells were segmented into the sequential chambers and any sediment remains within the chambers were manually removed with the Segmentation editor. The chambers were segmented by using the AmbientOcclusionField module and following the approach of Titschack et al. (2018) and Baum & Titschack (2016) (settings: number of rays: 156; ray length: ranging from 1 to 0.2 mm for every specimen and exceeding the cavity diameter in all other specimens). To separate the individual chambers within the shell, a DistanceMap of the intraspace was calculated as the basis for a CountourTreeSegmentation (persistence value: 0.05; see Titschack et al. 2018). The chamber separation was checked and manually corrected with the Segmentation editor. After this, the width, length, height, volume, flatness and elongation of the chambers and the width, length, height, and volume of the shell at different stages of growth were extracted with the ShapeAnalysis module, following Westin et al. (1997). To characterize the coiling geometry, we extracted the chambers centroids and used these to calculate the growth parameters introduced by Raup (1966) and Caromel et al. (2017): i) translation rate of the whorl (T), ii) expansion rate of the whorl (W), iii) the generating curve with respect to the coiling axis modified by Caromel et al. (2017) (D), and iv) the distance between the chambers centroid from the coiling axis in an x-y plane (R). For each specimen, we also recorded the total number of chambers and the number of whorls (#W) in the trochospire (Table S2).

Exceptionally well-preserved specimens of planktonic foraminifera from Chiuza and Jevíčko were used for stable isotopic characterisation of the habitat of the studied lineages. Despite a number of studies on the geochemistry of fossil planktonic foraminifera from the Central Paratethys (e. g., Báldi, 2006; Kováčová et al., 2009; Scheiner et al., 2018), the only analysis including *Velapertina* is the study by Durakiewicz et al. (1997) (Locality 6 in Fig. 1). This study indicates a shallow habitat for *Velapertina indigena*, overlapping with co-occurring *Orbulina*

suturalis and *Globigerinoides* sp., but the study has been conducted in an interval affected by the occurrence of evaporites, potentially biasing the oxygen isotopic results. Therefore, the stable isotopic habitat of the lineage relative to other planktonic foraminifera requires confirmation. The new measurements conducted here involved 15-20 specimens per species (approximately 100 µg), including individuals of *Praeorbulina g. circularis*, *Globigerina bulloides*, sinistrally and dextrally coiled *Neogloboquadrina* sp., and the benthic *Hansenisca soldanii* from Jevíčko, and *Velapertina indigena*, *Globigerina bulloides*, *Globoturborotalita* sp. and *Globigerinoides* sp. from Chiuza. Individuals of *Praeorbulina g. circularis* were further divided into small (< 200 µm) and large (> 200 µm) specimens, while in *Velapertina indigena* small (< 200 µm), moderate (200-300 µm) and large (> 300 µm) individuals were separated. The stable oxygen and carbon isotopic composition of the picked foraminifera were measured at MARUM, University of Bremen (Germany), with a Finnigan MAT 251 gas isotope ratio mass spectrometer connected to a Kiel 1 automated carbonate preparation device. The instrument was calibrated against the inhouse standard (ground Solnhofen limestone), which in turn was calibrated against the NBS 19 standard reference material. Over the measurement period, the standard deviations of the inhouse standard were 0.04 ‰ for $\delta^{13}C$ and 0.06‰ for $\delta^{18}O$. Data are reported in the delta-notation versus V-PDB.

3. Results

Our synthesis of literature occurrences reveals that both *Orbulina* lineage and *Velapertina* lineages were widespread throughout the middle Miocene Central Paratethys (Fig. 1). Because most of the records derive from outcrops, which only cover a small part of the middle Miocene sedimentary record, it was not possible to reconstruct the temporal occurrence with a precision higher than a foraminiferal biozone. At this resolution, the data synthesis indicates that the earliest representatives of *Praeorbulina* appeared in the Paratethys during the Langhian (M5 or NN4 Zone, early Badenian stage), likely originating from the Mediterranean region, where *Praeorbulina* is recorded from the earliest Langhian (Lirer et al., 2019), shortly after the global emergence of this lineage in the uppermost Burdigalian (M5 Zone, Wade et al., 2011). During the Langhian (M6 or base of NN5 Zone) we document the first occurrence of *Orbulina suturalis* and the co-occurrence of *Orbulina suturalis* with *Praeorbulina g. circularis* in a number of places throughout the Central Paratethys. This shows that this region displays the same species

succession in the evolving lineage as seen in the Mediterranean (Lirer et al., 2019) and in the world ocean (Wade et al., 2011).

Following the first appearance of *Orbulina*, *Velapertina indigena* evolved in the Central Paratethys in the Serravallian (M7-M9 or NN6 Zone, late Badenian). We identified 17 Serravallian localities where *Velapertina* was found, distributed throughout the Central Paratethys (Fig. 1). Of these, *Velapertina* co-occurred with *Orbulina* at 10 localities (co-occurrence implying the species were reported in the same sample) and there are only 9 localities, mainly in the Vienna Basin, where *Orbulina* has been reported but *Velapertina* was not. Within the stratigraphic resolution of our literature data synthesis, it is impossible to interpret whether the lack of *Velapertina* at some localities indicates an older age of those deposits. We can thus only conclude that at the given resolution of the Paratethyan stratigraphy, *Orbulina* and *Velapertina* had broadly overlapping distributions, with well documented co-occurrences, but we cannot identify where in Paratethys *Velapertina* originated.

Next to establishing the biogeography and the pattern of co-occurrence of the two lineages in the Central Paratethys, we analysed their shell geometry by X-ray imaging. Five of the six analysed specimens showed well-preserved internal shell features with minimal sediment infill, allowing us to manually reconstruct the pattern of chamber addition from the proloculus. The *Praeorbulina* specimens had 15 and 16 chambers, the *Orbulina* specimens had 12 and 13 chambers, and one of the *Velapertina* specimens had 14 chambers (Fig. 2 and 3). The initial whorl of the second *Velapertina* specimen proved to be damaged, with septa missing, and the shell architecture could therefore be reconstructed only for the last 10 chambers. The manual segmentation of the shell interior into the successive chambers reveals a pattern with rather constant and similar chamber growth rates throughout the ontogeny for all three taxa (Fig. 3), with a conspicuous acceleration of growth rate for the ultimate chamber occurring only in *Praeorbulina* and *Orbulina*. The average volume-based growth rate for six successive chambers starting with the penultimate chambers was in *Praeorbulina* 122% and 126%, in *Orbulina* 140% and 155% and in *Velapertina* 126% and 139% (Fig. 3). Whereas in *Praeorbulina* and *Orbulina*, the ultimate chamber became more spherical (similar width and height, Fig. 3c), in *Velapertina*, the ultimate chamber becomes conspicuously flatter, especially in one of the specimens (Fig. 3c and d).

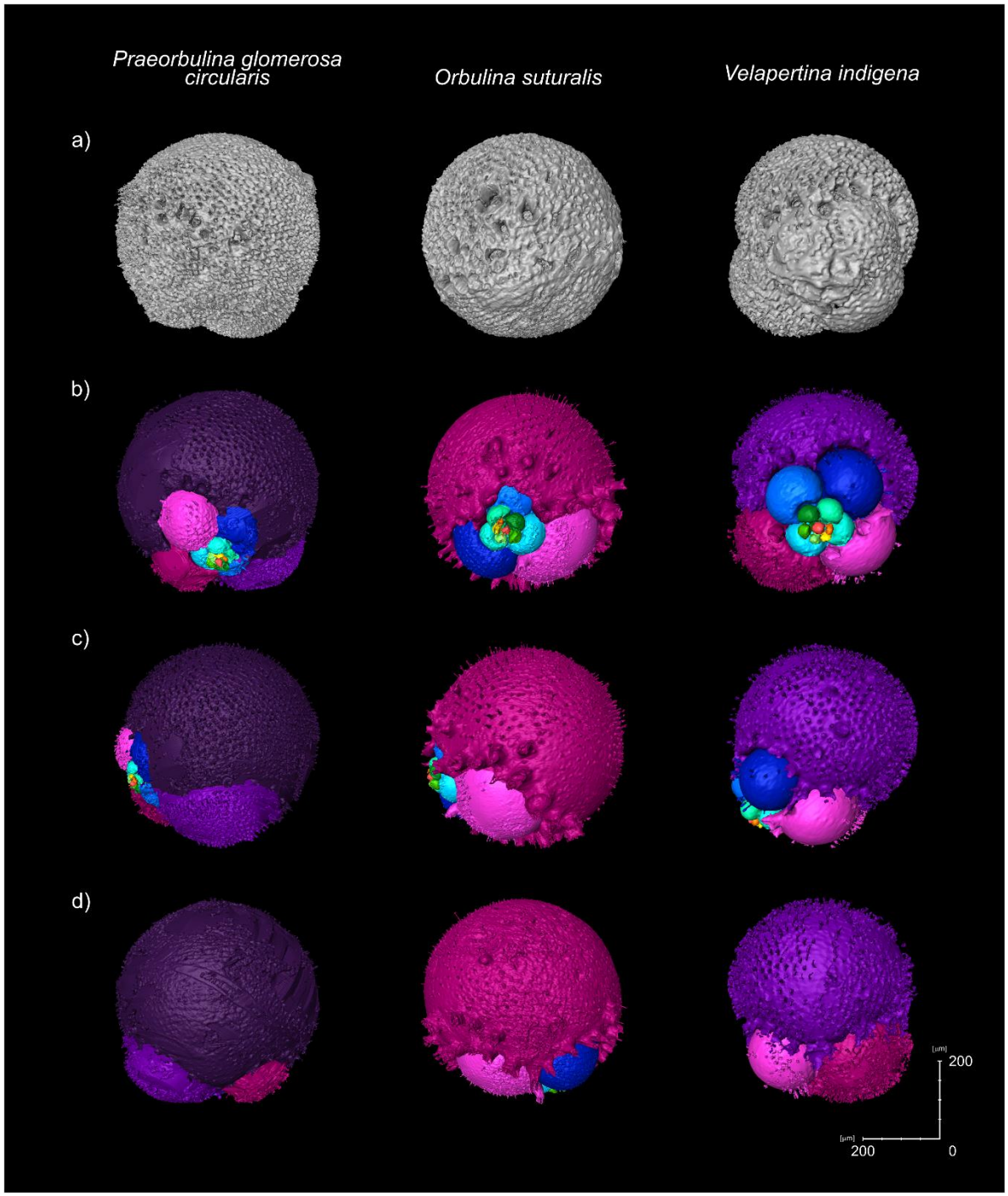

Figure 2. X-ray computed tomography imaging of shell architecture of *Praeorbulina glomerosa circularis*, *Orbulina suturalis* and *Velapertina indigena*. Species are shown from different perspectives: (a): spiral view of external morphology; (b): spiral view of internal morphology; (c): side view of internal morphology and (d): umbilical view of internal morphology. It appears, that the three species have similar external shell morphology with spherical shell shape and multiple apertures, but the CT data revealed distinct growth patterns of achieving the final encompassing chamber in *Orbulina* and *Velapertina* lineages.

The lack of growth acceleration towards the final chamber indicates that *Velapertina* must have achieved the spherical shell shape in a different manner than *Orbulina* and *Praeorbulina*. To assess the similarities in the ontogenetic trajectory preceding the ultimate chamber, we extracted the coordinates of the geometric centers of the five chambers added before to the ultimate chamber and used these to describe the shape of the logarithmic spire and the pattern of chamber addition along it for all six specimens. We combined these parameters with growth rate and chamber shape parameters for the same ontogenetic stage and analysed the resulting 10 parameters per specimen (Table S2) with cluster analysis, to visualise the similarity among the specimens. The outcome of this analysis shows higher similarity in the pre-adult ontogenetic trajectory and shell morphology between the two specimens of each species, indicating that the analysis likely captures a consistent aspect of the species pre-adult shell architecture. Next, the analysis reveals that the analysed shells of *Praeorbulina g. circularis* and *Orbulina suturalis* follow a more similar ontogeny, but the two specimens of *Velapertina indigena* are completely distinct (Fig. 4). These results suggest that the similar adult shell shape with encompassing final chamber in *Velapertina* and in the *Orbulina* lineage conceals a morphologically different pre-adult ontogenetic trajectory.

After analysing the shell architecture of the two lineages, we constrained the habitat of the lineages by comparing new stable isotopic analyses of their shells from Jevíčko and Chiuza with data from Durakiewicz et al. (1997). Our results at Jevíčko revealed a $\delta^{18}O$ offset of up to 1.5 ‰ between planktonic and benthic taxa. The benthic fauna at this site is represented by *Hansenisca soldanii*, which reveals the most enriched $\delta^{18}O$ signature. Among the analysed planktonic taxa, *Praeorbulina g. circularis* shows the heaviest $\delta^{18}O$ values and a distinct $\delta^{13}C$ enrichment, which is stronger in the larger individuals compared with smaller individuals, a signal consistent with the presence of symbionts (Fig. 5a). The Chiuza site, the best locality in terms of shell preservation of *Velapertina indigena*, lacks benthic foraminifera, but the overlap in the $\delta^{18}O$ values among all of the analysed planktonic species indicates that they likely all inhabited essentially the same surface layer. Here, we also found a conspicuous $\delta^{13}C$ enrichment in *Velapertina indigena*, especially among the larger specimens, which is of a similar magnitude as in the co-occurring *Globigerinoides* sp. These results are congruent with the earlier study by Durakiewicz et al. (1997), who recorded overall heavier $\delta^{18}O$ values, which may reflect the more northerly location of their material or an isotopic enrichment due to evaporation, as evidenced

by the presence of evaporites in their section. Nevertheless, those authors record a similar $\delta^{18}O$ offset between benthic and planktonic foraminifera and a similar $\delta^{13}C$ enrichment in *Velapertina indigena*, which is thus isotopically similar to *Orbulina suturalis* and *Globigerinoides* sp. Collectively, these results indicate that *Velapertina indigena* likely possessed symbionts and its stable isotopic habitat cannot be distinguished from that of the *Orbulina* lineage.

4. Discussion

Even though the external shell morphology of the *Orbulina* lineage and *Velapertina indigena* are similar (Fig. 2), with spherical shell shape, sutural and areal apertures, the CT data highlights a different internal shell architecture and a distinct growth pattern in *Velapertina* (Fig. 3 and 4). The high degree of overlap between the successive chambers and the negligible growth rate acceleration for the ultimate chamber found in *Velapertina* (Fig. 3a), indicate that this form achieved its terminal spherical shell morphology by progressively more overlapping chambers of similar size, whereas in *Orbulina*, the spherical shell emerges only in the final growth stage as a result of massive growth acceleration of the ultimate chamber that envelops the entire shell.

Indeed, next to the lack of growth acceleration, the final chamber in *Velapertina* is less globular (Fig. 3c and d) and does not completely encompass the earlier parts of the shell as is the case in *Praeorbulina* and *Orbulina* (Fig. 2). Instead, the analysed individuals of *Velapertina* bear consistent differences in shell architecture prior to the development of the ultimate chamber (Fig. 4), implying that their pre-adult morphology is not consistent with that of *Praeorbulina* and *Orbulina*. In other words, the ultimate chamber is not required to differentiate between the two lineages, because *Velapertina* is characterised by more overlap between the successive chambers, with centroids localized closer to the coiling axis (R = 87.36), throughout the early ontogeny, whereas in *Praeorbulina* - *Orbulina* the pre-adult part of the shell reveals a more loosely coiled, and more evolute growth geometry with less overlap between successive chambers, occupying more whorls and with chamber centroids disposed far from the coiling axes (R = 121.28). Thus, next to the Paleogene *Orbulinoides* (Cordey, 1968) and the Neogene *Orbulina* (d'Orbigny, 1839), *Velapertina* very likely represents the third example of the evolution of spherical shell shape among planktonic foraminifera.

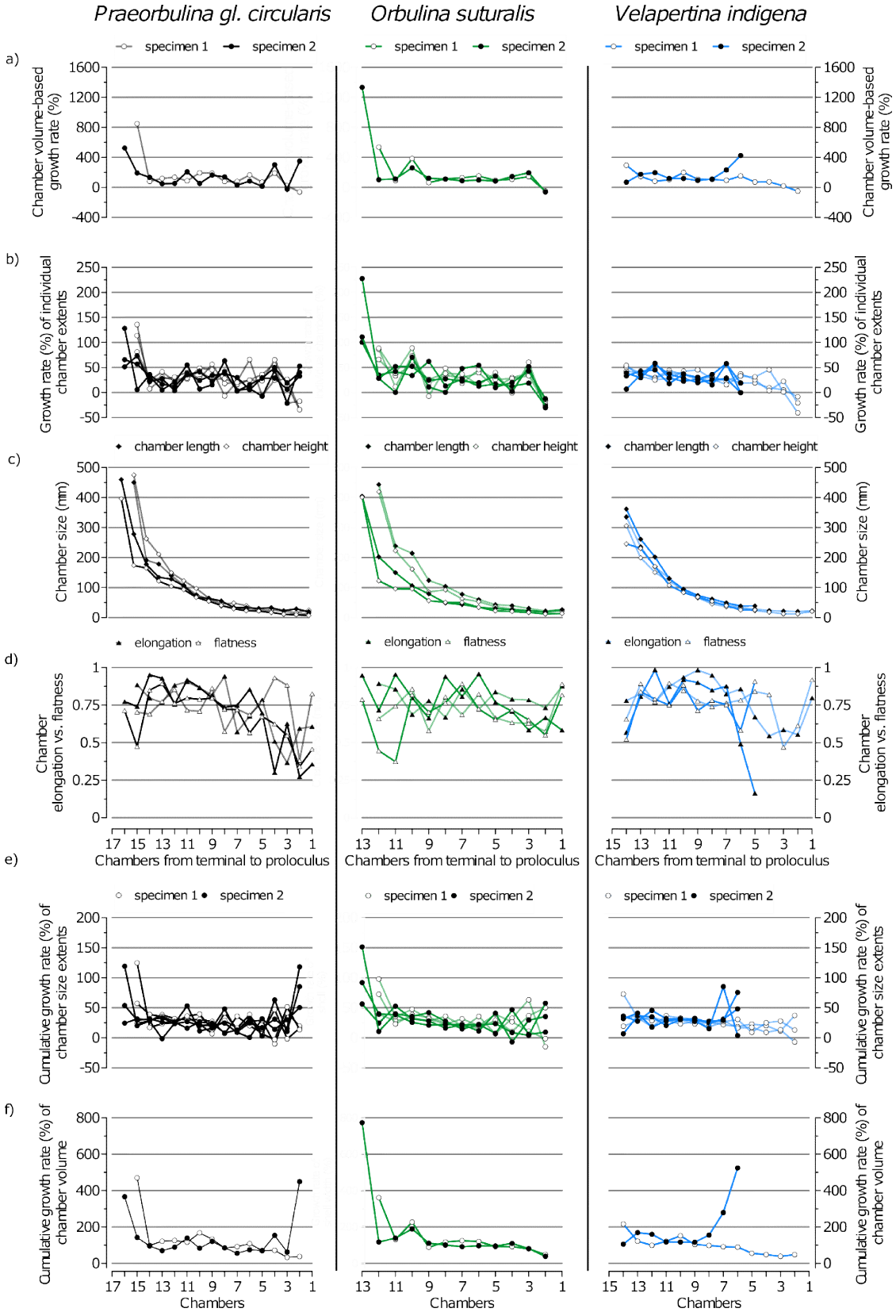
Praeorbulina gl. circularis
Orbulina suturalis
Velapertina indigena
a)
b)
c)
d)
e)
f)
specimen 1
specimen 2
Chamber volume-based growth rate (%)
Growth rate (%) of individual chamber extents
chamber length
chamber height
Chamber size (mm)
elongation
flatness
Chamber elongation vs. flatness
Chambers from terminal to proloculus
Cumulative growth rate (%) of chamber size extents
Cumulative growth rate (%) of chamber volume
Chambers

Figure 3. Ontogenetic trajectory of *Praeorbulina glomerosa circularis*, *Orbulina suturalis* and *Velapertina indigena* extracted from the X-ray computed tomography data. Different colours and lines denote different specimens, see legends. The growth trajectories of the analyzed species are plotted backward from the ultimate chamber to the proloculus: (a): growth rate based on the chamber-volume; (b): growth rate based on the chamber size extents (length, width and height); (c): chamber length and height ratio; (d): chamber flatness and elongation ratio; (e): cumulative growth rate based on the chambers size extents (length, width and height); (f): cumulative growth rate based on the chambers volume. The growth trajectories of the analyzed species are indeed similar, however the shape of the ultimate chamber and the lack of growth rate acceleration for the ultimate chamber in *Velapertina indicate* a different growth pattern as in the *Praeorbulina* - *Orbulina* lineage.

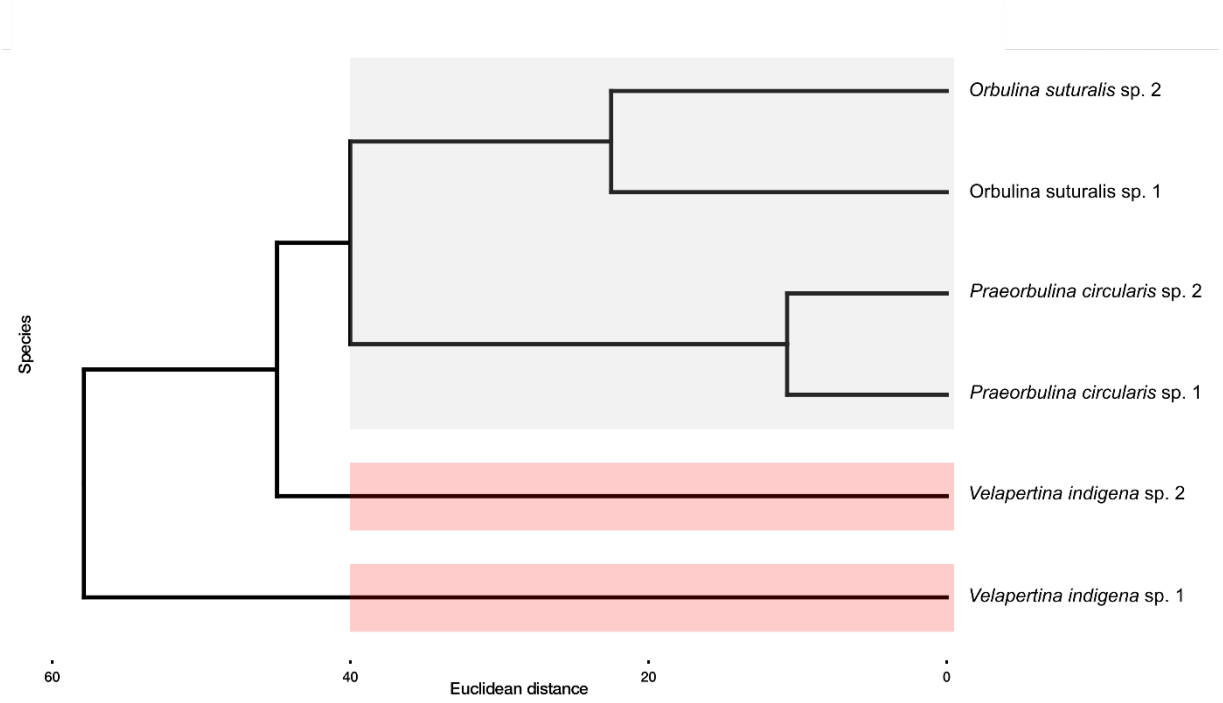

Figure 4. Cluster analysis (based on euclidean distance and single linkage clustering algorithm) of 10 variables describing the ontogenetic development of the adult morphology of the three analysed species. The variables are listed in Table S2 and include parameters describing the ontogeny of chamber shape and size and parameters of the logarithmic spiral determined from CT-rendering of internal volumes of the five chambers added prior to the final chamber. The clustering indicates that the convergent adult shape of *Velapertina indigena* is the result of a different ontogenetic sequence than in the *Praeorbulina* - *Orbulina* lineage.

The existence of a third independent case of the evolution of spherical shell shape in planktonic foraminifera, in *Velapertina*, allows us to assess the degree of developmental integration during the emergence of this character. When evolution is directed towards spherical shell geometry, the foraminifera are "faced" with the problem of retaining communication with the exterior through an aperture, without compromising the spherical shape. Both *Orbulinoides* and *Orbulina* exhibit a trend, where from a certain point along the transition towards a spherical shell, the large primary aperture transforms into a series of small sutural apertures. Remarkably, the same is observed in *Velapertina*, indicating that this may be the only solution available because of constructional constraints (Raup, 1966) during the morphogenesis of subsequent chambers. In *Orbulina*, where the terminal chamber encompasses the entire shell, this sequence had to go further, and the sutural apertures transformed further into multiple small openings covering evenly the entire surface of the shell (Blow, 1956). The Paratethyan *Velapertina* appears to have followed the same path of transformation: since the terminal chamber is not completely encompassing, there are still many sutural apertures, but it also possessed the first clearly identifiable areal apertures appearing in the final chamber (Popescu 1976; see also Fig. 2). This indicates a consistent connection between shell architecture and aperture types during the evolution of a spherical shell, with the emergence of areal apertures as the prerequisite for maintaining the trophic behaviour of the evolving lineage while possessing spherical shell shape.

The independent origin of spherical shells in *Velapertina indigena* implies that the similar morphological traits of *Velapertina* and *Orbulina* are the result of parallel evolution, a common phenomenon in the history of planktonic foraminifera (Coxall et al., 2007; Norris, 1991; Weiner et al., 2015). Coxall et al. (2007) documented the emergence of digitate chambers and concluded that there must have been an environmental driver that favoured this chamber morphology, associated with life in a deeper environment. Our stable isotopic analyses of *Velapertina indigena* indicates essentially the same habitat and presence of symbionts, as in the co-existing *Orbulina* lineage and the likely ancestral *Globigerinoides* (Fig 5.). This is in line with previous observations reporting no depth parapatry in the evolution of *Orbulina* (Pearson et al., 1997) and implies that the emergence of the spherical shell shape was not associated with a change in depth habitat. On the other hand, the independent evolution of the same trait in a co-existing lineage in the Central Paratethys indicates that there likely was a strong functional advantage of

this shape at that time. This prompts the question of why the spherical shell shape is so advantageous for planktonic foraminifera? As already recognised by Pearson et al. (1997), a spherical shell shape creates the minimum possible surface to volume ratio. Surface-to-volume ratio is a key parameter for cell physiology, determining the rate of key processes like gas exchange. Minimising this ratio implies a lifestyle where gas exchange is not limiting (no oxygen depletion), and its potential advantage could be that the spherical shell shape requires the least amount of material to achieve the maximum volume.

Having established that *Velapertina* evolved independently from *Orbulina*, it also has to be accepted that this peculiar form was endemic throughout its existence to the semi-isolated system of partly interconnected basins of the Central Paratethys (Fig. 1). The middle Miocene planktonic foraminifera composition in this complex marine realm was affected by tectonics and sea-level changes, creating marine gateways that facilitated population exchange between the Mediterranean and the Paratethys. The most prominent gateway during the Langhian was the Trans-Tethyan-Trench-Corridor, east of the Alps, which remained open until the Serravallian (Kováč et al., 2007; Kováč et al., 2017; Rögl, 1998) (Fig. 1). The timing of its restriction appears to coincide with the emergence of *Velapertina* and since *Velapertina* has never been reported outside of the Central Paratethys, the speciation of *Velapertina* likely took place in the then semi-isolated Central Paratethys. Here, the species clearly evolved in the presence of the *Orbulina* lineage, with which it co-occurred throughout the Central Paratethys (Fig. 1) and with which it shared its habitat (Fig. 5). It is unclear from the stratigraphic resolution of our data if *Velapertina indigena* evolved in the absence of *Orbulina* in some limited basins of the Paratethys, but certainly *Velapertina* co-occurred with *Orbulina* shortly after its emergence (Fig. 1). Assessing the spatial and temporal origin of *Velapertina* would require more detailed stratigraphic analysis of the basins, where the co-occurrence of the two lineages is documented. However, likely because of the restricted connection of the Central Paratethys in the Serravallian, the endemic *Velapertina* never succeeded to invade the world ocean. Like all other planktonic foraminifera inhabiting the Paratethyan basins it fell victim to the ongoing environmental transformation due to further restriction of the Central Paratethys, culminating in its transformation in the Tortonian into the Pannonian Lake (Kováč et al., 2007; Kováč et al., 2017).

As a result of its peculiar biogeography, *Velapertina* is one of only a few species of planktonic foraminifera with a known place of origin and an endemic distribution. Unlike the bipolar or Indopacific-Atlantic isolation known for some cryptic (Darling et al., 2003, 2007; Morard et al., 2011, 2019, Quillévéré et al., 2013; Weiner et al., 2015) or even morphologically distinguishable species (Kučera & Kennett, 2000; Lazarus et al., 1995), the distribution area of *Velapertina* was strikingly small and restricted. It is possible that this unusual degree of restriction facilitated speciation among the enclosed foraminifera, as evidenced by the existence of other endemic species that appear restricted to the Paratethys (Rögl, 1994).

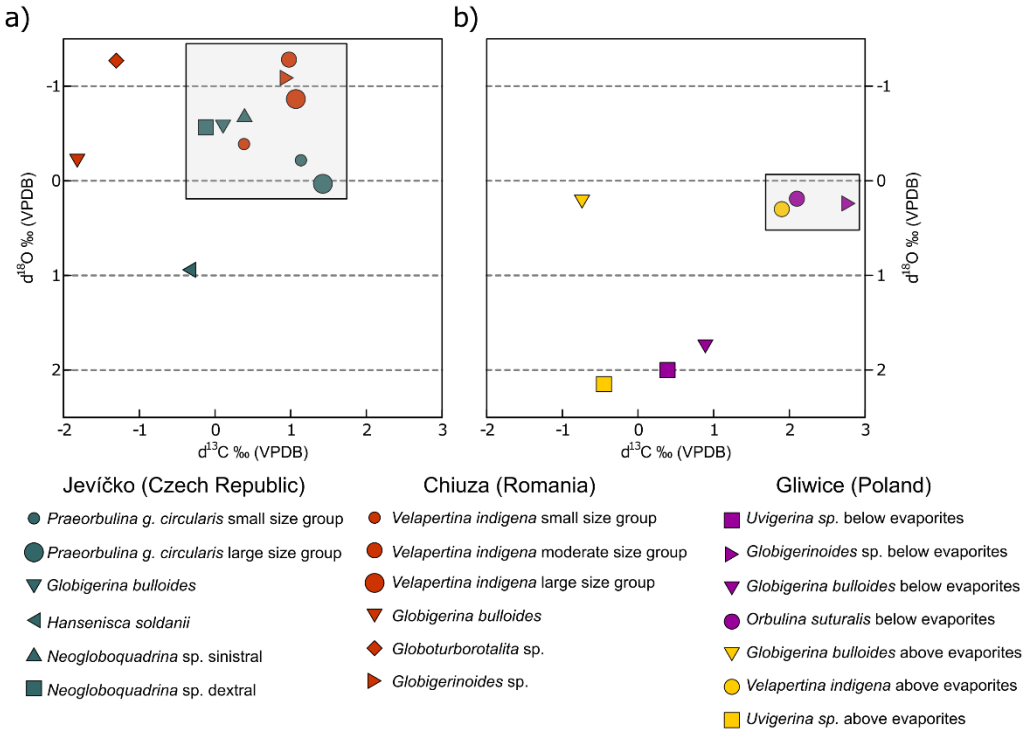

Figure 5. Multispecies habitat reconstruction of *Velapertina* relative to other planktonic foraminifera species based on $\delta^{13}C$ and $\delta^{18}O$ isotopes from (a) new measurements and (b) data from Durakiewicz et al. (1997).

5. Conclusions

The evolution of the spherical shell shape of *Orbulina universa* is a textbook example of an emergence of a complex character documented by a series of transitional steps, combining chamber growth rate and aperture modifications. Here we show that shortly after the emergence of *Orbulina*, the enigmatic lineage of *Velapertina* from the Central Paratethys iterated the same

steps of morphological integrations towards spherical shell shape. Through detailed CT analyses of *Praeorbulina glomerosa circularis*, *Orbulina suturalis* and *Velapertina indigena*, we revealed a consistent difference in the adult and pre-adult growth patterns of the two lineages, indicating that the *Velapertina* lineage had a different origin. This indicates that the final spherical morphology with areal apertures in *Velapertina indigena* results from convergent evolution with the *Orbulina* lineage. Because of increasing restriction of the biogeographical province, *Velapertina* remained endemic to the Paratethys throughout its short existence. The fact that it evolved shortly after *Orbulina* and shared the same habitat indicates a common environmental driver favouring spherical shells in planktonic foraminifera, implying that this complex character evolved in response to a specific environmental stimulus, such as the emergence of a specific habitat.

Acknowledgements

We thank Katarína Holcová for valuable discussions, Michael Jerry Sabo for proofreading the manuscript and Sorin Filipescu for providing material from Chiuza (Romania). The present study used a sample obtained during the Ocean Drilling Program (Leg 144).

P.K. was supported by the Collegium Talentum Programme of Hungary, by the Slovak Research and Development Agency under the contracts APVV 15-0575 and APVV 16-0121, by the Grants for Young Scientists of the Comenius University in Bratislava (UK/214/2019), by the German Academic Exchange Service (DAAD) Research Grant for Doctoral Candidates and Young Academic Scientists, by the German Academic Exchange Service (DAAD) STIBET Scholarship, by the National Scholarship Programme of the Slovak Republic and by the Erasmus+ Programme of the European Commission. We also acknowledge funding through the Cluster of Excellence ›The Ocean Floor – Earth's Uncharted Interface‹.

Site nr.	Lat (N)	Long (E)	Site name	Reference
1	50.64	22.80	Trzęsiny section, Poland	Szczechura (1984)
2	50.61	21.97	Jamnica M-83 core, Poland	Dumitriu et al. (2017)
3	50.53	21.66	Machów section, Poland	Dumitriu et al. (2017)
4	50.47	20.72	Busko Młyny borehole, Poland	Paruch-Kulczycka (2015)
5	50.35	20.67	Wiślica outcrop, Poland	Płonka (2017)
6	50.29	18.67	Gliwice boreholes, Poland	Bicchi et al. (2003)
7	50.14	19.91	Trojanowice 2 borehole, Poland	Olszewska (2014)
8	50.12	19.96	Bibice section, Poland	Machaniec & Pilarz (2011)
9	49.81	23.40	Bortiatyn-1 borehole, Poland	Garecka & Olszewska (2011)
10	49.50	23.60	Voloscha-1 borehole, Poland	Garecka & Olszewska (2011)
11	49.37	23.93	Pyatnychany-1 borehole, Poland	Garecka & Olszewska (2011)
12	49.64	16.69	Jevíčko outcrop, Czech Republic	in this study
13	49.56	16.96	Přemyslovice-3 borehole, Czech Republic	Holcová & Demény (2012)
14	49.40	16.41	Lomnice-1 core, Czech Republic	Scheiner et al. (2018)
15	49.27	17.07	HV-5 Rybníček core, Czech Republic	Kopecká (2012)
16	49.19	16.21	Králice and Oslavou section, Czech Republic	Zágoršek et al. (2007)
17	49.17	16.73	Šlapanice section, Czech Republic	Buriánek & Petrová (2013)
18	49.11	16.34	Oslovany sand pit, Czech Republic	Nehyba et al. (2016)
19	49.04	16.63	Židlochovice-1 borehole, Czech Republic	Doláková et al. (2014)
20	49.01	16.65	Nosislav-1 borehole, Czech Republic	Adámek et al. (2002)
21	48.86	16.47	Cf 600 Drnholec-5 borehole, Czech Republic	Petrová & Adámek (2005)
22	48.81	16.69	Mikulov section, Czech Republic	Brzobohatý et al. (2007)
23	48.69	16.87	Bernhardsthal borehole, Austria	Harzhauser et al. (2018)
24	48.61	16.54	Siebenhirten 3 borehole, Austria	Harzhauser et al. (2017)
25	48.61	16.08	Grund section, Austria	Spezzaferri & Rögl (2004)
26	48.56	16.08	KB-5 borehole, Austria	Gebhardt et al. (2009)
27	48.51	15.83	Mühlbach section, Austria	Harzhauser et al. (2003)
28	48.44	15.62	Gneixendorf, Austria	Spezzaferri & Rögl (2004)
29	48.48	17.93	Ratkovce-1 well, Slovak Republic	Rybár et al. (2015)
30	48.49	17.09	MZ 93 borehole, Slovak Republic	Koubová & Hudáčková (2010)
31	48.22	16.98	ZNV-1 Devínska Nová Ves borehole, Slovak Republic	Zlinská et al. (2013)
32	48.22	19.58	Trenč, Slovak Republic	unpublished/Kováč et al. (2017)
33	48.19	20.39	Sáta-75 borehole, Hungary	Selmeczi et al. (2012)
34	48.06	18.46	Pozba-3 borehole, Slovak Republic	Kováč et al. (2018)
35	47.87	18.46	Nová Vieska-1 borehole, Slovak Republic	Kováč et al. (2018)
36	47.85	18.37	Modrany-1 borehole, Slovak Republic	Kováč et al. (2018)
37	47.68	16.59	Sopron-89 borehole, Hungary	Selmeczi et al. (2012)
38	47.56	16.77	Nagylózs-1 borehole, Hungary	Selmeczi et al. (2012)
39	47.33	16.23	Bad Tatzmannsdorf 1 borehole, Austria	Friebe & Poltnig (1993)
40	47.24	24.43	Cepari section, Romania	Sant et al. (2019)
41	47.24	24.24	Chiuza section, Romania	Popescu & Crihan (2011)
42	47.24	24.03	Ciceu-Giurgești section, Romania	Sant et al. (2019)
43	47.32	22.25	Abrămuț section, Romania	Bojar et al. (2012)
44	47.15	23.86	Valea Dracului section, Romania	Sant et al. (2019)
45	47.01	23.64	Pâglișa section, Romania	Beldean et al. (2013)
46	47.05	16.08	Fürstenfeld 1 borehole, Austria	Friebe & Poltnig (1991)
47	46.99	15.69	Petersdorf-1 borehole, Austria	Hohenegger et al. (2009)
48	46.78	23.59	Piața Abator borehole, Romania	Suciu et al. (2005)
49	46.80	15.76	Perbersdorf-1 borehole, Austria	Hohenegger et al. (2009)
50	46.76	15.56	Wagna section, Austria	Hohenegger et al. (2009)

51	46.74	15.56	Retznei section, Austria	Hohenegger et al. (2009)
52	46.01	16.22	Donje Orešje section, Croatia	Vrsaljko et al. (2006)
53	45.98	16.11	Marija Bistrica section, Croatia	Sremac et al. (2018)
54	45.90	16.05	Čučurje section, Croatia	Ćorić et al. (2009)
55	45.83	15.90	Sveta Barbara section, Croatia	Pezelj et al. (2007)
56	45.84	15.90	Gornje Vrapče section, Croatia	Vrsaljko et al. (2006)
57	45.58	17.95	Ciprovac section, Croatia	Špišić et al. (2017)
58	45.17	16.25	Mt. Zrinska Gora section, Croatia	Martinuš et al. (2012)
59	45.11	19.79	B-11/08 borehole, Serbia	Rundić et al. (2013)
60	45.23	25.94	Slănic section, Romania	Bojar et al. (2018)
61	45.19	25.78	Brebu section, Romania	Sant et al. (2019)
62	45.14	25.71	Campinița section, Romania	Sant et al. (2019)
63	44.67	18.98	Ugljevik section, Bosnia and Herzegovina	Mandic et al. (2019)

Table S1. Localities used in the compilation of distribution of *Praeorbulina glomerosa circularis*, *Orbulina suturalis* and *Velapertina indigena* throughout the middle Miocene Central Paratethys. Site numbers refer to Figure 1.

Species	Specimen	Chamber number [#]	Chamber-length growth rate [%]	Chamber-width growth rate [%]	Chamber- height growth rate [%]	Chamber length and height ratio	Number of whorls [#W]	Chamber elongation and flatness ratio	Translation rate [T]	Generating curve [D]	Expansion rate [W]	Distance from the coiling axis [R]
P. g. circularis	1	1	NA	NA	NA	1.72	NA	0.73	NA	NA	NA	0.00
P. g. circularis	1	2	-34	-18	-35	1.72	0.00	1.56	0.17	0.60	NA	24.57
P. g. circularis	1	3	26	-22	14	1.92	0.15	0.41	0.01	0.63	189.09	28.28
P. g. circularis	1	4	25	57	65	1.45	0.30	0.54	0.09	0.51	100.65	30.06
P. g. circularis	1	5	-7	36	23	1.10	0.47	1.02	0.32	0.40	61.39	29.11
P. g. circularis	1	6	66	25	25	1.46	0.70	0.99	0.78	0.13	39.80	27.74
P. g. circularis	1	7	22	16	20	1.48	0.96	0.79	0.88	0.19	37.51	35.98
P. g. circularis	1	8	-7	28	18	1.17	1.17	1.64	0.52	0.32	44.69	52.48
P. g. circularis	1	9	45	26	56	1.09	1.41	0.95	0.90	0.07	38.26	53.99
P. g. circularis	1	10	49	42	28	1.27	1.76	1.22	1.72	-0.35	30.47	53.60
P. g. circularis	1	11	27	29	40	1.14	2.07	1.26	0.86	0.20	53.77	111.52
P. g. circularis	1	12	22	25	31	1.07	2.28	1.03	0.75	0.23	66.81	152.62
P. g. circularis	1	13	41	30	27	1.18	2.52	0.99	1.02	0.16	72.26	182.17
P. g. circularis	1	14	24	22	7	1.37	2.80	1.15	1.20	0.15	78.36	219.48
P. g. circularis	1	15	81	114	136	1.05	3.21	1.26	5.09	-3.33	28.27	90.78
P. g. circularis	2	1	NA	NA	NA	2.85	NA	0.78	NA	NA	NA	0.00
P. g. circularis	2	2	53	32	40	3.12	0.00	0.80	0.03	0.31	NA	18.56
P. g. circularis	2	3	-22	6	19	2.05	0.21	1.14	0.03	0.55	123.33	26.17
P. g. circularis	2	4	44	29	49	1.98	0.45	0.48	0.15	0.34	62.45	27.91
P. g. circularis	2	5	-8	28	29	1.42	0.65	1.03	0.00	0.46	54.67	35.53
P. g. circularis	2	6	8	15	6	1.45	0.80	1.51	0.14	0.43	51.66	41.52
P. g. circularis	2	7	4	3	30	1.16	0.96	1.04	0.58	0.35	41.33	39.72
P. g. circularis	2	8	63	42	38	1.37	1.19	1.02	1.00	0.05	30.48	36.41
P. g. circularis	2	9	15	22	34	1.18	1.48	1.00	0.77	0.15	37.90	56.01
P. g. circularis	2	10	7	41	24	1.01	1.72	1.10	0.71	0.23	41.32	71.25
P. g. circularis	2	11	55	35	38	1.14	1.98	1.15	1.58	-0.16	34.55	68.55
P. g. circularis	2	12	21	4	12	1.23	2.32	0.99	1.24	0.03	40.66	94.26
P. g. circularis	2	13	5	27	16	1.11	2.55	1.04	0.78	0.31	58.92	150.43
P. g. circularis	2	14	32	22	36	1.08	2.74	1.12	1.00	0.24	66.44	182.16
P. g. circularis	2	15	57	73	6	1.60	3.00	1.56	1.57	0.01	66.50	199.29
P. g. circularis	2	16	65	51	128	1.16	3.40	1.08	3.96	-2.04	35.07	119.20
Orbulina suturalis	1	1	NA	NA	NA	1.19	NA	0.98	NA	NA	NA	NA
Orbulina suturalis	1	2	-16	-31	-24	1.30	0.00	1.27	0.22	0.55	NA	0.00
Orbulina suturalis	1	3	39	60	33	1.36	0.16	1.25	0.46	0.48	241.93	0.16
Orbulina suturalis	1	4	29	-1	28	1.37	0.36	1.25	0.71	0.32	105.87	0.36
Orbulina suturalis	1	5	9	39	26	1.19	0.59	1.26	0.81	0.12	62.14	0.59
Orbulina suturalis	1	6	39	14	46	1.14	0.84	0.88	0.60	0.16	62.26	0.84
Orbulina suturalis	1	7	29	37	18	1.24	1.08	1.25	1.15	0.04	54.99	1.08
Orbulina suturalis	1	8	34	38	48	1.13	1.41	0.83	1.31	-0.01	51.57	1.41
Orbulina suturalis	1	9	19	26	-8	1.45	1.77	1.35	0.75	0.27	66.95	1.77

Orbulina suturalis	1	10	73	56	89	1.33	2.00	0.80	1.40	-0.09	67.48	2.00
Orbulina suturalis	1	11	11	33	38	1.07	2.29	1.15	2.16	-0.30	61.35	2.29
Orbulina suturalis	1	12	86	66	88	1.06	2.69	1.35	4.60	-2.63	34.51	2.69
Orbulina suturalis	2	1	NA	NA	NA	1.98	NA	0.71	NA	NA	NA	NA
Orbulina suturalis	2	2	-27	-30	-13	1.65	0.00	1.21	0.13	0.67	NA	0.00
Orbulina suturalis	2	3	19	51	43	1.37	0.15	0.89	0.38	0.54	196.41	0.15
Orbulina suturalis	2	4	12	2	20	1.29	0.32	0.99	0.33	0.44	100.54	0.32
Orbulina suturalis	2	5	17	32	10	1.37	0.52	1.18	0.59	0.28	58.54	0.52
Orbulina suturalis	2	6	12	19	54	1.00	0.76	1.32	0.79	0.10	39.59	0.76
Orbulina suturalis	2	7	27	22	48	0.86	1.01	0.90	0.77	0.25	44.34	1.01
Orbulina suturalis	2	8	13	27	0	0.96	1.24	1.23	0.84	0.21	43.94	1.24
Orbulina suturalis	2	9	62	25	11	1.41	1.56	0.94	1.30	-0.05	34.37	1.56
Orbulina suturalis	2	10	34	52	70	1.11	1.91	0.98	1.59	-0.24	36.18	1.91
Orbulina suturalis	2	11	42	52	0	1.57	2.27	2.56	1.00	0.25	64.54	2.27
Orbulina suturalis	2	12	35	28	28	1.65	2.52	1.60	1.35	0.14	64.02	2.52
Orbulina suturalis	2	13	100	111	228	1.01	2.93	1.20	4.30	-2.72	31.00	2.93
Velapertina indigena	1	1	NA	NA	NA	1.08	NA	0.87	NA	NA	NA	0.00
Velapertina indigena	1	2	-8	-21	-41	1.68	0.00	0.90	0.09	0.51	NA	11.58
Velapertina indigena	1	3	5	22	1	1.75	0.13	1.25	0.28	0.56	102.88	13.56
Velapertina indigena	1	4	9	4	45	1.31	0.27	0.66	0.35	0.52	54.82	14.71
Velapertina indigena	1	5	19	25	31	1.19	0.43	0.80	0.30	0.44	35.63	15.27
Velapertina indigena	1	6	19	37	33	1.07	0.62	1.09	0.44	0.30	26.66	16.50
Velapertina indigena	1	7	29	22	15	1.19	0.83	1.08	0.44	0.30	24.86	20.59
Velapertina indigena	1	8	20	31	27	1.13	1.04	1.28	0.93	0.19	21.92	22.76
Velapertina indigena	1	9	30	25	45	1.01	1.32	1.26	1.18	0.09	19.53	25.83
Velapertina indigena	1	10	36	36	42	0.97	1.60	1.10	0.98	0.14	24.48	39.14
Velapertina indigena	1	11	44	39	29	1.08	1.85	0.97	1.23	0.11	25.76	47.66
Velapertina indigena	1	12	30	28	25	1.12	2.09	1.00	1.22	0.12	28.25	59.12
Velapertina indigena	1	13	39	39	32	1.18	2.35	0.93	1.42	0.01	30.21	70.91
Velapertina indigena	1	14	42	51	54	1.10	2.75	1.19	4.97	-2.24	12.39	34.07
Velapertina indigena	2	1	NA	NA	NA	NA	NA	NA	NA	NA	NA	NA
Velapertina indigena	2	2	NA	NA	NA	NA	NA	NA	NA	NA	NA	NA
Velapertina indigena	2	3	NA	NA	NA	NA	NA	NA	NA	NA	NA	NA
Velapertina indigena	2	4	NA	NA	NA	NA	NA	NA	NA	NA	NA	NA
Velapertina indigena	2	5	NA	NA	NA	1.53	NA	0.18	NA	NA	NA	0.00
Velapertina indigena	2	6	0	19	-1	1.53	0.00	0.84	0.65	0.40	NA	42.09
Velapertina indigena	2	7	28	57	58	1.24	0.21	1.17	0.56	0.48	340.66	72.55
Velapertina indigena	2	8	26	15	36	1.14	0.40	1.09	0.42	0.33	179.34	72.06
Velapertina indigena	2	9	19	30	27	1.08	0.66	1.26	0.84	0.07	98.12	64.55
Velapertina indigena	2	10	29	37	22	1.14	0.99	1.04	2.54	-0.50	52.28	51.78
Velapertina indigena	2	11	37	18	29	1.20	1.27	1.01	1.16	0.24	103.80	132.21
Velapertina indigena	2	12	56	45	58	1.19	1.50	1.24	0.59	0.25	128.48	193.19
Velapertina indigena	2	13	29	43	35	1.13	1.74	0.96	1.31	-0.07	108.64	189.23
Velapertina indigena	2	14	38	33	7	1.47	2.14	1.09	3.32	-1.35	47.74	102.05

Table S2. Growth rates of chambers morphometric parameters (width, length and height), chamber length and height ratio and the parameters describing the shape of the logarithmic spire calculated based on the chambers geometric centroids of *Praeorbulina glomerosa circularis*, *Orbulina suturalis* and *Velapertina indigena*.

Conclusion

The calcite shells of planktonic foraminifera create a major component of the pelagic calcite flux. In the Cape Blanc upwelling area (Atlantic Ocean) during the 1990-1991 and 2007-2008 time series together, their contribution to the total calcite flux on the intra-annual timescale varied between 2 and 80 %, while their contribution for both time series together to the total calcite flux was ~21 %. The sedimentary time series from the tropical Atlantic (GeoB3104-1) revealed that their contribution to the total calcite flux beyond the intra-and interannual timescales is lower, approximately 9 %, with periods of higher relevance as during the Last Glacial Maximum, when the planktonic foraminifera calcite flux amounted for 24 % of the total calcite flux. Irrespective of the temporal domain, the contribution of planktonic foraminifera to the total calcite flux was constantly lower than the expected 20-50 % (Schiebel et al., 2007), which highlights the contribution of other groups of calcifying plankton to the total calcite flux.

Our inferences imply that the higher intra-annual variability in the planktonic foraminifera calcite flux is primarily driven by shell flux, since 82 % of the variability in the planktonic foraminifera calcite flux can be explained by shell flux alone. On the intra-annul time scale shell mass (shell size and calcification intensity) varied negligible, which probably results from intrinsic growth limitations, imposing minimum and maximum limits on the variability of shell size and calcification intensity of adult foraminifera shells. A similar variability in the regulating mechanisms was also reported elsewhere in the global ocean under seasonally varying environmental conditions (Deuser et al., 1981; Storz et al., 2009; Weinkauf et al., 2016). On the interannual timescales, multiple mechanisms act in concert to shape the variability in the planktonic foraminifera calcite flux, which prediction will require next to the knowledge of shell flux information about shell mass. Specifically, on the interannual timescales, the variability in shell size matched the variability in shell flux, implying that shell size for the prediction of temporal changes in the planktonic foraminifera calcite flux can be as much important as shell flux. The importance of shell size on the interannual timescale emerged from the fact that one of the studied years yielded foraminifera shells being 36 % on average smaller than in the second year. On longer timescales across major climate transitions, shell flux was the best predictor of variability in the planktonic foraminifera calcite flux. Despite the major changes in land and sea-surface temperature combined with modification in the carbonate chemistry across the

glacial-interglacial cycle, the shell mas remained relatively constant. The low variability in calcification intensity is supported by observations from the Miocene site, which reveals that despite different background climate state and millions of years of evolution, the calcification intensity of the studied species remained similar. This challenges earlier observations about the changes in calcification intensity in response to major climate transitions (Barker & Elderfield, 2002; Zarkogiannis et al., 2019).

Our analyses help to guide future research by setting priorities for modelling the variability in the planktonic foraminifera calcite flux and calcite budget. From our short-term and long-term observations, it appears, that calcification intensity was the least important predictor of planktonic foraminifera calcite flux. Irrespective of the temporal scale, the variability in the calcification intensity was constantly the lowest. In addition, the comparison of *Globigerina bulloides* calcification intensity between mid-Miocene and modern assemblages did not reveal substantial differences in the calcification intensity despite the species long-term evolution under warmer climate and elevated carbon dioxide concentration. The importance of shell size depends on the temporal scale since the accuracy of interannual predictions of variability in calcite flux can be significantly improved by the knowledge of shell size. Beyond the interannual timescale, the species derived shell size measurements imply minor variability and thus shell size can be ignored for predictions on geologically relevant timescales. Shell flux was clearly the most important predictor for the intra-and interannual variability in the planktonic foraminifer a calcite flux. It is the most variable mechanisms, probably because it reflects the connection between the environmental conditions and the ecological niches of the individual species (Žarić et al., 2006). Its relevance for predicting changes on centennial to millennial timescales depends on the environmental conditions. During climatically stable periods, shell flux, shell size, and calcification intensity are required to predict the variability in the planktonic foraminifera calcite flux. In contrast, across major climate transitions, such as during the last deglaciation, the shell flux captured the best the variability in the planktonic foraminifera calcite flux.

Outlook

Planktonic foraminifera are marine protists that produce calcite shells. Yet, the response of calcite production and export in planktonic foraminifera under global change, remained incompletely constrained. Understanding the variable export and production of planktonic foraminifera calcite under different environmental conditions is crucial for predicting the response of the pelagic carbonate flux and the marine carbon cycle on ocean acidification. As our inferences imply, shell flux and shell size are the most relevant predictors of changes in the planktonic foraminifera calcite flux. Therefore, it seems essential to understand the biotic and abiotic factors controlling shell flux and shell size variability. Indeed, the controlling mechanisms of planktonic foraminifera shell size have always been in a great interest of the scientific community (Hecht, 1976; Rillo et al., 2020; Schmidt et al., 2004). There are also a number of existing models aiming to constrain the spatio-temporal distribution of planktonic foraminifera (Fraile et al., 2008; Jonkers & Kučera, 2015; Kretschmer et al., 2018; Lombard et al., 2011; Žarić et al., 2006). Thus, by using a combination of inferences obtained in this dissertation, with the existing models concerning foraminifera size and shell flux variability, a model could be developed in order to understand the intensity of planktonic foraminifera calcite production and export under global warming and ocean acidification. This would also help us to understand how the final ranking of the mechanism's importance (1. Shell flux, 2. Shell size and 3. Calcification intensity) in shaping the variability in the planktonic foraminifera calcite flux will respond to global warming. With this knowledge, further hypothesis could be tested. For instance, i) how will the planktonic foraminifera calcite budget change under global warming; ii) what if calcification intensity decreases in the future and what will be the consequence of less heavily calcified shells in terms of the amount of exported calcite mass to the deep ocean; iii) if shell walls become thinner (de Moel et al., 2009), and shell weight decreases, will shell flux intensify or shells become larger, and compensate the less heavily calcified foraminifera shells in the planktonic foraminifera calcite flux?

References

Adámek, J., Petrová, P., & Švábenická, L. (2002). Preliminary results of the investigations at the Karpatian/lower Badenian boundary in the Carpathian Foredeep. *Geologické výzkumy na Moravě a ve Slezsku*, 16–19

Al-Sabouni, N., Kučera, M., & Schmidt, D. N. (2007). Vertical niche separation control of diversity and size disparity in planktonic foraminifera. *Marine Micropaleontology*, *63*(1–2), 75–90. https://doi.org/org/10.1016/j.marmicro.2006.11.002

Alderman, S. E. (1996). *Planktonic foraminifera in the Sea of Okhotsk: Population and stable isotopic analysis from a sediment trap* (Master's thesis). Cambridge: Massachusetts Institute of Technology/Woods Hole Oceanographic Institution.

Aldridge, D., Beer, C. J., & Purdie, D. A. (2012). Calcification in the planktonic foraminifera *Globigerina bulloides* linked to phosphate concentrations in surface waters of the North Atlantic Ocean. *Biogeosciences*, *9*(5), 1725-1739. https://doi.org/10.5194/bg-9-1725-2012

Allen, K. A., Hönisch, B., Eggins, S. M., Haynes, L. L., Rosenthal, Y., & Yu, J. (2016). Trace element proxies for surface ocean conditions: A synthesis of culture calibrations with planktic foraminifera. *Geochimica et Cosmochimica Acta*, *193*, 197–221. https://doi.org/10.1016/j.gca.2016.08.015

Archer, D. E. (1996). An atlas of the distribution of calcium carbonate in sediments of the deep sea. *Global Biogeochemical Cycles*, *10*(1), 159–174. https://doi.org/org/10.1029/95gb03016

Arz, H. W., Pätzold, J., & Wefer, G. (1998a). Calcium carbonate, total organic carbon and total carbon of sediment core GeoB3104-1. Dataset accessed [2020-01-18] at: https://doi.pangaea.de/10.1594/PANGAEA.54826. https://doi.org/10.1594/PANGAEA.54826

Arz, H. W., Pätzold, J., & Wefer, G. (1998b). Age determination of sediment core GeoB3104-1. Dataset accessed [2020-06-03] at: https://doi.pangaea.de/10.1594/PANGAEA.82333

Arz, H. W., Pätzold, J., & Wefer, G. (1999). The deglacial history of the western tropical Atlantic as inferred from high resolution stable isotope records off northeastern Brazil. *Earth and Planetary Science Letters*, *167*(1-2), 105–117. https://doi.org/10.1016/s0012-821x(99)00025-4

Asahi, H., & Takahashi, K. (2007). A 9-year time-series of planktonic foraminifer fluxes and environmental change in the Bering sea and the central subarctic Pacific Ocean, 1990–1999. *Progress in Oceanography*, *72*(4), 343–363. https://doi.org/org/10.1016/j.pocean.2006.03.021

Aurahs, R., Grimm, G. W., Hemleben, V., Hemleben, C., & Kučera, M. (2009). Geographical distribution of cryptic genetic types in the planktonic foraminifer *Globigerinoides ruber*. *Molecular Ecology*, *18*(8), 1692–1706. https://doi.org/org/10.1111/j.1365-294x.2009.04136.x

Baker, E. T., Milburn, H. B., & Tennant, D. A. (1988). Field assessment of sediment trap efficiency under varying flow conditions. *Journal of Marine Research*, *46*(3), 573–592. https://doi.org/10.1357/002224088785113522

Báldi, K. (2006). Paleoceanography and climate of the Badenian (Middle Miocene, 16.4–13.0 Ma) in the Central Paratethys based on foraminifera and stable isotope ($\delta^{18}O$ and $\delta^{13}C$) evidence. *International Journal of Earth Science (Geologische Rundschau)*, *95*, 119–142. https://doi.org/org/10.1007/s00531-005-0019-9

Balch, W. M., Bates, N. R., Lam, P. J., Twining, B. S., Rosengard, S. Z., Bowler, B. C., et al. (2016). Factors regulating the Great Calcite Belt in the Southern Ocean and its biogeochemical significance. *Global Biogeochemical Cycles*, *30*(8), 1124–1144. https://doi.org/10.1002/2016gb005414

Barker, S., & Elderfield, H. (2002). Foraminiferal calcification response to glacial-interglacial changes in atmospheric CO_2. *Science*, *297*(5582), 833–836. https://doi.org/10.1126/science.1072815

Baum, D., & Titschack, J. (2016), Cavity and pore segmentation in 3D images with ambient occlusion, in *Proceedings of the 18th EG/VGTC Conference on Visualization*, edited, pp. 113–117, Groningen, Netherlands.

Baumann, K.-H., Böckel, B., & Frenz, M. (2004). Coccolith contribution to South Atlantic carbonate sedimentation. In H. R. Thierstein, J. Young (Eds.), *Coccolithophores: from molecular processes to global impact*. (pp. 367–402). Berlin, Heidelberg: Springer Berlin Heidelberg.

Baumert, H. Z., & Petzoldt, T. (2008). The role of temperature, cellular quota and nutrient concentrations for photosynthesis, growth and light–dark acclimation in phytoplankton. *Limnologica*, *38*(3-4), 313–326. https://doi.org/10.1016/j.limno.2008.06.002

Bazin, L., Landais, A., Lemieux-Dudon, B., Toyé Mahamadou Kele, H., Veres, D., Parrenin, F., et al. (2013). Carbon dioxide composite data on AICC2012 chronology. Dataset accessed [2020-02-04] at: https://doi.pangaea.de/10.1594/PANGAEA.824893. https://doi.org/10.1594/PANGAEA.824893

Bé, A. W. H., Bishop, J. K., Sverdlove, M. S., & Gardner, W. D. (1985). Standing stock, vertical distribution and flux of planktonic foraminifera in the Panama Basin. *Marine Micropaleontology*, *9*(4), 307–333. https://doi.org/10.1016/0377-8398(85)90002-7

Beer, C. J., Schiebel, R., & Wilson, P. A. (2010). Testing planktic foraminiferal shell weight as a surface water CO_3^{2-} proxy using plankton net samples. *Geology*, *38*(2), 103–106. https://doi.org/org/10.1130/g30150.1

Behling, H., Arz, H. W., Pätzold, J., & Wefer, G. (2000). Late Quaternary vegetational and climate dynamics in northeastern Brazil, inferences from marine core GeoB 3104-1. *Quaternary Science Reviews*, *19*(10), 981–994. https://doi.org/10.1016/s0277-3791(99)00046-3

Beldean, C., Bercea, R., & Filipescu, S. (2013). Sedimentology and biostratigraphy of the early-middle Miocene transition in NW Transylvanian Basin (Păglişa and Dej sections). *Studia Universitatis Babes-Bolyai, Geologia*, *58*(1), 57–70. https://doi.org/org/10.5038/1937-8602.58.1.5

Berg, R. D., Solomon, E. A., & Teng, F. Z. (2019). The role of marine sediment diagenesis in the modern oceanic magnesium cycle. *Nature Communications*, *10*(1), 1–10. https://doi.org/org/10.1038/s41467-019-12322-2

Berner, R. A., & Honjo, S. (1981). Pelagic sedimentation of aragonite: Its geochemical significance. *Science*, *211*(4485), 940–942. https://doi.org/org/10.1126/science.211.4485.940

Bicchi, E., Ferrero, E., & Gonera, M. (2003). Palaeoclimatic interpretation based on middle Miocene planktonic foraminifera: the Silesia Basin (Paratethys) and Monferrato (Tethys) records. *Palaeogeography, Palaeoclimatology, Palaeoecology*, *196*(3–4), 265–303. https://doi.org/org/10.1016/s0031-0182(03)00368-7

Bicknell, R. D. C., Collins, K. S., Crundwell, M., Hannah, M., Crampton, J. S., & Campione, N. E. (2018). Evolutionary transition in the late Neogene planktonic foraminiferal genus *Truncorotalia*. *iScience*, *8*, 295–303. https://doi.org/org/10.1016/j.isci.2018.09.013

Bijma, J., Hönisch, B., & Zeebe, R. E. (2002). Impact of the ocean carbonate chemistry on living foraminiferal shell weight: Comment on "Carbonate ion concentration in glacial-age deep waters of the Caribbean Sea" by W. S. Broecker and E. Clark. *Geochemistry, Geophysics, Geosystems*, *3*(11), 1–7. https://doi.org/10.1029/2002gc000388

Bijma, W., Faber, W. W., & Hemleben, C. (1990). Temperature and salinity limits for growth and survival of some planktonic foraminifers in laboratory cultures. *Journal of Foraminiferal Research*, *20*(2), 95–116

Blow, W. H. (1956). Origin and evolution of the foraminiferal genus *Orbulina* d'Orbigny. *Micropaleontology*, *2*(1), 57–70. https://doi.org/org/10.2307/1484492

Bojar, A.-V., Barbu, V., & Bojar, H.-P. (2012). Middle Miocene zeolite-bearing turbidites, Abrămuţ Basin (Pannonian Basin), NW Romania. *Geological Quarterly*, 261–268. https://doi.org/org/10.7306/gq.1020

Bojar, A.-V., Barbu, V., Wójtowicz, A., Bojar, H.-P., Hałas, S., & Duliu, O. (2018). Miocene Slănic tuff, Eastern Carpathians, Romania, in the context of Badenian salinity crisis. *Geosciences*, *8*(2), 73–86. https://doi.org/org/10.3390/geosciences8020073

Bolton, C. T., Hernandez-Sanchez, M. T., Fuertes, M. A., Gonzalez-Lemos, S., Abrevaya, L., Mendez-Vicente, A., et al. (2016). Decrease in coccolithophore calcification and CO_2 since the middle Miocene. *Nat Commun*, *7*, 10284. https://doi.org/10.1038/ncomms10284

Brombacher, A., Elder, L. E., Hull, P. M., Wilson, P. A., & Ezard, T. H. G. (2018). Calibration of test diameter and area as proxies for body size in the planktonic foraminifer *Globoconella Puncticulata*. *Journal of Foraminiferal Research*, *48*(3), 241–245. https://doi.org/org/10.2113/gsjfr.48.3.241

Brönnimann, P. (1951). The genus *Orbulina* d'Orbigny in the Oligo-Miocene of Trinidad. *Contribution from the Cushman Foundation for foraminiferal research*, *2*(4), 132–138

Brummer, G.-J. A., Hemleben, C., & Spindler, M. (1986). Planktonic foraminiferal ontogeny and new perspectives for micropalaeontology. *Nature*, *319*(6048), 50-52. https://doi.org/10.1038/319050a0

Brummer, G.-J. A., Hemleben, C., & Spindler, M. (1987). Ontogeny of extant spinose planktonic foraminifera (*Globigerinidae*): A concept exemplified by *Globigerinoides sacculifer* (Brady) and *G. ruber* (d'Orbigny). *Marine Micropaleontology*, *12*, 357-381. https://doi.org/10.1016/0377-8398(87)90028-4

Brzobohatý, R., Nolf, D., & Kroupa, O. (2007). Fish otoliths from the middle Miocene of Kienberg at Mikulov, Czech Republic, Vienna Basin: their paleoenvironmental and paleogeographic significance. *Bull l'Institut R des Sci Nat Belqique Sci la Terre*, *77*, 167–196

Bubík, M. (2015). Tracking Richard Johann Schubert in Moravia: field-trip guide. In M. Bubík, A. Ciurej, M. A. Kaminski (Eds.), *16th Czech-Slovak-Polish Palaeontological Conference & 10th Polish Micropalaeontological Workshop, Abstracts Book and Excursion Guide*. (pp. 88–97). The Grzybowski Foundation & Micropress Europe, Kraków - New York.

Buitenhuis, E. T., Le Quéré, C., Bednaršek, N., & Schiebel, R. (2019). Large contribution of Pteropods to shallow $CaCO_3$ export. *Global Biogeochemical Cycles*, *33*(3), 458–468. https://doi.org/doi.org/10.1029/2018gb006110

Buriánek, D., & Petrová, P. T. (2013). Chemical composition and micropalaeontology of Badenian algal sandy limestone and calcareous sandstone. *Geologické výzkumy na Moravě a ve Slezsku*, 7–12

Caromel, A. G. M., Schmidt, D. N., Fletcher, I., & Rayfield, E. J. (2015). Morphological Change During The Ontogeny Of The Planktic Foraminifera. *Journal of Micropalaeontology*. https://doi.org/10.1144/jmpaleo2014-017

Caromel, A. G. M., Schmidt, D. N., & Rayfield, E. J. (2017). Ontogenetic constraints on foraminiferal test construction. *Evolution & Development*, *19*(3), 157–168. https://doi.org/org/10.1111/ede.12224

Catubig, N. R., Archer, D. E., Francois, R., deMenocal, P., Howard, W., & Yu, E.-F. (1998). Global deep-sea burial rate of calcium carbonate during the last glacial maximum. *Paleoceanography*, *13*(3), 298–310. https://doi.org/org/10.1029/98pa00609

Cicha, I., Čtyroká, J., Jiříček, R., & Zapletalová, I. (1975). Principal biozones of the Late Tertiary in the East Alps and West Carpathians. In I. Cicha (Eds.), *Biozonal division of the Upper Tertiary basins of the Eastern Alps and West Carpathians*. IUGS Proceedings of the VI Congress Bratislava.

Clark, P. U., Shakun, J. D., Baker, P. A., Bartlein, P. J., Brewer, S., Brook, E., et al. (2012). Global climate evolution during the last deglaciation. *Proc Natl Acad Sci U S A*, *109*(19), E1134-1142. https://doi.org/10.1073/pnas.1116619109

Comeau, S., Gorsky, G., Jeffree, R., Teyssié, J.-L., & Gattuso, J. P. (2009). Impact of ocean acidification on a key Arctic pelagic mollusc (Limacina helicina). *Biogeosciences*, *6*(9), 1877–1882. https://doi.org/10.5194/bg-6-1877-2009

Cordey, W. G. (1968). Morphology and phylogeny of Orbulinoides beckmanni (Saito, 1962). *Palaeontology*(11), 371–375

Ćorić, S., Pavelić, D., Rögl, F., Mandic, O., Vrabac, S., Avanić, R., et al. (2009). Revised middle Miocene datum for initial marine flooding of North Croatian Basins (Pannonian Basin System, Central Paratethys). *Geologia Croatica*, *62*(1), 31–43

Coxall, H. K., Wilson, P. A., Pearson, P. N., & Sexton, P. F. (2007). Iterative evolution of digitate planktonic foraminifera. *Paleobiology*, *33*(4), 495–516. https://doi.org/org/10.1666/06034.1

Curry, W. B., Ostermann, D. R., Guptha, M. V. S., & Ittekkot, V. (1992). Foraminiferal production and monsoonal upwelling in the Arabian Sea: Evidence from sediment traps. *Geological Society, London, Special Publications*, *64*(1), 93–106. https://doi.org/org/10.1144/gsl.sp.1992.064.01.06

d'Orbigny, A. (1839). Foraminifères. In A. Bertrand (Eds.), *De la Sagra R., Histoire physique et naturelle de l'Ile de Cuba*. (pp. 1–224).

Darling, K., Kučera, M., & Wade, C. M. (2007). Global molecular phylogeography reveals persistent Arctic circumpolar isolation in a marine planktonic protist. *Proceedings of the National Academy of Sciences*, *104*(12), 5002-5007. https://doi.org/doi/10.1073/pnas.0700520104

Darling, K., Kučera, M., Wade, C. M., von Langen, P., & Pak, D. (2003). Seasonal distribution of genetic types of planktonic foraminifer morphospecies in the Santa Barbara Channel and its paleoceanographic implications. *Paleoceanography*, *18*(2), 1032. https://doi.org/org/10.1029/2001pa000723

Darling, K., & Wade, C. M. (2008). The genetic diversity of planktic foraminifera and the global distribution of ribosomal RNA genotypes. *Marine Micropaleontology*, *67*(3-4), 216–238. https://doi.org/10.1016/j.marmicro.2008.01.009

Darwin, C. R. (1859). *On the origin of species by means of natural selection, or, The preservation of favoured races in the struggle for life*. London: John Murray

Davis, C. V., Badger, M. P. S., Bown, P. R., & Schmidt, D. N. (2013). The response of calcifying plankton to climate change in the Pliocene. *Biogeosciences*, *10*(9), 6131–6139. https://doi.org/10.5194/bg-10-6131-2013

de Moel, H., Ganssen, G. M., Peeters, F. J. C., Jung, S. J. A., Kroon, D., Brummer, G. A., & Zeebe, R. E. (2009). Planktic foraminiferal shell thinning in the Arabian Sea due to anthropogenic ocean acidification? *Biogeosciences*, *6*(9), 1917–1925. https://doi.org/10.5194/bg-6-1917-2009

de Villiers, S. (2003). Optimum growth conditions as opposed to calcite saturation as a control on the calcification rate and shell-weight of marine foraminifera. *Marine Biology*, *144*(1), 45–49. https://doi.org/10.1007/s00227-003-1183-8

Denton, G. H., Anderson, R. F., Toggweiler, J. R., Edwards, R. L., Schaefer, J. M., & Putnam, A. E. (2010). The last glacial termination. *Science*, *328*(5986), 1652-1656. https://doi.org/10.1126/science.1184119

Deuser, W. G. (1986). Seasonal and interannual variations in deep-water particle fluxes in the Sargasso Sea and their relation to surface hydrography. *Deep-Sea Research Part A: Oceanographic Research Papers*, *33*(2), 225–246. https://doi.org/org/10.1016/0198-0149(86)90120-2

Deuser, W. G., & Ross, E. H. (1989). Seasonally abundant planktonic foraminifera of the Sargasso Sea: Succession, deep-water fluxes, isotopic compositions, and paleoceanographic implications. *Journal of Foraminiferal Research*, *19*(4), 268–293. https://doi.org/org/10.2113/gsjfr.19.4.268

Deuser, W. G., Ross, E. H., Hemleben, C., & Spindler, M. (1981). Seasonal changes in species composition, numbers, mass, size, and isotopic composition of planktonic foraminifera settling into the deep Sargasso Sea. *Palaeogeography, Palaeoclimatology, Palaeoecology*, *33*(1–3), 103–127. https://doi.org/org/10.1016/0031-0182(81)90034-1

Doláková, N., Holcová, K., Nehyba, S., Hladilová, Š., Brzobohatý, R., Zágoršek, K., et al. (2014). The Badenian parastratotype at Židlochovice from the perspective of the multiproxy study. *Neues Jahrbuch für Geologie und Paläontologie - Abhandlungen*, *271*(2), 169–201. https://doi.org/org/10.1127/0077-7749/2014/0383

Doláková, N., Kováčová, M., & Utescher, T. (2020). Vegetation and climate changes during the Miocene climatic optimum and Miocene climatic transition in the northwestern part of Central Paratethys. *Geological Journal*, *56*(2), 729–743. https://doi.org/10.1002/gj.4056

Donner, B., & Wefer, G. (1994). Flux and stable-isotope composition of *Neogloboquadrina pachyderma* and other planktonic foraminifers in the Southern Ocean (Atlantic sector). *Deep-Sea Research Part I: Oceanographic Research Papers*, *41*(11–12), 1733–1743. https://doi.org/org/10.1016/0967-0637(94)90070-1

Dumitriu, S. D., Loghin, S., Dubicka, Z., Melinte-Dobrinescu, M. C., Paruch-Kulczycka, J., & Ionesi, V. (2017). Foraminiferal, ostracod, and calcareous nannofossil biostratigraphy of the latest Badenian – Sarmatian interval (Middle Miocene, Paratethys) from Poland, Romania and the Republic of Moldova. *Geologica Carpathica*, *68*(5), 419–444. https://doi.org/org/10.1515/geoca-2017-0028

Durakiewicz, T., Gonera, M., & Peryt, D. (1997). Oxygen and carbon isotopic changes in the middle Miocene (Badenian) foraminifera of the Gliwice area (SW Poland). *Bulletin of the Polish Academy of Sciences, Earth Sciences*, *45*(2–4), 145–155

Elderfield, H., Vautravers, M., & Cooper, M. (2002). The relationship between shell size and Mg/Ca, Sr/Ca, $\delta^{18}O$, and $\delta^{13}C$ of species of planktonic foraminifera. *Geochemistry, Geophysics, Geosystems*, *3*(8), 1–13. https://doi.org/doi.org/10.1029/2001gc000194

Fabry, V. J. (1989). Aragonite production by pteropod molluscs in the subarctic Pacific. *Deep-Sea Research Part a-Oceanographic Research Papers*, *36*(11), 1735–1751. https://doi.org/org/10.1016/0198-0149(89)90069-1

Fallet, U., Brummer, G.-J., Zinke, J., Vogels, S., & Ridderinkhof, H. (2010). Contrasting seasonal fluxes of planktonic foraminifera and impacts on paleothermometry in the Mozambique Channel upstream of the Agulhas Current. *Paleoceanography*, *25*(4), PA4223. https://doi.org/org/10.1029/2010pa001942

Fallet, U., Ullgren, J. E., Castañeda, I. S., van Aken, H. M., Schouten, S., Ridderinkhof, H., & Brummer, G.-J. A. (2011). Contrasting variability in foraminiferal and organic paleotemperature proxies in sedimenting particles of the Mozambique Channel (SW Indian Ocean). *Geochimica et Cosmochimica Acta*, *75*(20), 5834–5848. https://doi.org/org/10.1016/j.gca.2011.08.009

Fenton, I. S., Pearson, P. N., Dunkley Jones, T., Farnsworth, A., Lunt, D. J., Markwick, P., & Purvis, A. (2016). The impact of Cenozoic cooling on assemblage diversity in planktonic foraminifera. *Philos Trans R Soc Lond B Biol Sci*, *371*(1691), 20150224. https://doi.org/10.1098/rstb.2015.0224

Field, C. B., Behrenfeld, M. J., Randerson, J. T., & Falkowski, P. (1998). Primary production of the biosphere: integrating terrestrial and oceanic components. *Science*, *281*(5374), 237–240. https://doi.org/10.1126/science.281.5374.237

Filipescu, S. (1996). Stratigraphy of the Neogene from the western border of the Transylvanian Basin. *Studia Universitatis Babes-Bolyai, Geologia*, *41*(2), 3–78.

Fischer, G., Donner, B., Ratmeyer, V., Davenport, R., & Wefer, G. (1996). Distinct year-to-year particle flux variations off Cape Blanc during 1988–1991: Relation to δ^{18}O-deduced sea-surface temperatures and trade winds. *Journal of Marine Research*, *54*(1), 73–98. https://doi.org/org/10.1357/0022240963213484

Fischer, G., Romero, O. E., Merkel, U., Donner, B., Iversen, M., Nowald, N., et al. (2016). Deep ocean mass fluxes in the coastal upwelling off Mauritania from 1988 to 2012: Variability on seasonal to decadal timescales. *Biogeosciences*, *13*(10), 3071–3090. https://doi.org/org/10.5194/bg-13-3071-2016

Fischer, G., Romero, O. E., Toby, E., Iversen, M., Donner, B., Mollenhauer, G., et al. (2019). Changes in the dust-influenced biological carbon pump in the Canary Current System: Implications from a coastal and an offshore sediment trap record off Cape Blanc, Mauritania. *Global Biogeochemical Cycles*, *33*(8), 1100–1128. https://doi.org/org/10.1029/2019gb006194

Fraile, I., Schulz, M., Mulitza, S., & Kučera, M. (2008). Predicting the global distribution of planktonic foraminifera using a dynamic ecosystem model. *Biogeosciences*, *5*(3), 891–911. https://doi.org/org/10.5194/bg-5-891-2008

Frankignoulle, M., & Canon, C. (1994). Marine calcification as a source of carbon-dioxide: Positive feedback of increasing atmospheric CO_2. *Limnology and Oceanography*, *39*(2), 458–462. https://doi.org/org/10.4319/lo.1994.39.2.0458

Frenz, M., Baumann, K.-H., Boeckel, B., Hoppner, R., & Henrich, R. (2005). Quantification of foraminifer and coccolith carbonate in South Atlantic surface sediments by means of carbonate grain-size distributions. *Journal of Sedimentary Research*, *75*(3), 464–475. https://doi.org/org/10.2110/jsr.2005.036

Friebe, J. G., & Poltnig, W. (1991). Biostratigraphic results of deep drilling Fürstenfeld I. *Jahrbuch der Geologischen Bundesanstalt*, *134*(4), 689–700

Friebe, J. G., & Poltnig, W. (1993). Mikropaläontologische und regionalgeologische Ergebnisse der Bohrung Bad Tatzmannsdoff Thermal 1 (Steirisches Becken, Burgenland). *Jahrbuch der Geologischen Bundesanstalt*, *136*(2), 327–333

Garecka, M., & Olszewska, B. (2011). Correlation of the middle Miocene deposits in SE Poland and Western Ukraine based on foraminifera and calcareous nannoplankton. *Annales Societatis Geologorum Poloniae*, *81*, 309–330

Gebhardt, H., Zorn, I., & Roetzel, R. (2009). The initial phase of the early Sarmatian (middle Miocene) transgression. Foraminiferal and ostracod assemblages from an incised valley fill in the Molasse Basin of Lower Austria. *Australian Journal of Earth Sciences*, *102*(2), 100–119

Gerber, S., Eble, G. J., & Neige, P. (2008). Allometric space and allometric disparity: a developmental perspective in the macroevolutionary analysis of morphological disparity. *Evolution*, *62*(6), 1450–1457. https://doi.org/10.1111/j.1558-5646.2008.00370.x

Gould, S. J., & Eldredge, N. (1977). Punctuated equilibria: the tempo and mode of evolution reconsidered. *Paleobiology*, *3*(2), 115–151. https://doi.org/org/10.1017/s0094837300005224

Gould, S. J., & Eldredge, N. (1993). Punctuated equilibrium comes of age. *Nature*, *366*(6452), 223–227. https://doi.org/10.1038/366223a0

Guidi, L., Chaffron, S., Bittner, L., Eveillard, D., Larhlimi, A., Roux, S., et al. (2016). Plankton networks driving carbon export in the oligotrophic ocean. *Nature*, *532*(7600), 465–470. https://doi.org/10.1038/nature16942

Harzhauser, M., Daxner-Höck, G., Boon-Kristkoiz, E., Ćorić, S., Mandic, O., Miklas-Tempfer, P., et al. (2003). Paleoecology and biostratigraphy of the section Mühlbach (Gaindorf Formation, lower middle Miocene, lower Badenian, Austria). *104(A)*, 323–334

Harzhauser, M., Grunert, P., Mandic, O., Lukeneder, P., Gallardo, Á. G., Neubauer, T. A., et al. (2018). Middle and late Badenian palaeoenvironments in the northern Vienna Basin and their potential link to the Badenian salinity crisis. *Geologica Carpathica*, *69*(2), 149–168. https://doi.org/org/10.1515/geoca-2018-0009

Harzhauser, M., Theobalt, D., Strauss, P., Mandic, O., Carnevale, G., & Piller, W. E. (2017). Miocene biostratigraphy and paleoecology of the Mistelbach Halfgraben in the northwestern Vienna Basin (Lower Austria). *Jahrbuch der Geologischen Bundesanstalt*, *157*(1–4), 57–108

Hecht, A. D. (1976). An ecologic model for test size variation in recent planktonic foraminifera: Applications to the fossil record. *The Journal of Foraminiferal Research*, *6*(4), 295–311. https://doi.org/org/10.2113/gsjfr.6.4.295

Hemleben, C., Spindler, M., & Anderson, O. R. (1989). *Modern Planktonic Foraminifera*. Berlin: Springer-Verlag. https://doi.org/10.1007/978-1-4612-3544-6

Henehan, M. J., Evans, D., Shankle, M., Burke, J. E., Foster, G. L., Anagnostou, E., et al. (2017). Size-dependent response of foraminiferal calcification to seawater carbonate chemistry. *Biogeosciences*, *14*(13), 3287–3308. https://doi.org/org/10.5194/bg-14-3287-2017

Herbert, T. D., Lawrence, K. T., Tzanova, A., Peterson, L. C., Caballero-Gill, R., & Kelly, C. S. (2016). Late Miocene global cooling and the rise of modern ecosystems. *Nature Geoscience*, *9*(11), 843–847. https://doi.org/10.1038/ngeo2813

Hoegh-Guldberg, O., Jacob, D., Taylor, M., Guillen Bolanos, T., Bindi, M., Brown, S., et al. (2019). The human imperative of stabilizing global climate change at 1.5 °C. *Science*, *365*(6459), 1263–1275. https://doi.org/10.1126/science.aaw6974

Hohenegger, J., Ćorić, S., & Wagreich, M. (2014). Timing of the middle Miocene Badenian stage of the Central Paratethys. *Geologica Carpathica*, *65*(1), 55–66. https://doi.org/org/10.2478/geoca-2014-0004

Hohenegger, J., Rögl, F., Ćorić, S., Pervesler, P., Lirer, F., Roetzel, R., et al. (2009). The Styrian Basin: a key to the middle Miocene (Badenian/Langhian) Central Paratethys transgressions. *Australian Journal of Earth Sciences*, *102*, 102–132

Hók, J., Šujan, M., & Šipka, F. (2014). Tectonic division of the Western Carpathians: an overview and a new approach. *Acta Geologica Slovaca*, *6*(2), 135–143

Holcová, K., & Demény, A. (2012). The oxygen and carbon isotopic composition of Langhian foraminiferal tests as a paleoecological proxy in a marginal part of the Carpathian Foredeep (Czech Republic). *Geologica Carpathica*, *63*(2), 121–137. https://doi.org/org/10.2478/v10096-012-0010-x

Horner, T. J., Rickaby, R. E. M., & Henderson, G. M. (2011). Isotopic fractionation of cadmium into calcite. *Earth and Planetary Science Letters*, *312*(1–2), 243–253. https://doi.org/org/10.1016/j.epsl.2011.10.004

Horváth, F., Musitz, B., Balázs, A., Végh, A., Uhrin, A., Nádor, A., et al. (2015). Evolution of the Pannonian basin and its geothermal resources. *Geothermics*, *53*, 328–352. https://doi.org/10.1016/j.geothermics.2014.07.009

Huang, C.-y. (1981). Observations on the interior of some late Neogene planktonic foraminifera. *The Journal of Foraminiferal Research*, *11*(3), 173–190. https://doi.org/10.2113/gsjfr.11.3.173

Huber, B. T., Petrizzo, M. R., & MacLeod, K. G. (2020). Planktonic foraminiferal endemism at southern high latitudes following the terminal Cretaceous extinction. *Journal of Foraminiferal Research*, *50*(4), 382–402. https://doi.org/org/10.2113/gsjfr.50.4.382

Hudáčková, N., & Kováč, M. (1993). The Upper Badenian–Sarmatian events in the area of the Vienna Basin eastern margin. *Mineralia Slovaca*, *25*(3), 202–210

Incarbona, A., Jonkers, L., Ferraro, S., Sprovieri, R., & Tranchida, G. (2019). Sea surface temperatures and paleoenvironmental variability in the Central Mediterranean during historical times reconstructed using planktonic foraminifera. *Paleoceanography and Paleoclimatology*, *34*(3), 394–408. https://doi.org/10.1029/2018pa003529

Jenkins, D. G. (1968). Acceleration of the evolutionary rate in the *Orbulina* lineage. *Contributions of the Cushman Foundation for Foraminiferal Research*, *29*(4), 133–140

Jensen, S. (1998). Planktische Foraminiferen im Europäischen Nordmeer: Verbreitung und Vertikalfluß sowie ihre Entwicklung während der letzten 15000 Jahre. *Berichte Sonderforschungsbereich*, *313*(75), 1–105

Jonkers, L., Brummer, G.-J. A., Peeters, F. J. C., van Aken, H. M., & De Jong, M. F. (2010). Seasonal stratification, shell flux, and oxygen isotope dynamics of left-coiling *N. pachyderma* and *T. quinqueloba* in the western subpolar North Atlantic. *Paleoceanography*, *25*(2), 1–13. https://doi.org/org/10.1029/2009pa001849

Jonkers, L., Hillebrand, H., & Kučera, M. (2019). Global change drives modern plankton communities away from the pre-industrial state. *Nature*, *570*(7761), 372–375. https://doi.org/org/10.1038/s41586-019-1230-3

Jonkers, L., & Kučera, M. (2015). Global analysis of seasonality in the shell flux of extant planktonic foraminifera. *Biogeosciences*, *12*(7), 2207–2226. https://doi.org/org/10.5194/bg-12-2207-2015

Jonkers, L., van Heuven, S., Zahn, R., & Peeters, F. J. C. (2013). Seasonal patterns of shell flux, $\delta^{18}O$ and $\delta^{13}C$ of small and large *N. pachyderma* (s) and *G. bulloides* in the subpolar North Atlantic. *Paleoceanography*, *28*(1), 164–174. https://doi.org/org/10.1002/palo.20018

Kahn, M. I. (1981). Ecological and paleoecological implications of the phenotypic variation in three species of living planktonic foraminifera from the northeastern Pacific Ocean (50 degrees N, 145 degrees W). *The Journal of Foraminiferal Research*, *11*(3), 203–211. https://doi.org/org/10.2113/gsjfr.11.3.203

Keir, R. S. (1980). The dissolution kinetics of biogenic calcium carbonates in seawater. *Geochimica et Cosmochimica Acta*, *44*(2), 241–252. https://doi.org/org/10.1016/0016-7037(80)90135-0

Kelley, P. H. (1983). Evolutionary patterns of eight Chesapeake group molluscs: evidence for the model of punctuated equilibria. *Journal of Paleontology*, *57*(3), 581–598

Kennett, J. P., & Srinivasan, M. S. (1983). *Neogene planktonic foraminifera: a phylogenetic atlas*. Stroudsburg, Pennsylvania: Hutchinson Ross Publishing Company

Kincaid, E., Thunell, R. C., Le, J., Lange, C. B., Weinheimer, A. L., & Reid, F. M. H. (2000). Planktonic foraminiferal fluxes in the Santa Barbara Basin: Response to seasonal and interannual hydrographic changes. *Deep-Sea Research Part II: Topical Studies in Oceanography*, *47*(5–6), 1157–1176. https://doi.org/org/10.1016/s0967-0645(99)00140-x

King, A. L., & Howard, W. R. (2003). Planktonic foraminiferal flux seasonality in Subantarctic sediment traps: A test for paleoclimate reconstructions. *Paleoceanography*, *18*(1), 1019

Kiss, P., Jonkers, L., Hudáčková, N., Reuter, R. T., Donner, B., Fischer, G. & Kučera, M. (2021). Determinants of Planktonic Foraminifera Calcite Flux: Implications for the Prediction of Intra-and Interannual Pelagic Carbonate Budgets. Manuscript submitted for publication.

Kopecká, J. (2012). Foraminifera as environmental proxies of the middle Miocene (early Badenian) sediments of the central depression (Central Paratethys, Moravian part of the Carpathian Foredeep). *Bulletin of Geosciences*, 431–442. https://doi.org/org/10.3140/bull.geosci.1299

Koubová, I., & Hudáčková, N. (2010). Foraminiferal successions in the shallow water Sarmatian sediments from the MZ 93 borehole (Vienna Basin, Slovak part). *Acta Geologica Slovaca*, *2*(1), 47–58

Kováč, M., Andreyeva-Grigorovich, A., Bajraktarević, Z., Brzobohatý, R., Filipescu, S., Fodor, L., et al. (2007). Badenian evolution of the Central Paratethys Sea: paleogeography, climate and eustatic sea-level changes. *Geologica Carpathica*, *58*(6), 579–606

Kováč, M., Hudáčková, N., Halásová, E., Kováčová, M., Holcová, K., Oszczypko-Clowes, N., et al. (2017). The Central Paratethys palaeoceanography: a water circulation model based on microfossil proxies, climate, and changes of depositional environment. *Acta Geologica Slovaca*, *9*(2), 75–114

Kováč, M., Rybár, S., Halásová, E., Hudáčková, N., Šarinová, K., Šujan, M., et al. (2018). Changes in Cenozoic depositional environment and sediment provenance in the Danube Basin. *Basin Research*, *30*(1), 97–131. https://doi.org/org/10.1111/bre.12244

Kováčová, P., Emmanuel, L., Hudáčková, N., & Renard, M. (2009). Central Paratethys paleoenvironment during the Badenian (middle Miocene): evidence from foraminifera and stable isotope (δ^{13}C and δ^{18}O) study in the Vienna Basin (Slovakia). *International Journal of Earth Sciences*, *98*(5), 1109–1127. https://doi.org/org/10.1007/s00531-008-0307-2

Kováčová, P., & Hudáčková, N. (2009). Late Badenian foraminifers from the Vienna Basin (Central Paratethys): stable isotope study and paleoecological implications. *Geologica Carpathica*, *60*(1), 59–70. https://doi.org/org/10.2478/v10096-009-0006-3

Kretschmer, K. (2017). *Global assessment of species-specific habitats of planktonic foraminifera - An ecosystem modeling approach* (Doctoral dissertation). Bremen: University of Bremen.

Kretschmer, K., Jonkers, L., Kučera, M., & Schulz, M. (2018). Modeling seasonal and vertical habitats of planktonic foraminifera on a global scale. *Biogeosciences*, *15*(14), 4405–4429. https://doi.org/org/10.5194/bg-2017-429

Kučera, M., & Kennett, J. P. (2000). Biochronology and evolutionary implications of late Neogene California margin planktonic foraminiferal events. *Marine Micropaleontology*, *40*, 67–81. https://doi.org/org/10.1016/S0377-8398(00)00029-3

Kučera, M., Weinelt, M., Kiefer, T., Pflaumann, U., Hayes, A., Weinelt, M., et al. (2005). Reconstruction of sea-surface temperatures from assemblages of planktonic foraminifera: multi-technique approach based on geographically constrained calibration data sets and its application to glacial Atlantic and Pacific Oceans. *Quaternary Science Reviews*, *24*(7-9), 951–998. https://doi.org/10.1016/j.quascirev.2004.07.014

Kučera, M. (2007). Planktonic foraminifera as tracers of past oceanic environments. In C. Hillaire-Marcel, A. de Vernal (Eds.), *Proxies in Late Cenozoic Paleoceanography*. Amsterdam: Elsevier Science.

Kuroyanagi, A., Kawahata, H., Nishi, H., & Honda, M. C. (2002). Seasonal changes in planktonic foraminifera in the northwestern North Pacific Ocean: Sediment trap experiments from subarctic and subtropical gyres. *Deep-Sea Research Part II: Tropical Studies in Oceanography*, *49*(24–25), 5627–5645. https://doi.org/org/10.1016/s0967-0645(02)00202-3

Langer, M. R. (2008). Assessing the contribution of foraminiferan protists to global ocean carbonate production. *Journal of Eukaryotic Microbiology*, *55*(3), 163–169. https://doi.org/org/10.1111/j.1550-7408.2008.00321.x

Lazarus, D., Hilbrecht, H., Spencer-Cervato, C., & Thierstein, H. (1995). Sympatric speciation and phyletic change in *Globorotalia truncatulinoides*. *Paleobiology*, *21*(1), 28–51. https://doi.org/org/10.1017/s0094837300013063

Leclercq, N., Gattuso, J. P., & Jaubert, J. (2000). CO_2 partial pressure controls the calcification rate of a coral community. *Global Change Biology*, *6*(3), 329–334. https://doi.org/10.1046/j.1365-2486.2000.00315.x

Lirer, F., Foresi, L. M., Iaccarino, S. M., Salvatorini, G., Turco, E., Cosentino, C., et al. (2019). Mediterranean Neogene planktonic foraminifer biozonation and biochronology. *Earth-Science Reviews*, *196*. https://doi.org/org/10.1016/j.earscirev.2019.05.013

Locarnini, R. A., Mishonov, A. V., Baranova, O. K., Boyer, T. P., Zweng, M. M., Garcia, H. E., et al. (2019). World Ocean Atlas 2018, Volume 1: Temperature. A. Mishonov, Technical Editor. *NOAA Atlas NESDIS 81*, 52.

Lombard, F., da Rocha, R. E., Bijma, J., & Gattuso, J.-P. (2010). Effect of carbonate ion concentration and irradiance on calcification in planktonic foraminifera. *Biogeosciences*, *7*(1), 247–255. https://doi.org/org/10.5194/bg-7-247-2010

Lombard, F., Labeyrie, L., Michel, E., Bopp, L., Cortijo, E., Retailleau, S., et al. (2011). Modelling planktic foraminifer growth and distribution using an ecophysiological multi-species approach. *Biogeosciences*, *8*(4), 853–873. https://doi.org/org/10.5194/bg-8-853-2011

Łuczkowska, E. (1955). Tortonian foraminifera from the Chodenice and Grabowiec Beds in the vicinity of Bochnia. *Rocznik Polskiego Towarzystwa Geologicznego*, *23*

Łuczkowska, E. (1971). A new zone with *Praeorbulina indigena* (*Foraminiferida*, *Globigerinidae*) in the upper Badenian (Tortonian s.s.) of Central Paratethys. *Annales de la Sociéte Géologique de Pologne*, *40*, 445–448

Machaniec, E., & Pilarz, M. (2011), Upper Cretaceous and Miocene foraminiferal assemblages from the Bibice area (vicinity of Kraków), in *Eight Micropalaeontological Workshop "MIKRO-2011" and Annual TMS Foram-Nannofossil Group Meeting*, edited by M. Bąk, M. A. Kaminski, A. Waśkowska, pp. 109–110, Grzybowski Foundation Special Publication, Kraków, Poland.

Malmgren, B. A., Berggren, W. A., & Lohmann, G. P. (1983). Evidence for punctuated gradualism in the late Neogene *Globorotalia tumida* lineage of planktonic foraminifera. *Paleobiology*, *9*(4), 377–389. https://doi.org/org/10.1017/s0094837300007843

Malmgren, B. A., & Kennett, J. P. (1976). Biometric analysis of phenotypic variation in recent *Globigerina bulloides* d'Orbigny in the southern Indian Ocean. *Marine Micropaleontology*, *1*, 3–25. https://doi.org/org/10.1016/0377-8398(76)90003-7

Mandic, O., Sant, K., Kallanxhi, M.-E., Ćorić, S., Theobalt, D., Grunert, P., et al. (2019). Integrated bio-magnetostratigraphy of the Badenian reference section Ugljevik in southern Pannonian Basin - implications for the Paratethys history (middle Miocene, Central Europe). *Global and Planetary Change*, *172*, 374–395. https://doi.org/org/10.1016/j.gloplacha.2018.10.010

Marchant, M., Hebbeln, D., Giglio, S., Coloma, C., & González, H. E. (2004). Seasonal and interannual variability in the flux of planktic foraminifera in the Humboldt Current System off central Chile (30°S). *Deep-Sea Research Part II: Topical Studies in Oceanography*, *51*(20–21), 2441–2455. https://doi.org/org/10.1016/j.dsr2.2004.08.013

Marchant, M., Hebbeln, D., & Wefer, G. (1998). Seasonal flux patterns of planktic foraminifera in the Peru–Chile current. *Deep-Sea Research Part I: Oceanographic Research Papers*, *45*(7), 1161–1185. https://doi.org/org/10.1016/s0967-0637(98)00009-0

Marshall, B. J., Thunell, R. C., Henehan, M. J., Astor, Y., & Wejnert, K. E. (2013). Planktonic foraminiferal area density as a proxy for carbonate ion concentration: A calibration study using the Cariaco Basin ocean time series. *Paleoceanography*, *28*(2), 363–376. https://doi.org/org/10.1002/palo.20034

Martinuš, M., Fio, K., Pikelj, K., & Aščić, Š. (2012). Middle Miocene warm-temperate carbonates of Central Paratethys (Mt. Zrinska Gora, Croatia): paleoenvironmental reconstruction based on bryozoans, coralline red algae, foraminifera, and calcareous nannoplankton. *Facies*, *59*(3), 481–504. https://doi.org/org/10.1007/s10347-012-0327-z

Milliman, J. D. (1993). Production and accumulation of calcium carbonate in the ocean: Budget of a nonsteady state. *Global Biogeochemical Cycles*, *7*(4), 927–957. https://doi.org/org/10.1029/93gb02524

Mohiuddin, M. M., Nishimura, A., & Tanaka, Y. (2005). Seasonal succession, vertical distribution, and dissolution of planktonic foraminifera along the Subarctic Front: Implications for paleoceanographic reconstruction in the northwestern Pacific. *Marine Micropaleontology*, *55*(3–4), 129–156. https://doi.org/org/10.1016/j.marmicro.2005.02.007

Mohiuddin, M. M., Nishimura, A., Tanaka, Y., & Shimamoto, A. (2002). Regional and interannual productivity of biogenic components and planktonic foraminiferal fluxes in the northwestern Pacific Basin. *Marine Micropaleontology*, *45*(1), 57–82. https://doi.org/org/10.1016/s0377-8398(01)00045-7

Mohiuddin, M. M., Nishimura, A., Tanaka, Y., & Shimamoto, A. (2004). Seasonality of biogenic particle and planktonic foraminifera fluxes: Response to hydrographic variability in the Kuroshio Extension, northwestern Pacific Ocean. *Deep-Sea Research Part I: Oceanographic Research Papers*, *51*(11), 1659–1683. https://doi.org/org/10.1016/j.dsr.2004.06.002

Mohtadi, M., Steinke, S., Groeneveld, J., Fink, H. G., Rixen, T., Hebbeln, D., et al. (2009). Low-latitude control on seasonal and interannual changes in planktonic foraminiferal flux and shell geochemistry off south Java: A sediment trap study. *Paleoceanography*, *24*(1), PA1201. https://doi.org/10.1029/2008pa001636

Moller, T., Schulz, H., & Kučera, M. (2013). The effect of sea surface properties on shell morphology and size of the planktonic foraminifer *Neogloboquadrina pachyderma* in the North Atlantic. *Palaeogeography, Palaeoclimatology, Palaeoecology*, *391*, 34–48. https://doi.org/org/10.1016/j.palaeo.2011.08.014

Monnin, E., Indermuhle, A., Dallenbach, A., Fluckiger, J., Stauffer, B., Stocker, T. F., et al. (2001). Atmospheric CO_2 concentrations over the last glacial termination. *Science*, *291*(5501), 112–114. https://doi.org/10.1126/science.291.5501.112

Morard, R., Fullberg, A., Brummer, G. A., Greco, M., Jonkers, L., Wizemann, A., et al. (2019). Genetic and morphological divergence in the warm-water planktonic foraminifera genus *Globigerinoides*. *PLoS One*, *14*(12), e0225246. https://doi.org/org/10.1371/journal.pone.0225246

Morard, R., Quillevere, F., Douady, C. J., de Vargas, C., de Garidel-Thoron, T., & Escarguel, G. (2011). Worldwide genotyping in the planktonic foraminifer Globoconella inflata: implications for life history and paleoceanography. *PLoS One*, *6*(10), e26665. https://doi.org/org/10.1371/journal.pone.0026665

Moy, A. D., Howard, W. R., Bray, S. G., & Trull, T. W. (2009). Reduced calcification in modern Southern Ocean planktonic foraminifera. *Nature Geoscience*, *2*(4), 276–280. https://doi.org/org/10.1038/ngeo460

Müller, G. B., & Wagner, G. P. (1996). Homology, Hox genes, and developmental integration. *American Zoologist*, *36*(1), 4–13. https://doi.org/org/10.1093/icb/36.1.4

Müller, P. J. (2004). Density and water content of sediment core GeoB3104-1. Dataset accessed [2020-05-04] at: https://doi.pangaea.de/10.1594/PANGAEA.824893. https://doi.org/10.1594/PANGAEA.142622

Naik, S. S., Godad, S. P., Naidu, P. D., & Ramaswamy, V. (2013). A comparison of *Globigerinoides ruber* calcification between upwelling and non-upwelling regions in the Arabian Sea. *Journal of Earth System Science*, *122*(4), 1153–1159. https://doi.org/org/10.1007/s12040-013-0330-y

Nehyba, S., Holcová, K., Gedl, P., & Doláková, N. (2016). The lower Badenian transgressive-regressive cycles – a case study from Oslavany (Carpathian Foredeep, Czech Republic). *Neues Jahrbuch für Geologie und Paläontologie - Abhandlungen*, *279*(2), 209–238. https://doi.org/doi/10.1127/njgpa/2016/0548

NOAA National Centers for Environmental information, Climate at a Glance: Global Mapping. Dataset accessed [2021-03-06] at: https://www.ncdc.noaa.gov/cag/

Norris, R. D. (1991). Parallel evolution in the keel structure of planktonic foraminifera. *Journal of Foraminiferal Research*, *21*(4), 319–331. https://doi.org/org/10.2113/gsjfr.21.4.319

Northcote, L. C., & Neil, H. L. (2005). Seasonal variations in foraminiferal flux in the Southern Ocean, Campbell Plateau, New Zealand. *Marine Micropaleontology*, *56*(3–4), 122–137. https://doi.org/org/10.1016/j.marmicro.2005.05.001

Olszewska, B. (2014). Results of micropaleontological investigations of the Upper Jurassic, Upper Cretaceous and Miocene sediments in the Trojanowice 2 and Cianowice 2 boreholes (South-Eastern part of the Kraków-Częstochowa Upland). *Biuletyn Państwowego Instytutu Geologicznego*, *459*, 109–132

Orr, J. C., Fabry, V. J., Aumont, O., Bopp, L., Doney, S. C., Feely, R. A., et al. (2005). Anthropogenic ocean acidification over the twenty-first century and its impact on calcifying organisms. *Nature*, *437*(7059), 681–686. https://doi.org/10.1038/nature04095

Ortiz, J. D., & Mix, A. C. (1997). Comparison of Imbrie-Kipp Transfer Function and modern analog temperature estimates using sediment trap and core top foraminiferal faunas. *Paleoceanography*, *12*(2), 175–190. https://doi.org/10.1029/96pa02878

Paruch-Kulczycka, J. (2015). Foraminiferal biostratigraphy of the Miocene deposits from the Busko (Młyny) PIG-1 and Kazimierza Wielka (Donosy) PIG-1 boreholes (Northern part of the Carpathian Foredeep). *Biuletyn Państwowego Instytutu Geologicznego*, *461*, 115–132

Pearson, P. N., & Ezard, T. H. G. (2014). Evolution and speciation in the Eocene planktonic foraminifer *Turborotalia*. *Paleobiology*, *40*(1), 130–143. https://doi.org/org/10.1666/13004

Pearson, P. N., Shackleton, N. J., & Hall, M. A. (1997). Stable isotopic evidence for the sympatric divergence of *Globigerinoides trilobus* and *Orbulina universa* (planktonic foraminifera). *Journal of the Geological Society*, *154*(2), 295–302. https://doi.org/org/10.1144/gsjgs.154.2.0295

Pearson, P. N. (1995). Planktonic foraminifer biostratigraphy and the development of pelagic caps on guyots in the Marshall Islands Group. In J. A. Haggerty, S. Premoli, I. Rack, M. K. McNutt (Eds.), *Proceedings of the Ocean Drilling Program, Scientific Results, Vol. 144: College Station, TX (Ocean Drilling Program)*. (pp. 21–59).

Peeters, F., Ivanova, E., Conan, S., Brummer, G.-J., Ganssen, G., Troelstra, S., & van Hinte, J. (1999). A size analysis of planktic foraminifera from the Arabian Sea. *Marine Micropaleontology*, *36*(1), 31–63. https://doi.org/org/10.1016/s0377-8398(98)00026-7

Petrová, P., & Adámek, J. (2005). What brought revision of Cf 600 Drnholec-5 and 7 boreholes for solution of stratigraphy of the Karpatian/Badenian boundary? *Geologické výzkumy na Moravě a ve Slezsku*, 48–51

Pezelj, Đ., Sremac, J., & Sokač, A. (2007). Palaeoecology of the late Badenian foraminifera and ostracoda from the SW Central Paratethys (Medvednica Mt., Croatia). *Geologia Croatica*, *60*(2), 139–150

Pigliucci, M. (2003). Phenotypic integration: studying the ecology and evolution of complex phenotypes. *Ecology Letters*, *6*(3), 265–272. https://doi.org/org/10.1046/j.1461-0248.2003.00428.x

Płonka, K. (2017). Palaeontological analysis of middle Miocene siltstones at Wiślica (Carpathian Foredeep, Poland). *Geologos*, *23*(1), 29–43. https://doi.org/org/10.1515/logos-2017-0003

Poore, R. Z., Tedesco, K. A., & Spear, J. W. (2013). Seasonal flux and assemblage composition of planktic foraminifers from a sediment-trap study in the northern Gulf of Mexico. *Journal of Coastal Research*, *63*, 6–19. https://doi.org/org/10.2112/si63-002.1

Popescu, G. (1969). Some new *Globigerina* (*Foraminifera*) from the Upper Tortonian of the Transylvanian Basin and the Subcarpathians. *Revue Roumaine de Géologie, Géophysique et Géographie. Géologie*, *13*(1), 103–106

Popescu, G. (1973). Contributions to the microbiostratigraphy of the middle Miocene from the Northern Transylvania. *Studii şi cercetări de geologie, geofizică, geografie. Geologie*, *18*(1), 187–218

Popescu, G. (1976). Phylogenetic remarks on the genera *Candorbulina*, *Velapertina* and *Orbulina*. *Dări de Seamă ale Şedinţelor, Institutul de Geologie şi Geofizică*, *62*(3), 161–167

Popescu, G. (1987). Marine middle Miocene microbiostratigraphical correlation in Central Paratethys. *Dări de Seamă ale Şedinţelor, Institutul de Geologie şi Geofizică*, *72–73*(3), 149–167

Popescu, G., & Crihan, I.-M. (2011). Middle Miocene Globigerinas of Romania. *Acta Palaeontologica Romaniae*, *7*, 291–313

Qin, B., Li, T., Xiong, Z., Algeo, T. J., & Jia, Q. (2020). Calcification of planktonic foraminifer *Pulleniatina obliquiloculata* controlled by seawater temperature rather than ocean acidification. *Global and Planetary Change*, *193*. https://doi.org/10.1016/j.gloplacha.2020.103256

Quillévéré, F., Morard, R., Escarguel, G., Douady, C. J., Ujiié, Y., de Garidel-Thoron, T., & de Vargas, C. (2013). Global scale same-specimen morpho-genetic analysis of T*runcorotalia truncatulinoides*: a perspective on the morphological species concept in planktonic foraminifera. *Palaeogeography, Palaeoclimatology, Palaeoecology*, *391*, 2–12. https://doi.org/org/10.1016/j.palaeo.2011.03.013

Raup, D. M. (1966). Geometric analysis of shell coiling: general problems. *Journal of Paleontology*, *40*, 1178–1190

Rembauville, M., Meilland, J., Ziveri, P., Schiebel, R., Blain, S., & Salter, I. (2016). Planktic foraminifer and coccolith contribution to carbonate export fluxes over the central Kerguelen Plateau. *Deep-Sea Research Part I: Oceanographic Research Papers*, *111*, 91–101. https://doi.org/org/10.1016/j.dsr.2016.02.017

Reuss, E. A. (1854). Beitrage zur geognostischen Kenntniss Mährens. *Jahrbuch der Kaiserlich-Königlichen Geologischen Reichsanstalt*, *5*(4), 657–765

Reynolds, C. E., Richey, J. N., & Poore, R. Z. (2013). *Seasonal flux and assemblage composition of planktic foraminifera from the northern Gulf of Mexico, 2008–2012*. Reston, Virginia: U.S. Geological Survey. https://doi.org/10.3133/ofr20131243

Reynolds, R. W., Smith, T. M., Liu, C., Chelton, D. B., Casey, K. S., & Schlax, M. G. (2007). Daily high-resolution-blended analyses for sea surface temperature. *Journal of Climate*, *20*(22), 5473–5496. https://doi.org/doi.org/10.1175/2007jcli1824.1

Riebesell, U., Zondervan, I., Rost, B., Tortell, P. D., Zeebe, R. E., & Morel, F. M. (2000). Reduced calcification of marine plankton in response to increased atmospheric CO2. *Nature*, *407*(6802), 364–367. https://doi.org/10.1038/35030078

Rigual-Hernández, A. S., Sierro, F. J., Bárcena, M. A., Flores, J. A., & Heussner, S. (2012). Seasonal and interannual changes of planktic foraminiferal fluxes in the Gulf of Lions (NW Mediterranean) and their implications for paleoceanographic studies: Two 12-year sediment trap records. *Deep-Sea Research Part I: Oceanographic Research Papers*, *66*, 26–40. https://doi.org/org/10.1016/j.dsr.2012.03.011

Rigual Hernández, A. S., Trull, T. W., Nodder, S. D., Flores, J. A., Bostock, H., Abrantes, F., et al. (2020). Coccolithophore biodiversity controls carbonate export in the Southern Ocean. *Biogeosciences*, *17*(1), 245–263. https://doi.org/org/10.5194/bg-17-245-2020

Rillo, M. C., Miller, C. G., Kučera, M., & Ezard, T. H. G. (2019). Supplementary Material: Intraspecific size variation in planktonic foraminifera cannot be consistently predicted by the environment. Dataset accessed [2020-12-17] at: Natural History Museum Data Portal: https://doi.org/10.5519/qd.g69gdih9

Rillo, M. C., Miller, C. G., Kučera, M., & Ezard, T. H. G. (2020). Intraspecific size variation in planktonic foraminifera cannot be consistently predicted by the environment. *Ecology and Evolution*, *10*(20), 11579–11590. https://doi.org/10.1101/468165

Rögl, F. (1994). *Globigerina ciperoensis* (*Foraminiferida*) in the Oligocene and Miocene of the Central Paratethys. *Annalen des Naturhistorischen Museums in Wien*, *96A*, 133–159

Rögl, F. (1998). Paleogeographic considerations for Mediterranean and Paratethys seaways (Oligocene to Miocene). *Annalen des Naturhistorischen Museums in Wien*, *99A*, 279–310

Romero, O. E., Baumann, K.-H., Zonneveld, K. A. F., Donner, B., Hefter, J., Hamady, B., et al. (2020). Flux variability of phyto- and zooplankton communities in the Mauritanian coastal upwelling between 2003 and 2008. *Biogeosciences*, *17*(1), 187–214. https://doi.org/org/10.5194/bg-17-187-2020

Romero, O. E., Kim, J.-H., & Donner, B. (2008). Submillennial-to-millennial variability of diatom production off Mauritania, NW Africa, during the last glacial cycle. *Paleoceanography*, *23*(3), PA3218. https://doi.org/org/10.1029/2008pa001601

Roy, T., Lombard, F., Bopp, L., & Gehlen, M. (2015). Projected impacts of climate change and ocean acidification on the global biogeography of planktonic Foraminifera. *Biogeosciences*, *12*(10), 2873–2889. https://doi.org/org/10.5194/bg-12-2873-2015

Rundić, L., Knežević, S., & Rakijaš, M. (2013). Middle miocene badenian transgression: new evidences from the Vrdnik coal basin (Fruska Gora Mt., Northern Serbia). *Geoloski anali Balkanskoga poluostrva*(74), 9–23. https://doi.org/org/10.2298/gabp1374009r

Rybár, S., Halásová, E., Hudáčková, N., Kováč, M., Kováčová, M., Šarinová, K., & Šujan, M. (2015). Biostratigraphy, sedimentology and paleoenvironments of the northern Danube Basin: Ratkovce 1 well case study. *Geologica Carpathica*, *66*(1), 51–67. https://doi.org/org/10.1515/geoca-2015-0010

Sabine, C. L., Feely, R. A., Gruber, N., Key, R. M., Lee, K., Bullister, J. L., et al. (2004). The oceanic sink for anthropogenic CO_2. *Science*, *305*(5682), 367–371. https://doi.org/10.1126/science.1097403

Salgueiro, E., Voelker, A., Abrantes, F., Meggers, H., Pflaumann, U., Lončarić, N., et al. (2008). Planktonic foraminifera from modern sediments reflect upwelling patterns off Iberia: Insights from a regional transfer function. *Marine Micropaleontology*, *66*(3-4), 135–164. https://doi.org/10.1016/j.marmicro.2007.09.003

Salmon, K. H., Anand, P., Sexton, P. F., & Conte, M. (2015). Upper ocean mixing controls the seasonality of planktonic foraminifer fluxes and associated strength of the carbonate pump in the oligotrophic North Atlantic. *Biogeosciences*, *12*(1), 223–235. https://doi.org/org/10.5194/bg-12-223-2015

Salter, I., Schiebel, R., Ziveri, P., Movellan, A., Lampitt, R., & Wolff, G. A. (2014). Carbonate counter pump stimulated by natural iron fertilization in the Polar Frontal Zone. *Nature Geoscience*, *7*(12), 885–889. https://doi.org/org/10.1038/ngeo2285

Sant, K., Palcu, D. V., Turco, E., Di Stefano, A., Baldassini, N., Kouwenhoven, T., et al. (2019). Litho- and biostratigraphic data of lower-middle Miocene sections in the Transylvanian basin and SE Carpathian Foredeep (Romania). *Data Brief*, *24*, 103904. https://doi.org/org/10.1016/j.dib.2019.103904

Sautter, L. R., & Thunell, R. C. (1989). Seasonal succession of planktonic foraminifera: Results from a four-year time-series sediment trap experiment in the Northeast Pacific. *Journal of Foraminiferal Research*, *19*(4), 253–267. https://doi.org/org/10.2113/gsjfr.19.4.253

Selmeczi, I., Lantos, M., Bohn-Havas, M., Nagymarosy, A., & Szegő, É. (2012). Correlation of bio- and magnetostratigraphy of Badenian sequences from western and northern Hungary. *Geologica Carpathica*, *63*(3), 219–232. https://doi.org/org/10.2478/v10096-012-0019-1

Shakun, J. D., Clark, P. U., He, F., Marcott, S. A., Mix, A. C., Liu, Z., et al. (2012). Global warming preceded by increasing carbon dioxide concentrations during the last deglaciation. *Nature*, *484*(7392), 49–54. https://doi.org/10.1038/nature10915

Shapiro, G. I., Aleynik, D. L., & Mee, L. D. (2010). Long term trends in the sea surface temperature of the Black Sea. *Ocean Science*, *6*(2), 491–501. https://doi.org/10.5194/os-6-491-2010

Scheiner, F., Holcová, K., Milovský, R., & Kuhnert, H. (2018). Temperature and isotopic composition of seawater in the epicontinental sea (Central Paratethys) during the middle Miocene Climate Transition based on Mg/Ca, $\delta^{18}O$ and $\delta^{13}C$ from foraminiferal tests. *Palaeogeography, Palaeoclimatology, Palaeoecology*, *495*, 60–71. https://doi.org/org/10.1016/j.palaeo.2017.12.027

Schiebel, R. (2002). Planktic foraminiferal sedimentation and the marine calcite budget. *Global Biogeochemical Cycles*, *16*(4), 1065. https://doi.org/org/10.1029/2001gb001459

Schiebel, R., Barker, S., Lendt, R., Thomas, H., & Bollmann, J. (2007). Planktic foraminiferal dissolution in the twilight zone. *Deep-Sea Research Part II: Topical Studies in Oceanography*, *54*(5–7), 676–686. https://doi.org/org/10.1016/j.dsr2.2007.01.009

Schiebel, R., & Hemleben, C. (2005). Modern planktic foraminifera. *Paläontologische Zeitschrift*, *79*(1), 135–148. https://doi.org/org/10.1007/bf03021758

Schiebel, R., & Hemleben, C. (2017). *Planktic Foraminifers in the Modern Ocean*. Berlin, Heidelberg: Springer Berlin Heidelberg. https://doi.org/10.1007/978-3-662-50297-6

Schlitzer, R. (2019). Ocean Data View. https://odv.awi.de

Schmidt, D. N., Renaud, S., Bollmann, J., Schiebel, R., & Thierstein, H. R. (2004). Size distribution of Holocene planktic foraminifer assemblages: Biogeography, ecology and adaptation. *Marine Micropaleontology*, *50*(3–4), 319–338. https://doi.org/org/10.1016/s0377-8398(03)00098-7

Siegel, D. A., & Deuser, W. G. (1997). Trajectories of sinking particles in the Sargasso Sea: Modeling of statistical funnels above deep-ocean sediment traps. *Deep-Sea Research Part I: Oceanographic Research Papers*, *44*(9-10), 1519–1541. https://doi.org/org/10.1016/s0967-0637(97)00028-9

Sigman, D. M., & Boyle, E. A. (2000). Glacial/interglacial variations in atmospheric carbon dioxide. *Nature*, *407*(6806), 859–869. https://doi.org/10.1038/35038000

Singh, A. D., & Conan, S. M. H. (2008). Aragonite pteropod flux to the Somali Basin, NW Arabian Sea. *Deep-Sea Research Part I: Oceanographic Research Papers*, *55*(5), 661–669. https://doi.org/doi.org/10.1016/j.dsr.2008.02.008

Smith, M. R., & Myers, S. S. (2018). Impact of anthropogenic CO_2 emissions on global human nutrition. *Nature Climate Change*, *8*(9), 834–839. https://doi.org/10.1038/s41558-018-0253-3

Spanbauer, T. L., Fritz, S. C., & Baker, P. A. (2018). Punctuated changes in the morphology of an endemic diatom from Lake Titicaca. *Paleobiology*, *44*(1), 89–100. https://doi.org/org/10.1017/pab.2017.27

Spezzaferri, S., Kučera, M., Pearson, P. N., Wade, B. S., Rappo, S., Poole, C. R., et al. (2015). Fossil and genetic evidence for the polyphyletic nature of the planktonic foraminifera *Globigerinoides*, and description of the new genus *Trilobatus*. *PLoS One*, *10*(5), e0128108. https://doi.org/org/10.1371/journal.pone.0128108

Spezzaferri, S., & Rögl, F. (2004). Bolboforma (phytoplankton *Incertae Sedis*), *Bachmayerella* and other *Calciodinelloidea* (phytoplankton) from the middle Miocene of the Alpine–Carpathian Foredeep (Central Paratethys). *Journal of Micropalaeontology*, *23*(2), 139–152. https://doi.org/org/10.1144/jm.23.2.139

Sremac, J., Tripalo, K., Repac, M., Bošnjak, M., Vrsaljko, D., Marjanac, T., et al. (2018). Middle Miocene drowned ramp in the vicinity of Marija Bistrica (Northern Croatia). *The Mining-Geology-Petroleum Engineering Bulletin*, *33*(4), 23–43. https://doi.org/org/10.17794/rgn.2018.4.3

Stalling, D., Westerhoff, M., & Hege, H.-C. (2005). Amira - a highly interactive system for visual data analysis. In C. D. Hansen, C. R. Johnson (Eds.), *The Visualization Handbook*. (pp. 749–767). Butterworth-Heinemann, Burlington.

Storz, D., Schulz, H., Waniek, J. J., Schulz-Bull, D. E., & Kučera, M. (2009). Seasonal and interannual variability of the planktic foraminiferal flux in the vicinity of the Azores Current. *Deep-Sea Research Part I: Oceanographic Research Papers*, *56*(1), 107–124. https://doi.org/org/10.1016/j.dsr.2008.08.009

Suciu, A. A., Chira, C., & Popa, M. V. (2005). Late Badenian foraminifera, calcareous nannofossils and pteropod assemblages identified in boreholes from Cluj-Napoca. *Acta Palaeontologica Romaniae*, *5*, 451–461

Super, J. R., Thomas, E., Pagani, M., Huber, M., O'Brien, C., & Hull, P. M. (2018). North Atlantic temperature and pCO_2 coupling in the early-middle Miocene. *Geology*, *46*(6), 519–522. https://doi.org/10.1130/g40228.1

Szczechura, J. (1984). Morphologic variability in the *Globigerinoides-Orbulina* group from the middle Miocene of the Central Paratethys. *Acta Palaeontologica Polonica*, *29*, 3–27

Špišić, M., Bakrač, K., Hajek-Tadesse, V., Filjak, R., Brlek, M., Avanić, R., et al. (2017), Micropaleontological study of the middle Miocene section Ciprovac, Dilj Mt., in *Neogene of Central and South-Eastern Europe, 7th International Workshop*, edited by M. Horvat, L. Wacha, pp. 66–68, Croatian Geological Society, Velika, Croatia.

Takahashi, K., & Bé, A. W. H. (1984). Planktonic foraminifera: Factors controlling sinking speeds. *Deep-Sea Research Part A: Oceanographic Research Papers*, *31*(12), 1477–1500. https://doi.org/org/10.1016/0198-0149(84)90083-9

Takahashi, T., Feely, R. A., Weiss, R. F., Wanninkhof, R. H., Chipman, D. W., Sutherland, S. C., & Takahashi, T. T. (1997). Global air-sea flux of CO_2: an estimate based on measurements of sea-air pCO_2 difference. *Proc Natl Acad Sci U S A*, *94*(16), 8292-8299. https://doi.org/10.1073/pnas.94.16.8292

Tans, P., & Keeling, R. (2020). Trends in atmospheric Carbon Dioxide. Dataset accessed [2021-03-06] at: www.esrl.noaa.gov/gmd/eegg/trends/

Tedesco, K. A., & Thunell, R. C. (2003). Seasonal and interannual variations in planktonic foraminiferal flux and assemblage composition in the Cariaco Basin, Venezuela. *The Journal of Foraminiferal Research*, *33*(3), 192–210. https://doi.org/org/10.2113/33.3.192

Titschack, J., Baum, D., Matsuyama, K., Boos, K., Färber, C., Kahl, W. A., et al. (2018). Ambient occlusion – a powerful algorithm to segment shell and skeletal intrapores in computed tomography data. *Computers & Geosciences*, *115*, 75–87. https://doi.org/org/10.1016/j.cageo.2018.03.007

Vlček, T., Hudáčková, N., Jamrich, M., Halásová, E., Franců, J., Nováková, P., et al. (2020). Hydrocarbon potential of the Oligocene and Miocene sediments from the Modrany-1 and Modrany-2 wells (Danube Basin, Slovakia). *Acta Geologica Slovaca*, *12*(1), 43–55

Voigt, I., Cruz, A. P. S., Mulitza, S., Chiessi, C. M., Mackensen, A., Lippold, J., et al. (2017). Variability in mid-depth ventilation of the western Atlantic Ocean during the last deglaciation. *Paleoceanography*, *32*(9), 948–965. https://doi.org/10.1002/2017pa003095

Vrsaljko, D., Pavelić, D., Miknić, M., Brkić, M., Kovačić, M., Hećimović, I., et al. (2006). Middle Miocene (upper Badenian/Sarmatian) palaeoecology and evolution of the environments in the area of Medvednica Mt. (North Croatia). *Geologia Croatica*, *59*(1), 51–63

Wade, B. S., Pearson, P. N., Berggren, W. A., & Pälike, H. (2011). Review and revision of Cenozoic tropical planktonic foraminiferal biostratigraphy and calibration to the geomagnetic polarity and astronomical time scale. *Earth-Science Reviews*, *104*(1–3), 111–142. https://doi.org/org/10.1016/j.earscirev.2010.09.003

Wan, S., Jian, Z., Cheng, X., Qiao, P., & Wang, R. (2010). Seasonal variations in planktonic foraminiferal flux and the chemical properties of their shells in the southern South China Sea. *Science China-Earth Sciences*, *53*(8), 1176–1187. https://doi.org/org/10.1007/s11430-010-4039-3

Watson, A. J., Schuster, U., Shutler, J. D., Holding, T., Ashton, I. G. C., Landschutzer, P., et al. (2020). Revised estimates of ocean-atmosphere CO_2 flux are consistent with ocean carbon inventory. *Nat Commun*, *11*(1), 4422. https://doi.org/10.1038/s41467-020-18203-3

Weiner, A. K. M., Weinkauf, M. F. G., Kurasawa, A., Darling, K. F., & Kučera, M. (2015). Genetic and morphometric evidence for parallel evolution of the *Globigerinella calida* morphotype. *Marine Micropaleontology*, *114*, 19–35. https://doi.org/org/10.1016/j.marmicro.2014.10.003

Weinkauf, M. F. G., Kunze, J. G., Waniek, J. J., & Kučera, M. (2016). Seasonal variation in shell calcification of planktonic foraminifera in the NE Atlantic reveals species-specific response to temperature, productivity, and optimum growth conditions. *PLoS One*, *11*(2), e0148363. https://doi.org/org/10.1371/journal.pone.0148363

Weinkauf, M. F. G., Moller, T., Koch, M. C., & Kučera, M. (2013). Calcification intensity in planktonic Foraminifera reflects ambient conditions irrespective of environmental stress. *Biogeosciences*, *10*(10), 6639–6655. https://doi.org/org/10.5194/bg-10-6639-2013

Weldeab, S., Schneider, R. R., & Kölling, M. (2006). Sea surface temperature and salinity reconstruction of sediment core GeoB3129-1. Dataset accessed [2020-02-04] at: https://doi.pangaea.de/10.1594/PANGAEA.738284

Westin, C. F., Peled, S., Gudbjartsson, H., Kikinis, R., & Jolesz, F. A. (1997). Geometrical diffusion measures for MRI from tensor basis analysis. In (Eds.), *Proceedings of the 5th Annual Meeting of ISMRM*. (pp. 1742). Vancouver, Canada.

Wigley, T. M. L. (1983). The pre-indutrial carbon dioxide level. *Climatic Change*, *5*(4), 315–320. https://doi.org/10.1007/bf02423528

Wolfteich, C. M. (1994). *Sattelite-derived sea surface temperature, mesoscale variability, and foraminiferal production in the North Atlantic* (Master's thesis). Cambridge: Massachusetts Institute of Technology/Woods Hole Oceanographic Institution.

You, Y., Huber, M., Müller, R. D., Poulsen, C. J., & Ribbe, J. (2009). Simulation of the Middle Miocene Climate Optimum. *Geophysical Research Letters*, *36*(4). https://doi.org/10.1029/2008gl036571

Young, R. W., Carder, K. L., Betzer, P. R., Costello, D. K., Duce, R. A., DiTullio, G. R., et al. (1991). Atmospheric iron inputs and primary productivity: Phytoplankton responses in the North Pacific. *Global Biogeochemical Cycles*, *5* (2), 119–134. https://doi.org/10.1029/91gb00927

Zágoršek, K., Vávra, N., & Holcová, K. (2007). New and unusual bryozoa from the Badenian (middle Miocene) of the Moravian part of the Vienna Basin (Central Paratethys, Czech Republic). *Neues Jahrbuch für Geology and Paläontologie*, *243*(2), 201–215

Zarkogiannis, S. D., Antonarakou, A., Tripati, A., Kontakiotis, G., Mortyn, P. G., Drinia, H., & Greaves, M. (2019). Influence of surface ocean density on planktonic foraminifera calcification. *Sci Rep*, *9*(1), 533. https://doi.org/10.1038/s41598-018-36935-7

Zeebe, R. E., & Wolf-Gladrow, D. (2001). *CO_2 in Seawater: Equilibrium, Kinetics, Isotopes*. Amsterdam: Elsevier Science

Zlinská, A., Zágoršek, K., & Zorn, I. (2013). Upper Badenian sediments around Bratislava (Vienna Basin). *Geologické výzkumy na Moravě a ve Slezsku*, 69–71

Žarić, S., Donner, B., Fischer, G., Mulitza, S., & Wefer, G. (2005). Sensitivity of planktic foraminifera to sea surface temperature and export production as derived from sediment trap data. *Marine Micropaleontology*, *55*(1–2), 75–105. https://doi.org/org/10.1016/j.marmicro.2005.01.002

Žarić, S., Schulz, M., & Mulitza, S. (2006). Global prediction of planktic foraminiferal fluxes from hydrographic and productivity data. *Biogeosciences*, *3*(2), 187–207. https://doi.org/org/10.5194/bg-3-187-2006